from W.S. Thompson 1/24/64

Bellcomm Mission assurance Dept.

GU-68

Working Paper No. 13

December 6, 1963

APPLICATION OF PROBABILISTIC MODELING TECHNIQUES TO A TILT STABILIZATION ASSEMBLY

Prepared by

C. L. Britt

Prepared for
National Aeronautics and Space Administration
under
Contract No. NASw-334

ACKNOWLEDGEMENT

The work summarized herein represents a joint effort by several persons. The experimental designs, statistical analyses, and computer studies were under the direction of Dr. D. W. Gaylor. The experimental work and the construction of special equipment was under the direction of C. D. Parker in the Solid State Laboratory of R.T.I. H. B. Lyon conducted the experiments and recorded the data. The majority of the typing of this report was done by Mrs. Martha Self.

TABLE OF CONTENTS

LIST OF FIGURES

1.0. INTRODUCTION

The proof of the adaptability and acceptability of any methodology lies in the ability to apply it in practice to real complex systems. To provide another application of the probabilistic model techniques developed at RTI, and to aid in the development of these techniques, a representative electro-mechanical control system has been purchased by RTI, has undergone extensive tests in RTI laboratory facilities, and will remain available for further tests if required. The system chosen as an example was designed to be used as a stabilization mechanism for an aircraft radar antenna. The system is designated as a "Tilt Stabilization Assembly," and will be referred to in this paper as the T.S.A. System. The general methodology developed for estimating the reliability-performance of complex systems has been applied to this specific system, with results as outlined in the following sections of this paper.

The application of a general methodology to a specific example system serves several useful purposes. First, this approach shows what approximations and assumptions are required in order to stay within the limitations of time, available equipment, and costs. Secondly, any gaps or missing details in the methodology become evident during the step by step application to the specific system. These gaps must be filled in either with new or existing theory, or singled out for future study. Third, an example, written in language that is familiar to the engineer will insure acceptance and quick reduction to practice of those techniques that the engineer recognizes as assisting him in performing his job.

In this report, the emphasis is on the application of certain techniques that may prove useful in the <u>early design</u> stages of an equipment when the complete equipment is not yet available for test, and the mission input-environmental conditions may be unknown, or partially known. The components of the equipment are subjected to tests, and the component test data and data from past experience with similar components are used to construct a probabilistic model of the equipment. This mathematical model then becomes useful for:

1. Evaluating the given design in terms of the probability of successful performance of a given mission.
2. Determining the effect of proposed design changes on the probability of successful performance.
3. Determining the critical components and/or input conditions.
4. Evaluating the effect of different inputs and environmental conditions on the probability of successful performance of the mission.
5. Determining the effect of specifications at the interface of equipments on the probability of successful performance.

It is important to note also that it is possible to estimate either the probability that one specific system will perform as desired, or the probability that any sample system from a population of nearly identical systems will perform as desired. In the first case, observations are made of the behavior of the specific system components, and the variations and parameter values of these components are used in the mathematical model of the system. In the second case, manufacturing tolerances introduce additional variability into the mathematical model. For the example considered in this report, observations are taken on one set of components and an estimate is made of the probability of successful operation of a system made up of these particular components.

The step by step procedure followed in evaluating the reliability of the T.S.A. system may be outlined in general form as follows:

1. The equipment for which the reliability investigation is to be conducted is defined. The equipment reliability is defined as the probability of no failure in a specified time interval 0,t.
2. The operating conditions of the equipment during the mission of interest are defined.
3. The mission is subdivided into convenient time intervals during which the mode of operation of the equipment remains fixed.
4. The failure of the equipment during each mode is carefully defined in terms of the behavior of certain measurable attributes of the equipment.
5. The equipment is subdivided into convenient elements for which failure data is available or for which data may be generated by suitable experiments.

6. For each element, attributes are selected that define the performance of the element.
7. The inputs and environmental conditions for each element are investigated. By experience, intuition, or screening experiments, the important inputs and environmental conditions are selected for analysis.
8. The selected inputs and environmental conditions are classified as to expected behavior over time, and are described mathematically. In most cases, a probabilistic description is required, since exact values to be encountered in the mission are unknown.
9. A generalized transfer characteristic relating the element attributes to the element inputs and environmental measures is developed using theoretical and empirical techniques, or alternatively, the behavior over time of the element attribute is determined by observation as the inputs and environmental conditions expected to be encountered in the mission are simulated.
10. The functional relationships between the elements are used to propagate attribute behavior through the various elements to determine the behavior of the equipment attribute. The equipment reliability is then calculated from the definition of equipment failure and the estimated attribute behavior.
11. The reliability function for each mode or time interval is properly combined to estimate the probability that the equipment will perform successfully during the assigned mission.

2.0. DESCRIPTION OF THE TILT STABILIZATION ASSEMBLY

The T.S.A. is described in some detail in reference 2, section 2. A brief general description will be repeated here.

The function of the T.S.A. is to provide horizontal stabilization of an aircraft radar antenna over aircraft tilt angles of $\pm$ 20^{o} from the horizontal. A vertical seeking gyroscope is used as a horizontal reference sensor.

Physically, the TSA consists of three separate major components, a gyro-torque unit, servo amplifier, and rotary inverter. Functionally, the components comprise an a.c. position servomechanism with both position and rate feedback loops. A pictorial sketch of the system is shown in figure 1. A functional block diagram with the definition of important variables is shown in figure 2. With reference to these figures, the system operation is described as follows:

A change in aircraft pitch angle, ϕ_a, is detected by comparison with the gyroscope outer gimbal angle ϕ_r. Ideally, the gyro gimbal angles remain fixed with respect to an inertial coordinate system. The aircraft motion therefore displaces the autosyn rotor with respect to the stator and the autosyn generates an a.c. error signal e_e. The error signal is then amplified and used to drive the servo motor in a direction to null the error signal by rotation of the autosyn stator. Since the servo motor is also connected through a gear train to the output arm of the system, the output arm angle tends to remain fixed with respect to a horizontal inertial reference plane.

The two degree of freedom gyroscope uses a ball and disk erection device to cause the spin axis of the gyro to tend to align itself with the local gravity vector.

A caging-uncaging motor is used to hold the gyro rotor fixed with respect to the equipment case upon command of the operator. This motor mechanically locks both gyro gimbals. A relay in the amplifier converts the d.c. (caging-uncaging) command signal to the a.c. signal that is required to operate the motor.

A typical mission profile for the T.S.A. is shown in figure 3. For this mission, four modes of operation of the system may be identified.

1. Power off
2. Power on - gyro caged
3. Cage - uncage
4. Stabilization

For the purpose of calculating the probability of successful operation during this mission, the power off mode is eliminated from consideration by making the assumption that the system is functioning properly at t = 0, immediately after the power is turned on.

In the assumed mission profile, a warmup time of 45 minutes has been allowed before stabilization is required. Also, a 15 minute period between uncaging of the gyro and the stabilization mode has been allowed so that any transient disturbances caused by uncaging will have time to dampen out. These specific time periods are chosen to permit a numerical calculation of the probability that the system will have no failure up to the time t = 1 hr. (just prior to recaging), given that the system is operating properly at t = 0. The failure event is defined in the following section.

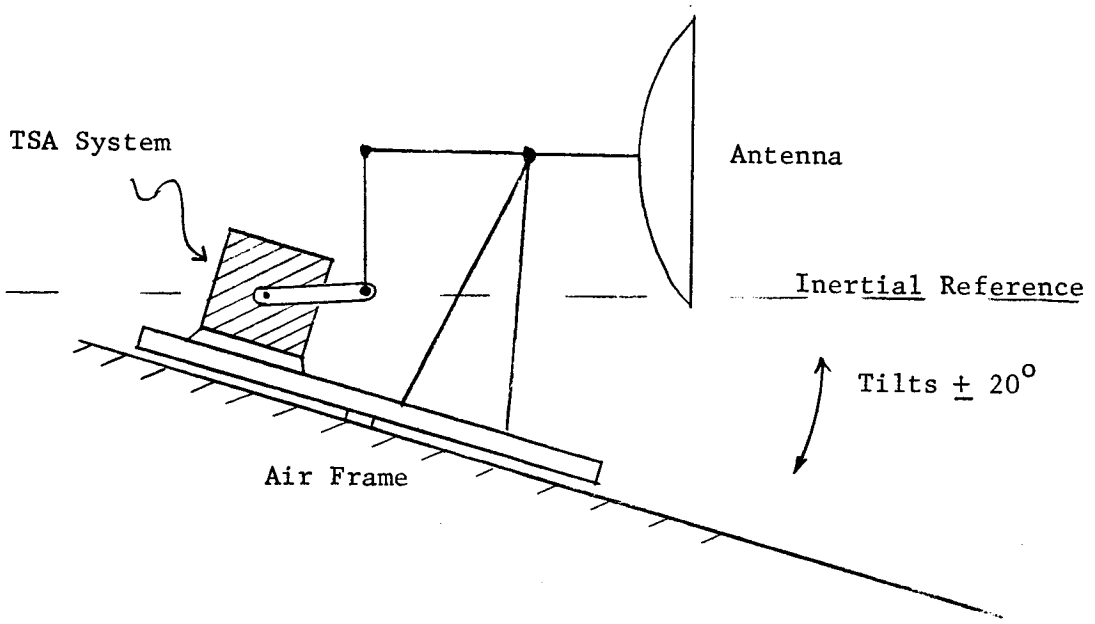

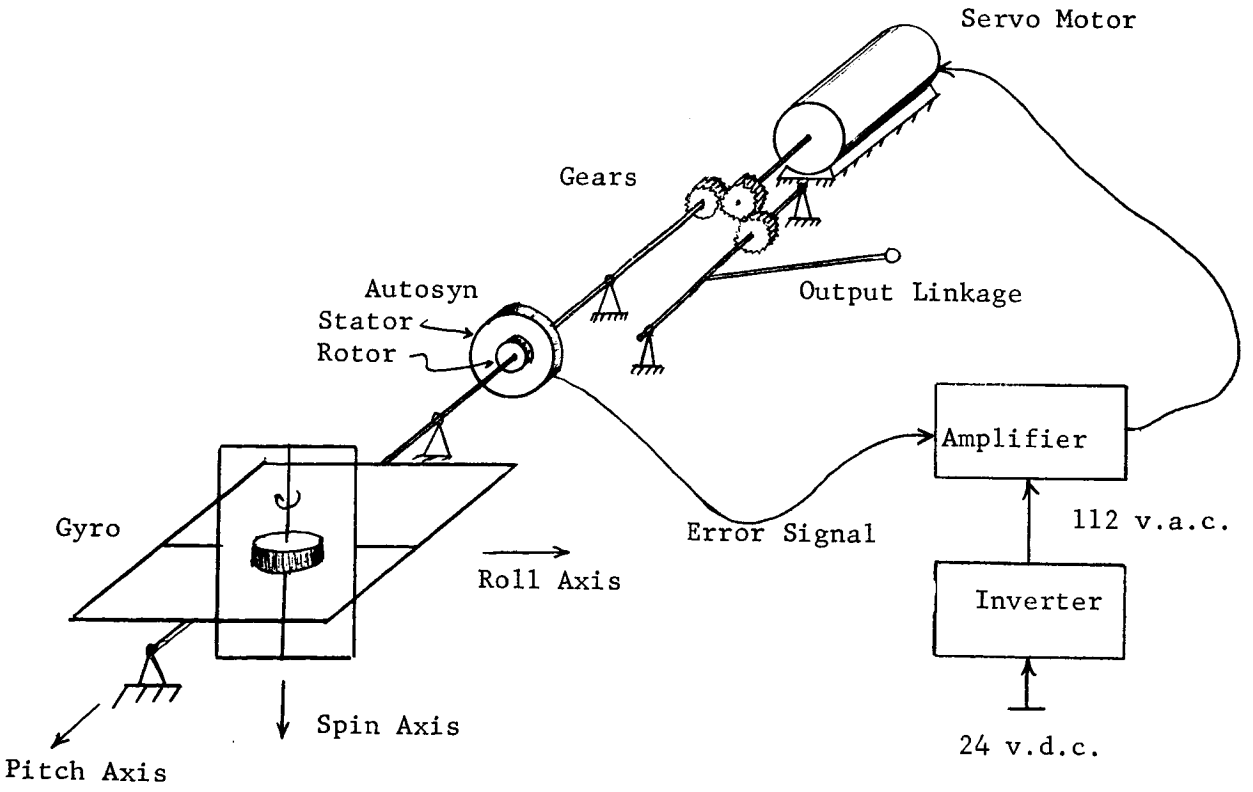

Figure 1. Pictorial Sketches of TSA System

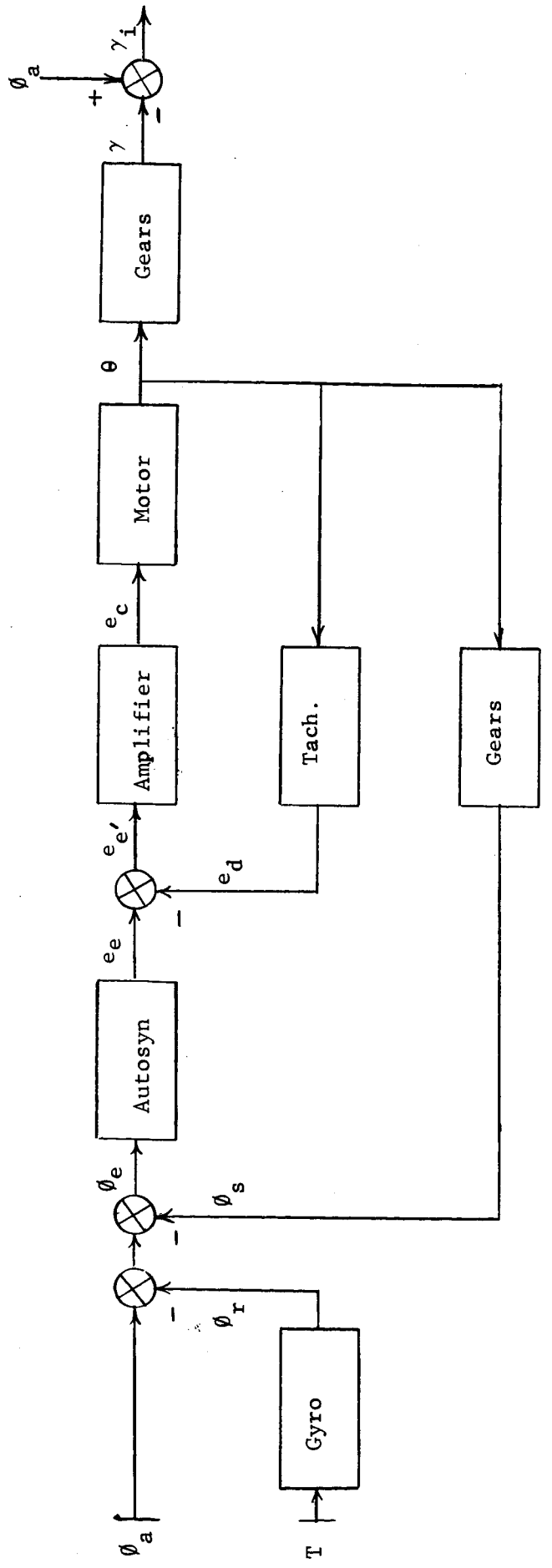

e_e = Error signal from autosyn
e_d = Rate damping signal
e_c = Control voltage
θ = Motor shaft angle
T = Stray torques on gyro gimbals
γ = Linkage arm angle (case reference)
$\gamma_i = \phi_a - \gamma$ = Linkage arm angle (inertial)

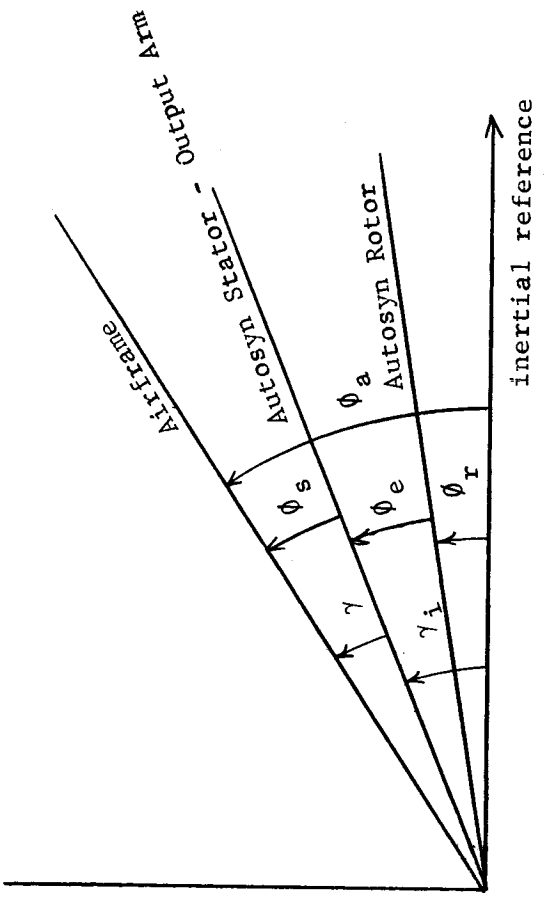

Figure 2 - Block Diagram of TSA System

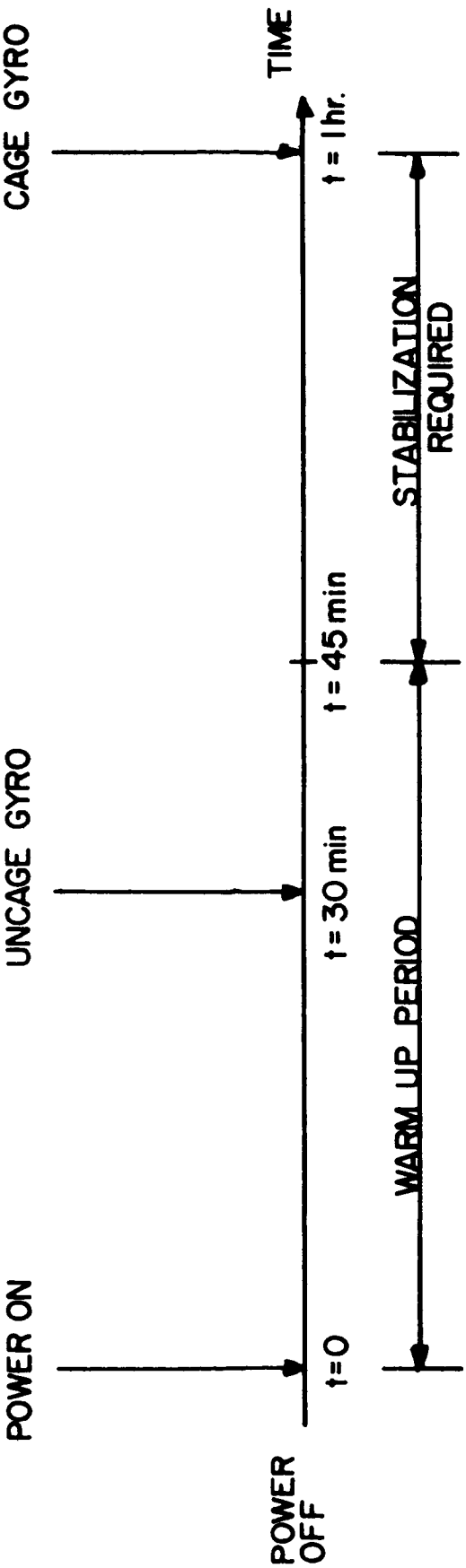

Figure 3. MISSION PROFILE - SEQUENCE OF OPERATIONS

3.0. DEFINITION OF THE RELIABILITY OF THE T.S.A.

To determine the probability of successful operation of the T.S.A., the event "successful operation" must be carefully defined. To define this term, a quantitative measure of performance must be found for the system, and bounds must be placed on this measure so that all observers will agree that a particular trial of the system is either a success or a failure.

The purpose of the T.S.A. is to maintain the output arm angle γ_i, measured in an inertial coordinate system, within limits such that the radar system of the aircraft will operate successfully. Hence, a suitable definition of failure might be: "failure occurs if the output arm angle γ_i exceeds a limit of $\pm$ c degrees, at any time during the time period when stabilization is required." This is not the only definition of failure that could be used, and others have been suggested in reference 1. Using this definition, it is evident that a failure cannot occur before stabilization is required, hence the system reliability as defined must be unity up to this time. The operation of the system prior to stabilization is best handled by subdividing the mission into time intervals, as follows:

$T_1 = 0 \leq t < t_1$ = gyro caged, system power on

$T_2 = t_1 \leq t < t_2$ = uncaging takes place

$T_3 = t_2 \leq t < t_3$ = gyro uncaged, stabilization not required

$T_4 = t_3 \leq t \leq t_4$ = stabilization required

The system is assumed to be operating properly at $t = 0$. Any malfunctions in the system during the interval $0 \leq t < t_3$, in accordance with the definition of failure, will be detected at time t_3. A plot of the probability of no failure vs. time will thus contain a sharp jump at time t_3. System malfunctions during the period 0 to t_3 are taken into account by estimating the probability that no malfunction occurs during the period 0 to t_3 that will cause the output arm angle γ_i to exceed a level $\pm$ c at time t_3, with certainty. To define the notation, let S_{T1} represent the event of no malfunction during time period T_1 that would cause certain system failure at time t_3. Further, define:

$$R_{T1} = Pr(S_{T1})$$

$$R_{T2} = Pr(S_{T2}/S_{T1})$$

$$R_{T3} = Pr(S_{T3}/S_{T2}S_{T1})$$

$$R_{T4}(t;c) = PR(|\gamma_i| < c \text{ in } t_3 \leq t \leq t_4/S_{T3}S_{T2}S_{T1})$$

Then the system reliability is given over the mission interval $0 \leq t \leq t_4$ by:

$$R(t;c) = 1 \qquad 0 \leq t < t_3$$

$$R(t;c) = R_{T4}(t;c)\, R_{T1}R_{T2}R_{T3} \qquad t_3 \leq t \leq t_4$$

The reliability $R_{T4}(t;c)$ will be called the probability of successful operation of the system during the stabilization mode, and will be estimated first.

The above probabilities are also considered to be conditional on the inputs to the system, including environmental inputs, being within certain acceptable ranges, or:

$$R_{T4}(t;c) = Pr(|\gamma_i| < c \text{ in } t_3,\ t/S_{T1}S_{T2}S_{T3}\ X_1X_2 \ldots X_n)$$

where X_1 = event of acceptable input x_1

X_n = event of acceptable input x_n

In most cases, these acceptable ranges are determined by the definition of failure of the equipment that supplies the particular input. In the mathematical model of the system, these input ranges may be considered as variables of the model if it is desired to find optimum ranges or specifications at the interface of equipments.

For the T.S.A. system, the inputs that are considered include the D.C. supply voltage from the aircraft (E), the ambient temperature (T) and the pitching motions of the airplane (ϕ_a). The system, considered as a single element, is represented as follows:

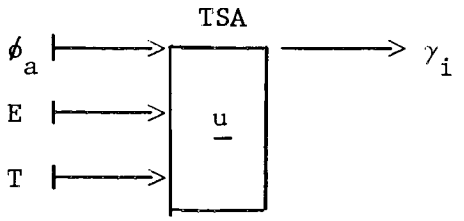

Here ϕ_a is a random process that will be discussed in detail in the following sections of this report. E and T are considered to be random variables that will have fixed values over any given mode of operation during the mission, but the exact value is unknown a priori. $\underline{u}$ represents variations within the system that in turn cause variations in the system output γ_i. The ranges on E and T are taken to be:

$$20 \leq E \leq 30 \text{ volts}$$

$$0 \leq T \leq 90^{\circ}C$$

These ranges will serve as guides for the tests to be conducted on the system. In selecting these ranges, it is important that they include the actual values that might be encountered in the mission, if possible.

The environmental conditions that are not considered, such as linear accelerations, humidity, radiation, and pressure, are considered to be of secondary importance, but it should be realized that any reliability estimate obtained will be conditional on these inputs having values that correspond to their values under the laboratory conditions at which the component tests are conducted.

To simplify the equations to follow, the notation of the acceptable input conditions, and the condition of no prior malfunctions will be dropped, but should be understood to be implied in the probability statements.

In the expression for the reliability of the TSA in the stabilization mode, it is convenient to consider the probability of a "catastrophic" failure separately:

$$R_{T4}(t;c) = \Pr(\text{n.c.f. in } t_3,\ t)\ \Pr(|\gamma_i| < c \text{ in } t_3,\ t/\text{n.c.f.})$$

where n.c.f. - no catastrophic failure

The first probability will include sudden changes in the system that are certain to cause the output arm angle to exceed the assigned limits.

A specialization of the above expression suggested in reference 1, "Probabilistic Models for System Reliability" by J. B. Lewis and W. T. Wells is:

$$R(t;c) = \int_{\Gamma} [e^{-\int_0^t h(\tau/\underline{v})\, d\tau}][\int_c f(w;t/\underline{v})\, dw]\, f_T(\underline{v})\, d\underline{v}$$

Where:

Γ is the region of the input space where the inputs are considered acceptable.

$\underline{v}$ represents the random variables that describe the inputs.

w is some monotonic function of the output attribute.

c represents the bounds on the w function.

$f(w;t/\underline{v})$ is the conditional time changing density function of w.

$f_T(\underline{v})$ represents the joint truncated density function of the input random variables, truncated at the boundary Γ.

$h(\tau/\underline{v})$ is the conditional catastrophic hazard rate, generally time dependent.

To apply this general model to the T.S.A. system, assumptions will be made as follows:

1. For catastrophic failures, the hazard rate is constant throughout the time interval considered.
2. The inputs E, T, and ϕ_a are independent.
3. The input process $\phi_a(t)$ will be a stationary process, and component tests will be conducted with this input simulated as closely as possible.

Also, to aid in the numerical calculations, the multiple integral over the input space will be approximated by finite sums.

With these assumptions and approximations, there is obtained:

$$R_{T4}(t;c) = \sum_{i=1}^{n} \sum_{j=1}^{m} [e^{-(h_4/E_iT_j)(t-t_3)}][R_D(t;c/E_iT_j] \; X$$

$$[Pr(E_{i-1/2} < E < E_{i+1/2}) \; Pr(T_{j-1/2} < T < T_{j+1/2}]$$

Here R_D has been used to represent the conditional probability of a failure due to causes other than random catastrophic, and includes drift, degradation, and performance failures. R_D is used here instead of the integral of a density function because the choice of a suitable density function will depend upon the behavior of the output attribute, and this behavior must be determined first. The sums are over the region of the acceptable input space, and the last two probabilities are normalized so that:

$$\sum_{i=1}^{n} \sum_{j=1}^{m} [Pr(E_{i-1/2} < E < E_{i+1/2}) \; Pr(T_{j-1/2} < T < T_{j+1/2}] = 1$$

The objective in the following sections of this report will be to obtain estimates of the various terms in the above expressions using data from past experience with similar equipment, data from component tests, and analytical techniques where required.

4.0 ESTIMATION OF THE PROBABILITY OF NO DRIFT OR PERFORMANCE FAILURE

To estimate the probability that the inertial output arm angle remains within limits of $\pm$ c degrees, given that no catastrophic failures have occurred, the information desired is:

a) A generalized transfer characteristic relating the system attribute to the system inputs, and describing the internal variations of the system:

$$\gamma_i(t) = g[E, T, \phi_a(t), \underline{u}(t)]$$

b) Adequate statistical descriptions of E, T, $\phi_a(t)$, and $\underline{u}(t)$.

c) Numerical values for the limits $\pm$ c.

With this information, the process γ_i may be simulated on an analog or digital computer, or known analytical techniques may be used, to calculate the desired probability.

To develop the generalized transfer characteristic for the T.S.A., the system is first broken down into convenient elements. Each element is examined separately, and an expression developed for the output as a function of the inputs, insofar as known. This development of theoretical element transfer functions is done in the conventional manner, using the physical laws that apply in a particular case. The parameters of the theoretical transfer function are then considered as attributes of the element; that is, these parameters are considered as describing the performance of the element. For example, for the gyro-autosyn considered as an element, it is expected that the output signal will be proportional to the angular displacement of the autosyn rotor with respect to the stator, or:

$$e_e = K_e|\phi_e| \sin(\omega_o t+\Psi) \qquad \text{(volts)}$$

where:

K_e = constant of proportionality or "autosyn gain"
ω_o = frequency of autosyn reference voltage
Ψ = phase angle (+ $\pi/2$ or - $\pi/2$ depending upon direction of displacement)

The angle ϕ_e may be expressed in terms of the angles defined previously in Figure 2 so that:

$$e_e = K_e|\phi_a - \phi_r - \phi_s| \sin(\omega_o t+\Psi) \qquad \text{(volts)}$$

or in terms of rms volts:

$$V_e = K_e(\phi_a - \phi_s) + N_G \ . \qquad \text{(rms volts)}$$

Where:

$N_G = -K_e \phi_r$

$+V_e$ = corresponds to clockwise motor rotation($\Psi = +\pi/2$)

$-V_e$ = corresponds to counter-clockwise motor rotation ($\Psi = -\pi/2$).

N_G represents the component of the output voltage due to gyro drift.

The parameter K_e and variable N_G are selected as the important attributes of the gyro-autosyn combination, and the behavior of these attributes over time is of interest for predicting the behavior of the system over time. Other parameters of the gyro autosyn are considered to be of secondary importance in the particular application under study. Tests are to be conducted on this element to determine if the theoretical expression is reasonably valid, and also to determine the behavior of the attributes over time as a function of the environmental inputs such as ambient temperature and supply voltage.

Proceeding in this manner for each element, a functional diagram for the system is developed showing the inputs and selected performance attributes of each element. The choice of elements and attributes and the functional relationship between them for the T.S.A. is shown in Figure 4. Note that it has been assumed that each element of the system operates in the same ambient temperature. If this were not the case, it would be indicated on the functional diagram by using a dummy element, as shown below for an example where the ambient temperature in which element B operates is thought to be about 20% higher than the ambient temperature of element A.

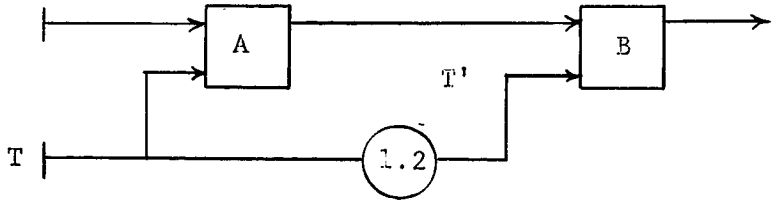

The system functional diagram is used as a guide for the tests to be conducted on each element, and as a guide for obtaining the system transfer characteristic from the element transfer characteristics.

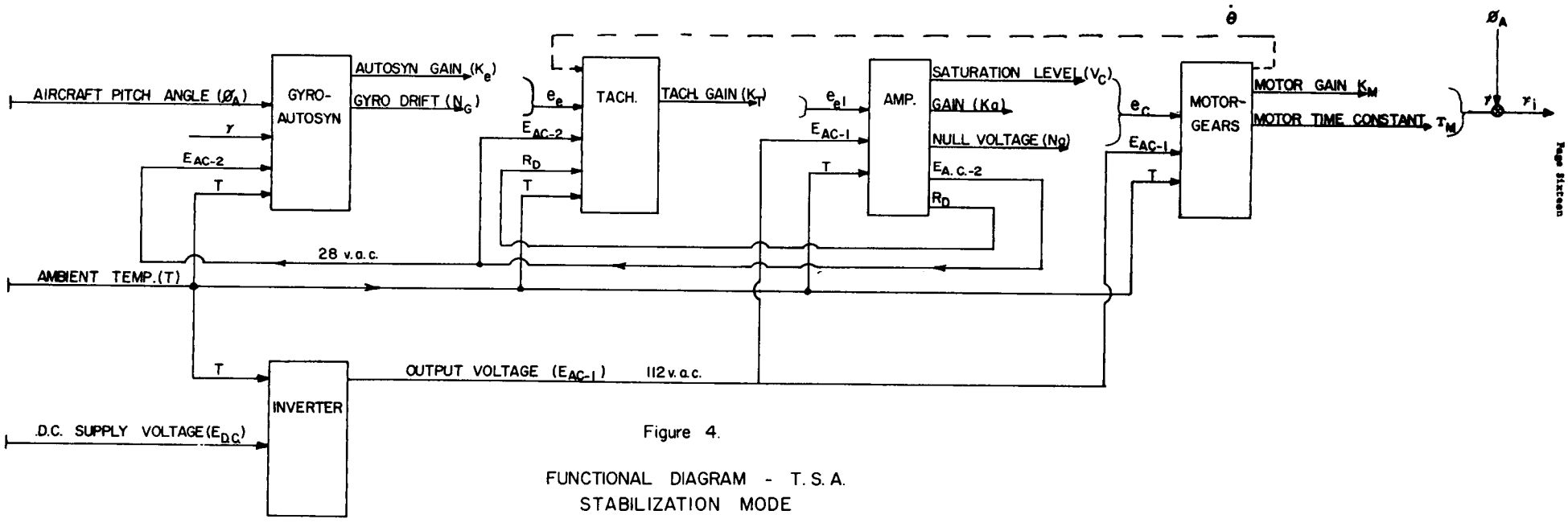

Figure 4.

FUNCTIONAL DIAGRAM - T. S. A.
STABILIZATION MODE

4.1 DEVELOPMENT OF ELEMENT TRANSFER CHARACTERISTICS

4.1.1 Amplifier

From the system functional diagram, it follows that the amplifier considered alone is represented as:

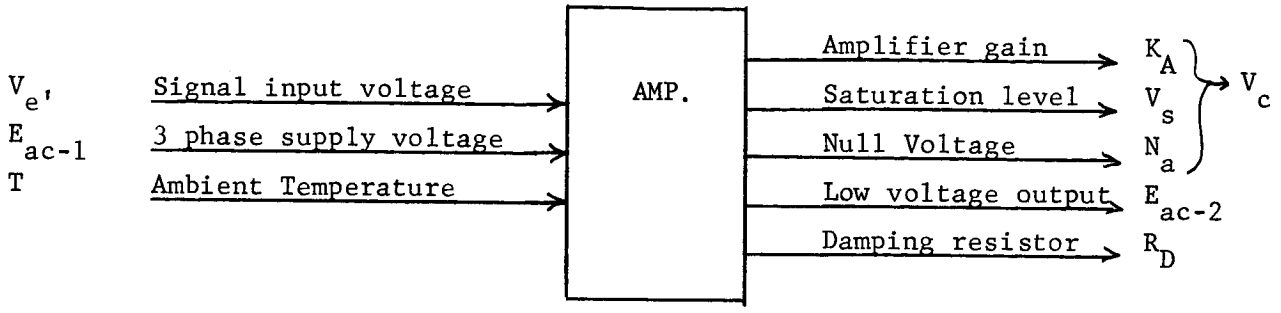

and it is desired to express each of the amplifier attributes as functions of the inputs and internal variations of the amplifier, if any.

The specific procedure used for empirically obtaining these expressions is as follows:

1. Holding E_{ac-1} and T fixed at design value and room temperature, respectively, the rms value of the output voltage (V_c) is measured as the signal input voltage ($V_{e'}$) is set at various levels. A load impedance similar to the impedance that the element will encounter in the system is used.
2. From the results of (1), we find that the amplifier output voltage may in fact be approximately described by the attributes: gain (K_A), saturation level (V_s), and null voltage (N_a). That is:

$$V_c \approx K_A V_{e'} + N_a \qquad \text{for } |V_{e'}| < \frac{V_s}{K_A}$$

$$V_c \approx V_s \qquad \text{for } |V_{e'}| \geq \frac{V_s}{K_A}$$

The value of K_A is determined by the method of least squares, fitting a linear slope to the data points of the V_c vs. $V_{e'}$ curve. The degree of approximation is measured by the goodness of fit of the least squares slope. The nominal value of V_s is obtained by averaging the positive and negative data points in the region of the $V_c$vs. $V_{e'}$ curve where the curve is flat, (Figure 5, page 20).

3. Next, the amplifier output voltage is observed at three levels of input voltage, while the supply voltage and temperature are

set at high, nominal, and low levels in a full factorial experiment. The measurements are made at 5 minute intervals over a time period of thirty minutes, to detect any short term drift of the attributes. The attributes E_{ac-2} and R_D are also measured at the 5 minute intervals. From this data, the value of K_A may be calculated, while V_s, $|N_a|$, E_{ac-2}, and R_D are measured directly. Data taken in this experiment is recorded in appendix D.

4. To express the test results in a usable mathematical form, the linear and quadratic terms of a Taylor's Series are used to approximate the relationship between a particular attribute of an element (Y), and the input-environmental random variables. As an example of this model, for an attribute that is time invariant, we have:

$$Y = b_o + b_1T + b_2T^2 + b_3E + b_4E^2 + b_5TE$$

where the b's are constants estimated by the method of least squares from the data. The term (b_5TE) represents the contribution of the linear x linear interaction of T and E. The IBM 7072 computer at Duke University was used for the actual computational analysis of the data. The computer program is based on a step-wise multiple regression procedure whereby only the statistically significant terms of the Taylor's expansion are included in the model. In this way the final regression is simplified by including only those terms that significantly reduce the variance. The program is an expansion of the program written for the IBM 650 "Multiple Regression by Step-wise Procedure," No. 6015-3112, reference [10].

5. For the case where the test data indicates that an attribute must be described by a time changing probability density function, a suitable functional form is postulated, and the coefficients of the function are estimated from the data. For the amplifier null voltage, an equation of the form:

$$|N_a| = \frac{K}{1 + be^{-at}}$$

was found to fit the data reasonably well. The coefficients a, b, and K were then estimated from the data. H. Hotelling (Journal of the American Statistical Association 22, 1927, p. 283) gives a technique for estimating these coefficients. The data indicated

that K was a function of the input conditions, hence K was subjected to the multiple regression analysis described in (4).

Analysis of the test data by the above described procedures gives results for the amplifier attributes as follows:

$$K_A = 3409 + 41.7\ \Delta E_{ac-1} - 1.10(\Delta E_{ac-1})^2$$

$(s = 34)$

$$V_s = 115.2 + .058\ \Delta T - .0011(\Delta T)^2 + 1.21\ \Delta E_{ac-1} - .055(\Delta E_{ac-1})^2 + .0025\ \Delta E_{ac-1}\ \Delta T$$

$(s = .9)$

$|N_a|$ = random process, normally distributed at any t, with:

$$\text{estimated mean} = \frac{1.86 + .0122\ \Delta T - .0425\ \Delta E_{ac-1}}{1 + .218e^{-.247t}}$$

estimated standard deviation = .29

R_D = 304 ohms, independent of time, temperature and supply voltage

$E_{ac-2} = .24\ E_{ac-1}$ independent of time, temperature

where: $\Delta E_{ac-1} = (E_{ac-1} - 112V)$

$\Delta T = (T - 26^{\circ}C)$

t = time in minutes,

t = 0 corresponds to power on time plus 10 minutes.

s = goodness of fit (Standard deviation)

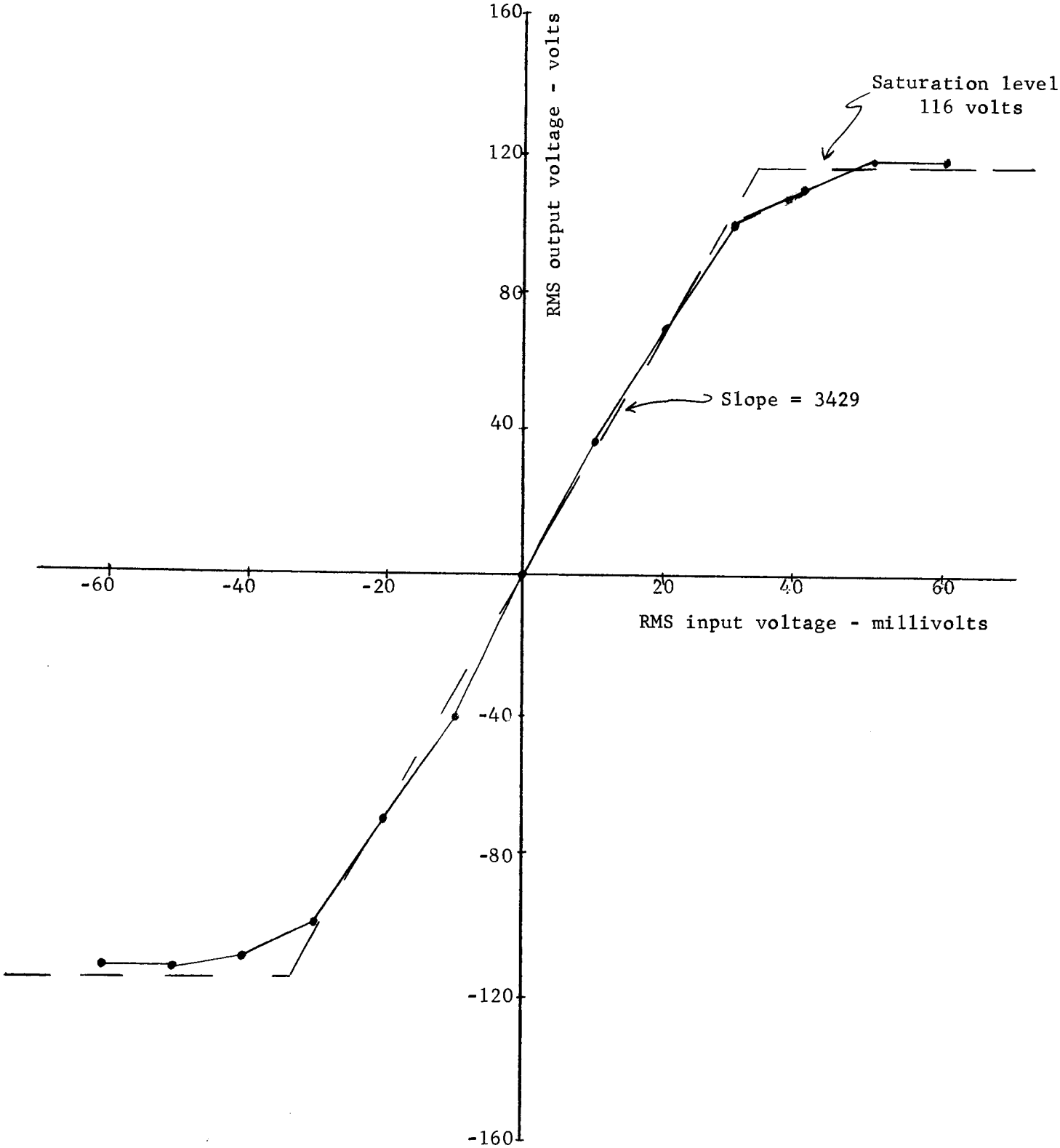

Figure 5 - Nominal Amplifier Characteristics

4.1.2 Gyro-Autosyn

The gyro-autosyn, considered as a single element, has attributes and inputs as shown below:

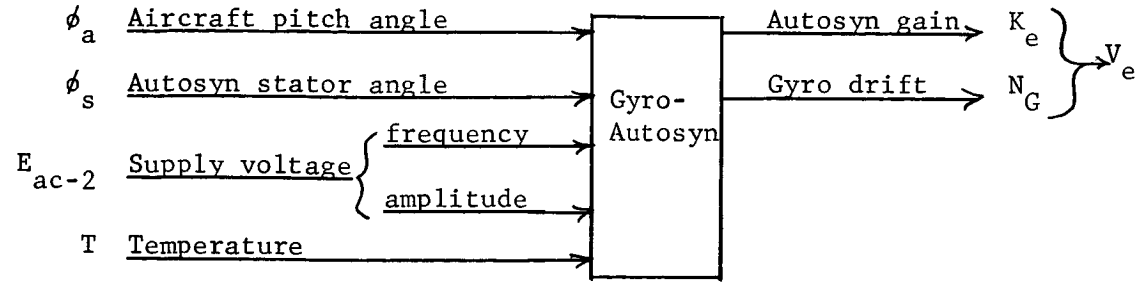

This element presents a more complicated situation than the amplifier because of the mechanical input processes $\phi_a(t)$ and $\phi_s(t)$. It is desirable to simulate these inputs as closely as possible with motions that the gyro will encounter in the mission.

The processes $\phi_a(t)$ and $\phi_s(t)$ will have no effect on the autosyn gain attribute in the linear approximation by definition. The input $\phi_a(t)$ will affect the gyro drift attribute because of the friction at the gyro gimbal bearings. When the angle ϕ_a changes value, an unwanted torque will be applied to the gyro through this gimbal friction, and this torque will cause unwanted drift of the gyro. The input $\phi_s(t)$, stator angle, could affect the gyro drift attribute since torque will be applied to the gyro through electromagnetic coupling in the autosyn. The magnitude of this torque is determined by the current flowing in the autosyn windings, the difference between ϕ_a and ϕ_s, and the design parameters of the autosyn. Since the current flowing in the autosyn windings is extremely small, and since the system operation keeps the difference $\phi_a - \phi_s$ very small, it is felt that the torque applied to the gyro through this means of coupling will be negligible as compared to the torque applied through friction in the gimbal bearings. The input $\phi_s(t)$ is therefore held at a fixed value during the gyro tests.

To simulate the process $\phi_a(t)$ realistically, the literature was searched to obtain data on the characteristics of aircraft pitch motion. From reference [4], as described in detail in appendix B, a statistical description of the characteristics of atmospheric turbulance is obtained, along with sufficient information to translate these atmospheric disturbances into typical aircraft pitching motions.

To provide the pitching motion input to the gyro-autosyn, a voltage analogous to the angle ϕ_a is generated on an analog computer, using a noise generator as a source, and shaping the noise on the computer to achieve the proper statistical characteristics. The voltage thus generated is used to drive a platform on which the gyro is mounted. The platform motion then closely simulates the motion that the gyro-autosyn will encounter in a typical mission.

Tests are conducted on the gyro-autosyn element to measure the attributes K_A and N_G over a time period of thirty minutes under various input-environmental conditions. Observations are made of the autosyn output voltage minus a voltage proportional to the gyro platform motion. This results in a voltage output proportional to $N_G = K_e \phi_r$, when $\phi_s = 0$. Twenty trials at nominal conditions were conducted to establish the form and distribution of the gyro drift attribute. Next, the variables temperature (T), supply voltage frequency (ω_o), and supply voltage amplitude $|E_{ac-2}|$, were each set at two levels in a full factorial experiment, with four replications at each condition. To avoid any bias in the data due to the effect of the earth's rotation on gyro drift, each of the four replications are taken with a different orientation of the gyro (N,E,S,W). This experiment yielded 52 sample functions of gyro drift. Examination of the data indicated that the variable ω_o had no apparent affect on the gyro drift attribute over the range considered. Thus, for the variables temperature and supply voltage, the data effectively is as shown below:

Temperature T

Supply Voltage E_{ac-2}	Low	Nom.	High
Low	8 trials		8 trials
Nom		20 trials	
High	8 trials		8 trials

To more accurately determine the effect of temperature and supply voltage amplitude, the blank blocks in the above experiment were later filled in with 4 trials in each block, resulting in data as follows:

Supply Voltage E_{ac-2}		Temperature T: Low	Nom.	High
	Low	8 trials	4 trials	8 trials
	Nom.	4 trials	24 trials	4 trials
	High	8 trials	4 trials	8 trials

For the gyro drift attribute, each trial is in the form of a continuous record over a time period of thirty minutes. A typical sample function of gyro drift is shown in Figure 6. The maximum amplitude of the gyro drift over the last 15 minute portion of each trial is recorded in appendix D. The analysis of the gyro drift data is discussed in Section 4.3 of this report, "Analysis of Drifts."

The behavior of the attribute K_e, autosyn gain, is determined by holding the angles ϕ_s and ϕ_a constant, while supply voltage and temperature are set at three levels; low, nominal, and high. No drift of this attribute over time is noted under fixed input conditions. Data on the attribute K_e is subjected to the multiple regression procedure described previously to obtain:

$$K_e = .1119 - .000289\,\Delta T + .00093\,\Delta E_{ac-1} \qquad \text{Volts/degree}$$

$$(s = .0029)$$

A plot of autosyn output voltage vs. angular displacement is shown in Figure 7, under nominal conditions of temperature and supply voltage. The curve is reasonably linear over most of the range of importance.

4.1.3 Motor and Gears

The motor and gears are considered as a single element, and are represented as:

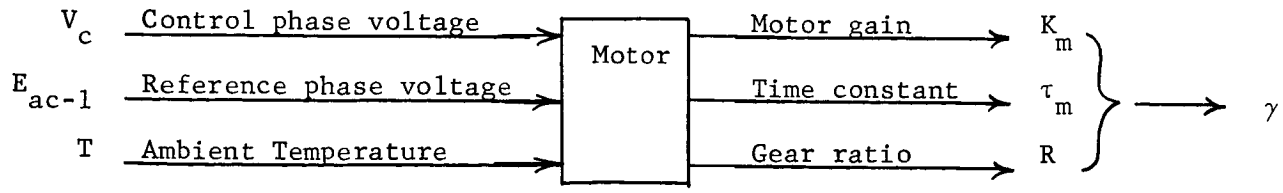

Where the theoretical linear motor transfer function is derived in reference [2] as:

$$\frac{\hat{\theta}}{\hat{V}_c} \approx \frac{K_m}{s(\tau_m s+1)} \; ; \qquad \frac{\gamma}{\theta} = R.$$

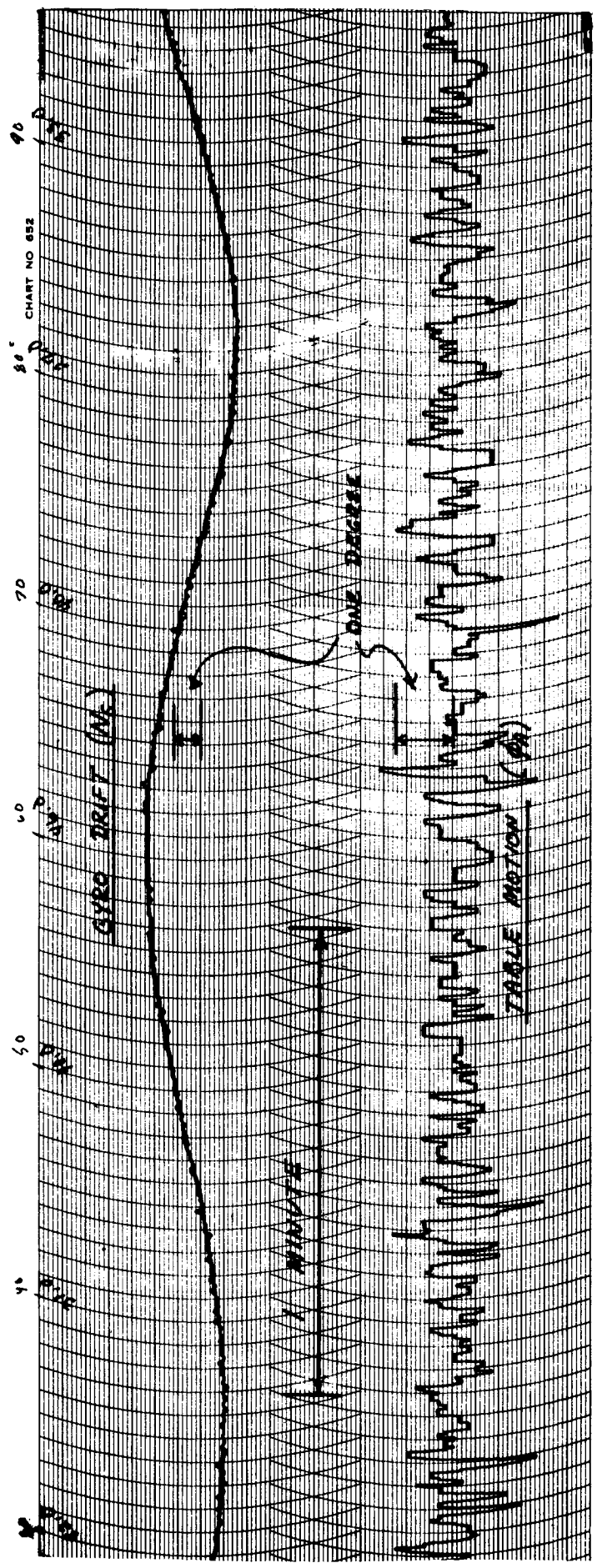

FIGURE 6 - SAMPLE FUNCTION OF GYRO DRIFT

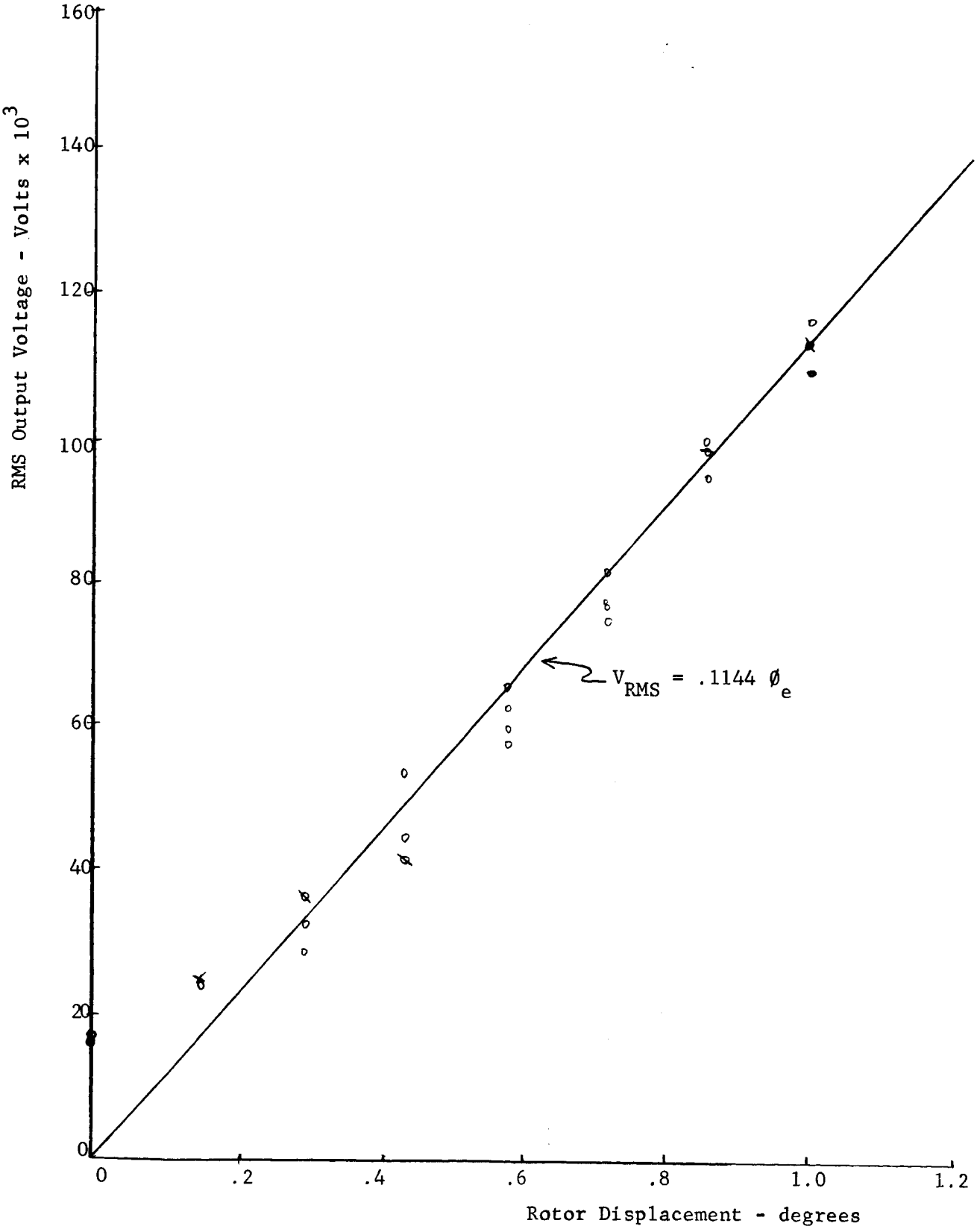

Figure 7 - Nominal Autosyn Gain Characteristics

To check the validity of this expression, the motor speed and the motor "time constant" are observed at various values of control voltage, while the reference phase voltage and the ambient temperature are held fixed at nominal conditions. A plot of θ vs. V_c is shown in Figure 8. This plot shows that the motor exhibits a deadband characteristic, in that no rotation of the motor takes place until the control phase voltage is at least ten volts. The linear least squares slope that represents the nominal value of K_m is also shown in Figure 8. This linear approximation, which neglects the deadband effect, should give reasonable results if V_c does not remain in the interval $-10 < V_c < 10$ volts for a large percentage of the time, with the signal levels that are simulated. The value $V_c = 10$ v. corresponds to a system angular error of .026 degrees. This error can exist before any corrective action will be initiated by the system.

The motor time constant, τ_m, is measured by introducing step voltage inputs to the motor, and recording the resultant change in the motor speed on a continuous chart recorder. The experimental results indicate how the time constant changes with the magnitude of the step input voltage. This data is recorded in appendix D. The value of τ_m obtained from a step voltage change of $V_c = \pm 41$ volts is selected as being the most representative value to use in the approximate linear transfer function.

To determine the effect of the environmental inputs on the attributes K_m and τ_m, the supply voltage and temperature are set at three levels, and at each condition of supply voltage and temperature, the motor gain and time constant are measured. The resulting data is listed in appendix D, and analysis of the data by the methods as described previously gives:

$$K_m = 437 + 1.81\ \Delta T - .40\ \Delta E_{ac-1} \qquad \text{degrees/sec/volt}$$

$$(s = 27)$$

$$\tau_m = .368 + .00074\ \Delta T - .0000213\ (\Delta T)^2 - .0053\ \Delta E_{ac-1} - .00018\ (\Delta E_{ac-1})^2 \qquad \text{sec.}$$

$$(s = .011)$$

$$R = 1/306 \qquad \text{degrees/degree}$$

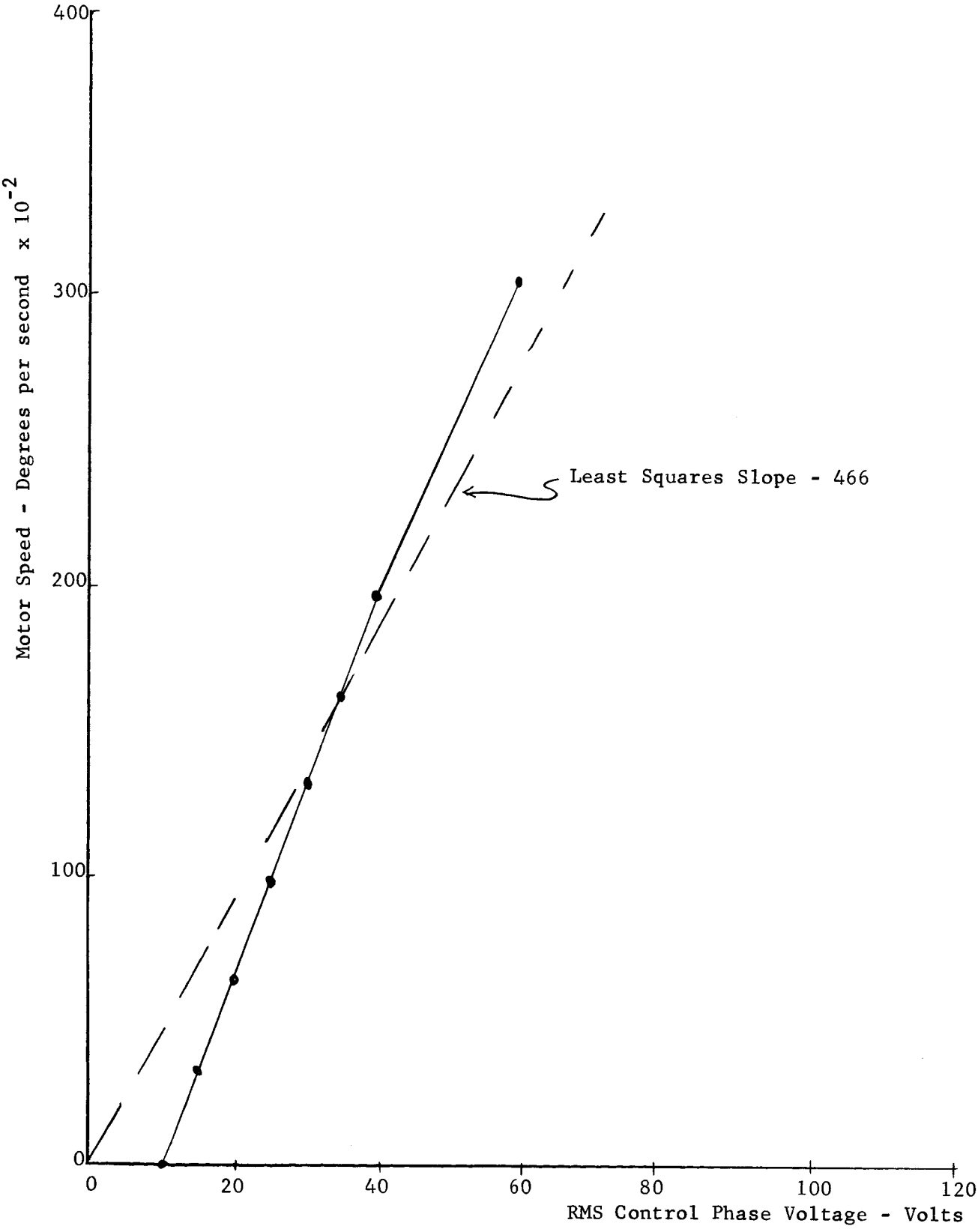

Figure 8 - Nominal Motor Speed - Voltage Characteristics

4.1.4 Tachometer

The tachometer, although physically contained in the motor, is treated as a separate element because of its entirely different function in the system. From the system functional diagram, the selected inputs and attributes are identified as:

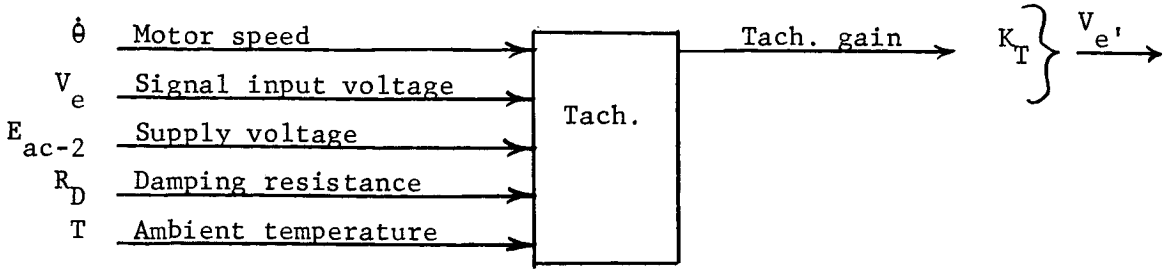

The actual output voltage versus motor speed, with the other inputs held fixed, is shown in Figure 9. From this plot the degree of approximation required in assuming a linear transfer function of the form:

$$\frac{\hat{V}_{e'}}{\hat{\theta}} = K_T s$$

is shown.

The input resistor R_D was found from tests on the amplifier element to remain constant within measurement accuracy with changing ambient temperature and supply voltages. Hence, this input is held fixed during the tests on the tachometer. The attribute K_T is measured while temperature and supply voltage are set at three levels by recording the output voltage and motor speed at each level of supply voltage and temperature. Knowing these variables permits the calculation of K_T at each condition. The data is recorded in appendix D. The tachometer gain did not appear to change over time when observed for thirty minutes, hence the attribute is considered a function of the supply voltage and temperature only. The mathematical expression obtained is:

$$K_T = [1178 - 3.38\,\Delta T + 8.9\,\Delta E_{ac-1}]\,10^{-8} \quad \text{Volts/deg per sec.}$$

$$(s = 76 \times 10^{-8}) \quad .$$

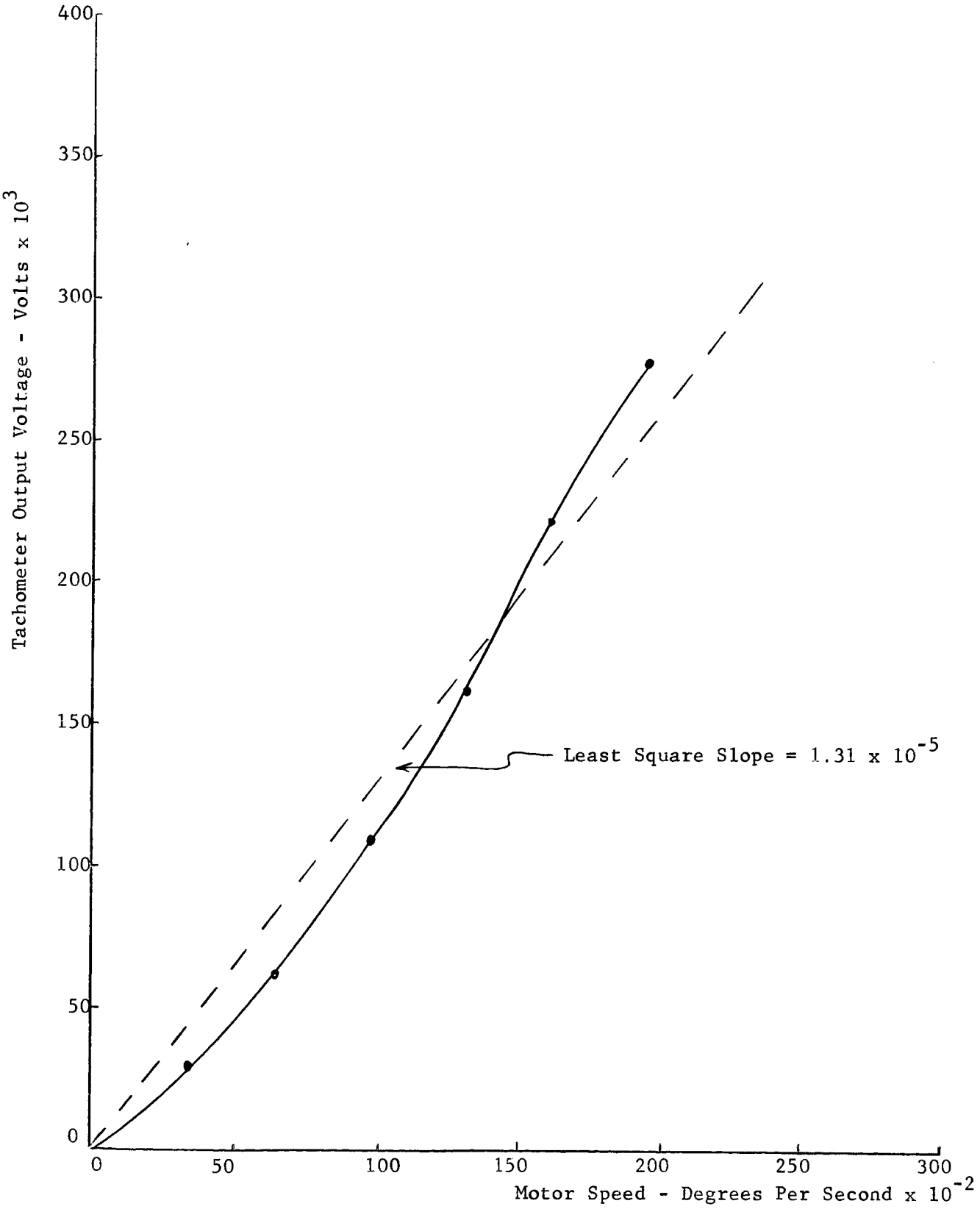

Figure 9 - Nominal Tachometer Gain Characteristic

4.1.5 Inverter

The selected attributes of the inverter include the magnitude and frequency of the a.c. voltage output. The element is represented as:

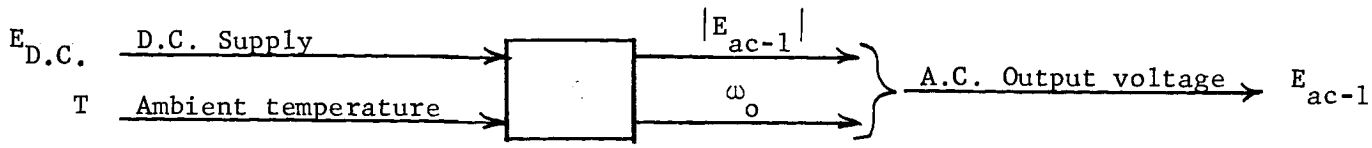

To determine the behavior of the attributes, the temperature is held at fixed levels and the output voltage magnitude and frequency are recorded as the D.C. supply voltage is set at several levels. The test results are shown in graphical form in Figure 10. With fixed inputs, no time variation in the attributes is observed. The variation with ambient temperature is small. For nominal input conditions, the output voltage and frequency are given approximately by:

$$|E_{ac-1}| = 7.70\ E_{D.C.} - .125(E_{D.C.})^2 \quad \text{volts} \qquad (18 < E_{D.C.} < 30\ \text{v})$$

$$\omega_o = 28.84\ E_{D.C.} - .495(E_{D.C.})^2 \ \text{cps} .$$

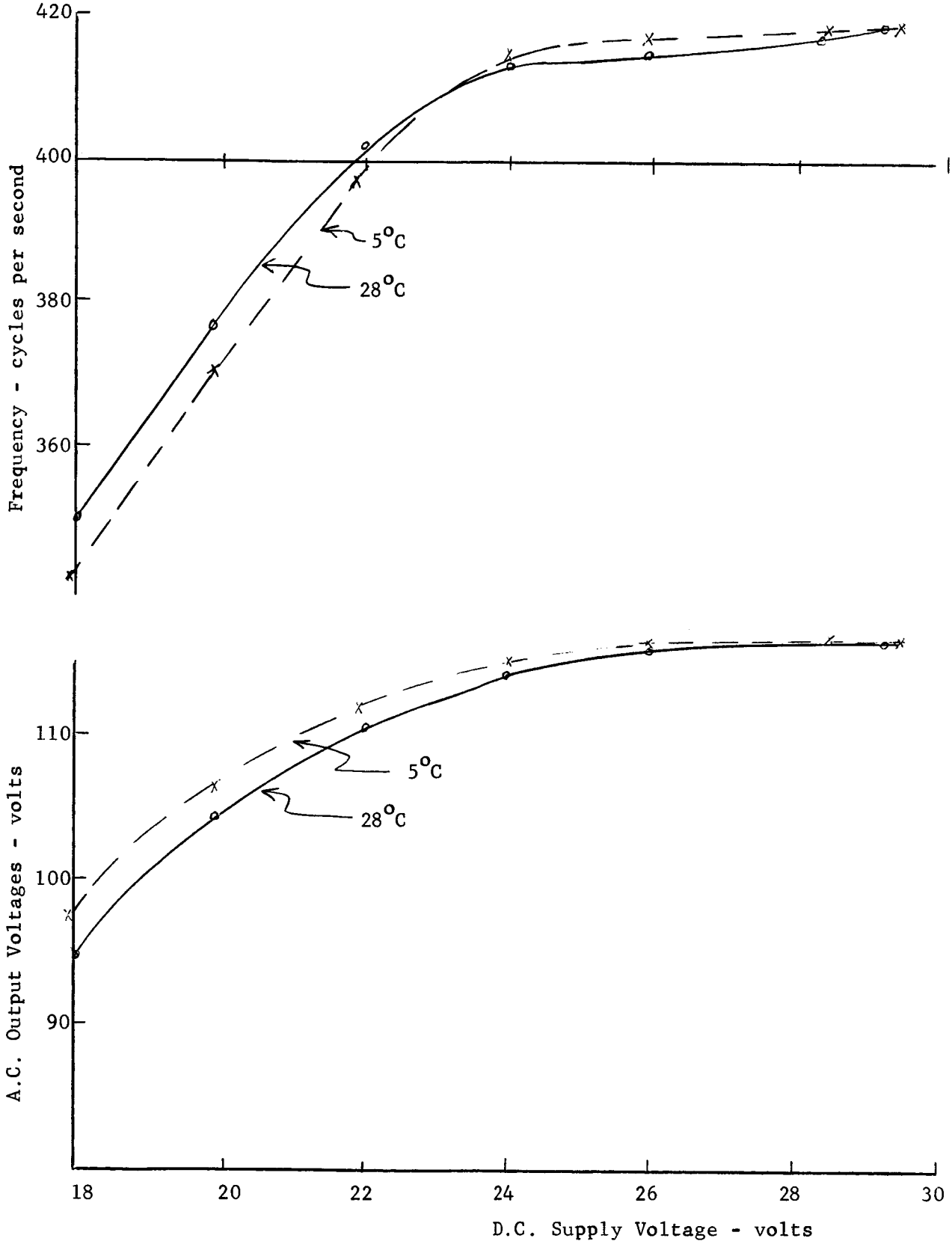

Figure 10 - Inverter Characteristics

4.2 SYSTEM TRANSFER CHARACTERISTIC

From the mathematical representation of the elements of the system, the error model of the complete system is developed. The linear system representation is shown in Figure 11. From this diagram, an expression for the system attribute is obtained in Laplace transform form as:

$$\hat{\gamma}_i = \frac{1}{As^2 + Bs + 1} \left[Bs\left(\frac{A}{B} s + 1\right) \hat{\phi}_a + \hat{\phi}_r + \frac{\hat{N}_a}{K_A K_e} \right]$$

where: $A = \dfrac{\tau_m}{K_e R K_A K_m}$

$$B = \frac{1 + K_A K_m K_T}{K_e R K_A K_m}$$

$$\hat{\phi}_a = \phi_a(s) = \int_o^\infty \phi(t) e^{-st}\, dt$$

and K_A, K_m, K_T, K_e, τ_m, $\hat{\phi}_r$, and $\hat{N}_a$ are functions of the environmental inputs.

If the processes $\phi_r(t)$ and $N_a(t)$ are slowly varying quantities in comparison with $\phi_a(t)$, the above expression may be simplified to obtain:

$$\hat{\gamma}_i \approx \frac{Bs\left(\frac{A}{B} s + 1\right)}{As^2 + Bs + 1} \hat{\phi}_a + \hat{\phi}_r + \frac{\hat{N}_a}{K_A K_e} \quad .$$

The coefficients A and B are random variables that will take on values determined by the random variables E_{DC} and T. From the known values that the terms in the expressions for A and B take on as functions of E_{ac-1} and T, it is possible to obtain an expression for the coefficients A and B as:

$$A \approx [622 - 1.45\, \Delta T - 28.4\, \Delta E_{ac-1} + .87(\Delta E_{ac-1})^2 + .127\, \Delta T\, \Delta E_{ac-1}]\, 10^{-6}$$

$$(s = 41 \times 10^{-6})$$

$$B \approx 341 \times 10^{-4}$$

$$(s = 6 \times 10^{-4}) \quad .$$

As would be expected, the feedback configuration decreases the effect of the

individual part parameter variations. Even though the terms in the expression for the coefficient B vary considerably with supply voltage and temperature, the combination of these terms remains constant, to a high degree of approximation. The feedback configuration also reduces the effect of amplifier null voltage drift, N_a, on system error.

The system error model, together with adequate descriptions of the behavior of the drift and input processes, permits the calculation of the probable time behavior of the system attribute. This calculation will certainly be tedious, if not impossible, by hand. However, if each time dependent process is considered separately, the task is not difficult.

The first step in determining the behavior of the system attribute γ_i will thus be to investigate the magnitude and importance of each time process in the error model, considering each separately. The system attribute will be considered to be made up of these components:

$$\hat{\gamma}_{ia} = \frac{Bs(\frac{A}{B}s + 1)}{As^2 + Bs + 1}\,\hat{\phi}_a \qquad \text{(error due to system time delays)}$$

$$\hat{\gamma}_{ib} = \hat{\phi}_r \qquad \text{(error due to gyro drift)}$$

$$\hat{\gamma}_{ic} = \frac{\hat{N}_a}{K_a K_e} \qquad \text{(error due to amplifier drift) .}$$

The importance of each component is considered in the following sections of this paper.

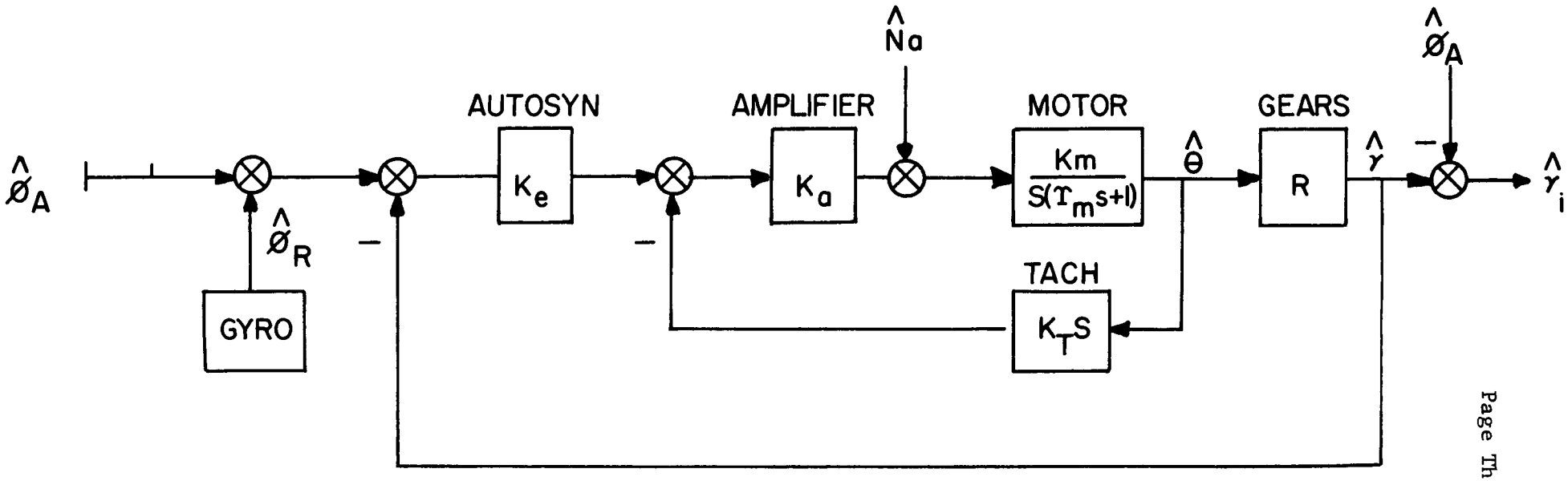

$K_e = .1119 - .000289\,\Delta T + .00093\,\Delta E_{ac-1}$ VOLTS/DEGREE

$K_a = 3409 + 41.7\,\Delta E_{ac-1} - 1.10(\Delta E_{ac-1})^2$ VOLTS/VOLT

$K_m = 437 + 1.81\,\Delta T - .40\,\Delta E_{ac-1}$ DEG. PER SEC./VOLT

$\tau_m = .368 + .00074\,\Delta T - .0000213(\Delta T)^2 - .0053\,\Delta E_{ac-1} - .00018(\Delta E_{ac-1})^2$ SEC.

$K_T = [1178 - 3.38\,\Delta T + 8.9\,\Delta E_{ac-1}]\,10^{-8}$ VOLTS/DEG. PER SEC.

$R = 1/306$

FIGURE 11
SYSTEM REPRESENTATION

4.3 ANALYSIS OF DRIFT PROCESSES

4.3.1 Analysis of Gyro Drift ϕ_r

The gyro drift data is first corrected for changes in autosyn gain. That is, the observed data is $N_G(t) = K_e \phi_r(t)$, and the desired data is $\phi_r(t)$. Knowing the variations in K_e as a function of the environmental inputs permits the correction of the data.

The observed drift recordings indicate that a model of the form:

$$\phi_r(t) = (\bar{A} + \bar{B}t\bar{\alpha}e^{\bar{\beta}t}) \sin(\omega t + \bar{\phi})$$

where: $\bar{A}$, $\bar{B}$, $\bar{\alpha}$, $\bar{\beta}$, and $\bar{\phi}$ are random variables and $\bar{A}$, $\bar{\beta}$, and $\bar{\alpha}$ depend upon supply voltage and temperature.

will be required to describe the data. In considering the gyro drift alone, however, it is not necessary to estimate the coefficients above. The data is taken over the full mission time, hence the probability that the attribute γ_i does not exceed a level $\pm$ c due to gyro drift only can be calculated from the probability density of the maximum amplitude of the drift over the simulated mission interval. Using this approach, with each sample of gyro drift, there is associated a random variable w, the maximum amplitude of the gyro drift over the last 15 minutes of a 30 minute test period. For example:

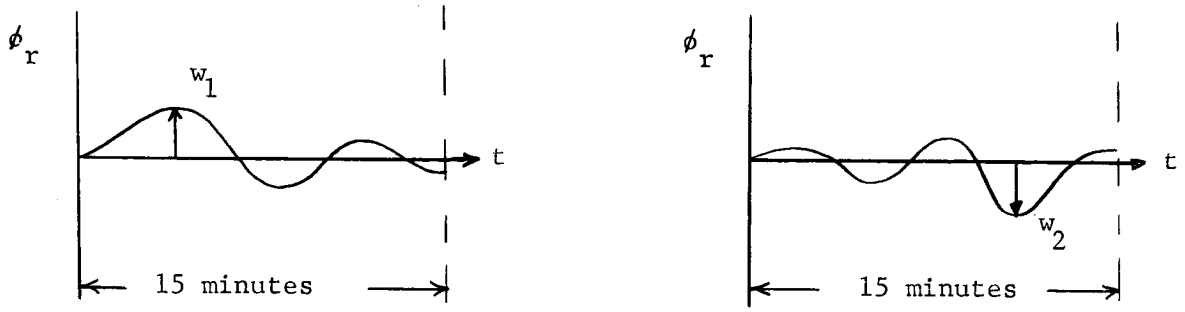

The random variable w obtained from the twenty drift samples at room temperature and nominal supply voltage is found to have a log-normal probability distribution. The twenty amplitudes are plotted on log-normal paper in figure (12). The assumption is made that the underlying distribution at conditions other than nominal is log-normal also. With this assumption, a conditional probability density function is found for each set of input conditions. The mean value of these conditional density functions is subjected to the multiple regression

analysis described previously to obtain:

$$\text{mean } (\ln w) = .453 - .05094\,\Delta T + .0104\,\Delta E_{ac-1}$$

$$+ .0006188(\Delta T)^2 + .00153(\Delta E_{ac-1})^2$$

$$\text{S.D. } (\ln w) = .409$$

The probability that the system attribute γ_i will not exceed a level $\pm$ c due to gyro drift during a 15 minute interval is then calculated from:

$$R_{T4}(c;15/E_{ac-1},T) = \int_0^{+c} f(w,\ 15/E_{ac-1},T)^{*}\,dw \quad .$$

This calculation for $|c| = 1^{o}, 2^{o}, 3^{o}$, and 5^{o} is shown in table 1, for 5 levels each of E_{ac-1} and T. (page 37)

4.3.2 Amplifier Null Voltage Drift

The amplifier null voltage amplitude is described by a time changing normal density function:

$$\text{mean } |N_a| = \frac{1.86 + .0122\,\Delta T - .0425\,\Delta E_{ac-1}}{1 + .218e^{-.247t}} \quad \text{volts}$$

$$\text{S.D.} = .29 \text{ volts} .$$

The effect of this drift process on the system attribute will be analyzed with the other drift processes considered zero.

To convert the voltage N_a to degrees variation of the system attribute, we have:

$$\gamma_{ic}(t) = \frac{N_a(t)}{K_A K_e} \quad .$$

The term $K_A K_e$ is a random variable whose value is determined by the value of the supply voltage and ambient temperature.

The importance of this process can be determined by considering the effect of null voltage drift in a "worse case" sense. The term $K_A K_e$ is a function of truncated random variables, and from information obtained previously, the

$$^{*}\ f(w,15/E_{ac-1},T) = \frac{1}{.409\sqrt{2\pi}}\ \text{Exp} - \left[\frac{\ln w - \text{mean } (\ln w)}{2(.409)^2}\right]$$

Temperature (^{o}C)

a.c. Supply Voltage E_{ac-1} (Volts)	T = 0	20	40	60	80
100	.0001	.0180	.5400	.8800	.8400
106	.0001	.0300	.6400	.9200	.8900
112	.0001	.0300	.6400	.9200	.8900
118	.0001	.0160	.5200	.8550	.8200
124	.0001	.0026	.3000	.7000	.6400

$c = \pm 1^{o}$

Temperature

E_{ac-1}	0	20	40	60	80
100	.0001	.3300	.9640	.9980	.9965
106	.0001	.4300	.9800	.9990	.9984
112	.0001	.4300	.9800	.9990	.9984
118	.0001	.3200	.9600	.9970	.9960
124	.0001	.1400	.8850	.9870	.9800

$c = \pm 2^{o}$

Temperature

E_{ac-1}	0	20	40	60	80
100	.0014	.7000	.9975	.9999	.9999
106	.0035	.7900	.9990	.9999	.9999
112	.0035	.7900	.9990	.9999	.9999
118	.0012	.6900	.9970	.9999	.9999
124	.0002	.4700	.9870	.9994	.9990

$c = \pm 3^{o}$

Temperature

E_{ac-1}	0	20	40	60	80
100	.0450	.9600	.9999	.9999	.9999
106	.0750	.9805	.9999	.9999	.9999
112	.0750	.9805	.9999	.9999	.9999
118	.0400	.9550	.9999	.9999	.9999
124	.0100	.8800	.9997	.9999	.9999

$c = \pm 5^{o}$

TABLE 1

Probability of output arm angle γ_i exceeding a level $\pm c$ due to gyro drift only.

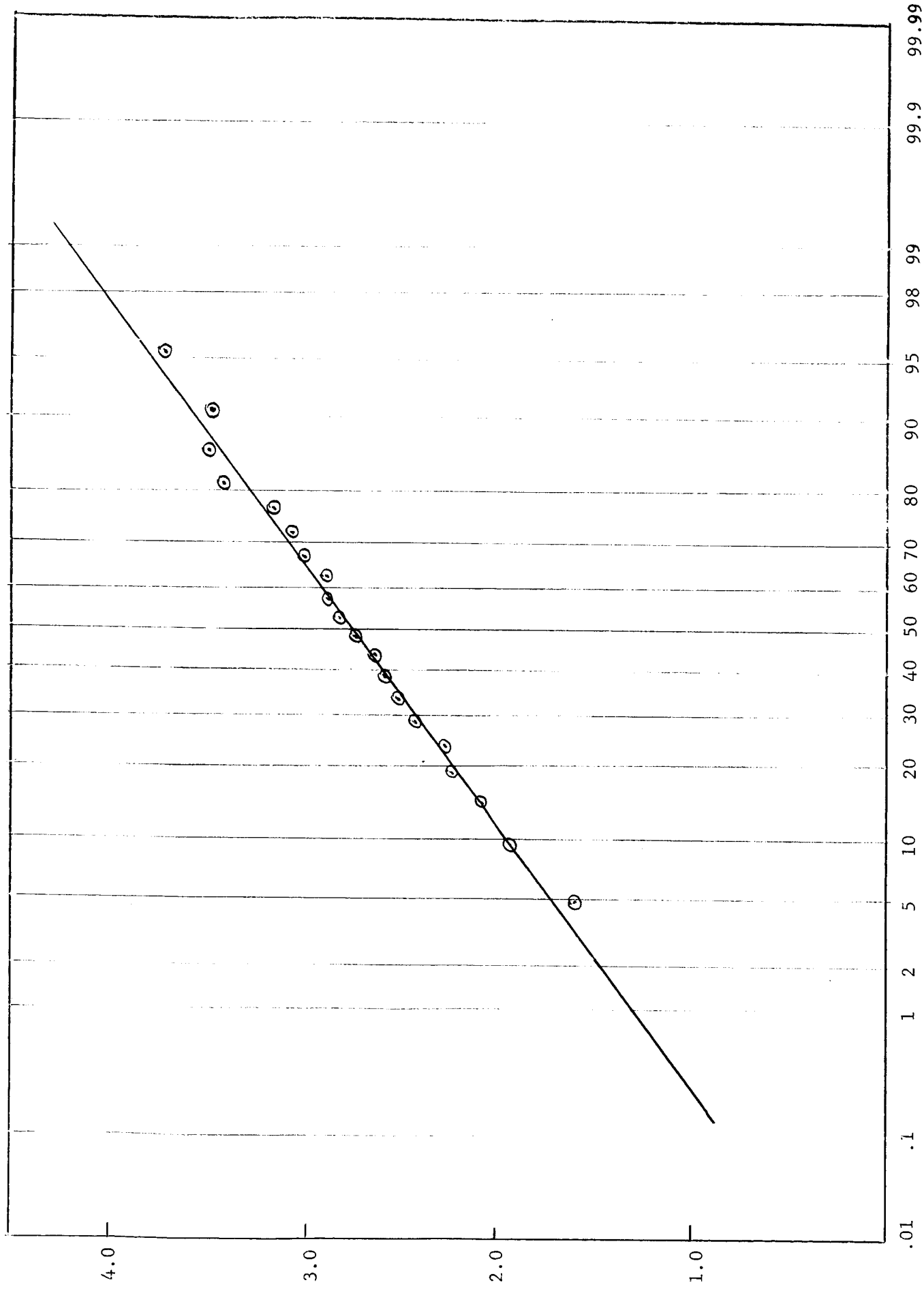

Figure 12 - Plot of ln w (maximum amplitude of gyro drift in mm) at nominal conditions - 20 samples

smallest value that the term can take on may be found. This value is found from the equations:

$$K_A = 3409 + 41.7\ \Delta E_{ac-1} - 1.10\ (\Delta E_{ac-1})^2$$

$$K_e = .1119 - .000289\ \Delta T + .00093\ \Delta E_{ac-1}$$

$$E_{ac-1} = 7.70\ E_{D.C.} - .125\ (E_{D.C.})^2$$

$$\Delta E_{ac-1} = (E_{ac-1} - 112)$$

$$\Delta T = (T - 26)$$

$$20 < E_{D.C.} < 30\ ;\ 0 < T < 90 \quad .$$

Going through the calculations, we find that the minimum value of $K_A K_e$ will occur at a temperature of $90^{\circ}C$ and a d.c. supply voltage of 20 volts. At these conditions:

$$K_e K_A \big|_{min.} = 258 \qquad \text{volts/degree.}$$

The mean value of $|N_a|$ will be maximum under the same conditions, and with $t \longrightarrow \infty$.

$$\text{mean } |N_a| \text{ max.} = 2.98 \quad \text{volts.}$$

Hence, the error in the system attribute for the worse conditions of temperature and supply voltage is described by the normal density function with:

$$\text{mean } |\gamma_{ic}| = \frac{2.98}{258} = .01155 \quad \text{degrees}$$

$$\text{S.D.} = \frac{.29}{258} = .00112 \text{ degrees.}$$

From this density function, we see that with a probability of .9999, the error in γ_i due to amplifier null voltage considered alone will be:

$$|\gamma_{ic}| < .0156 \quad \text{degrees} .$$

This source of drift can therefore be considered negligible in comparison to the gyro drift.

4.3.3 Error due to the System Time Delays

The third component contributing to the variations in the system attribute is the component that arises because of time lags in the system. With gyro drift and null voltage drift zero, the expression for this error is:

$$\hat{\gamma}_{ia} = \frac{Bs(\frac{\overline{A}}{B}s + 1)}{\overline{A}s^2 + Bs + 1} \quad \hat{\phi}_a \quad .$$

Where $\phi_a(t)$ is a stationary Gaussian process with zero mean, and known spectral density.

To investigate the importance of this component of system error, the spectral density of the random process $\gamma_{ia}(t)$ can be found for particular values of the random variable $\overline{A}$, and this, in conjunction with the methods outlined in reference [3], will be useful in making probability statements about the behavior of $\gamma_{ia}(t)$.

The spectral density of $\gamma_{ia}(t)$ is given by:

$$\Phi_\gamma(\omega) \Big|_{A_{ij}} = \left| \frac{Bs(\frac{A_{ij}}{B}s + 1)}{A_{ij}s^2 + Bs + 1} \right|^2 \Phi_\phi(\omega) \quad .$$

Where: A_{ij} is a value of $\overline{A}$ corresponding to values of supply voltage E_i and temperature T_j.

The spectral density of the input process $\phi_a(t)$ is obtained from the transfer function from white noise to ϕ_a, as derived in appendix B. The expression for this spectral density is:

$$\Phi_\phi(\omega) = \left| \frac{K_1 j\omega(1 + j\frac{\omega}{52.7})}{(1 + j\frac{\omega}{30.3})(1 + j\frac{\omega}{.488})(1 - \frac{\omega^2}{(4.93)^2} + j\omega\frac{2(.84)}{4.93})(1 + j\frac{\omega}{.5})} \right|^2$$

A plot of this function is shown in Figure 13, using a log scale, and in Figure 14, using a linear scale. The constant K_1 is determined from the assumed mean square (ms) value of the wind gust vertical velocity $W_G/V(t)$, as follows:

$$K_1 = .391\sqrt{\frac{4(ms)}{\pi}} \quad \text{radians}$$

and for $ms(\frac{W_G}{V}) = 46 \times 10^{-4}$, we obtain $K_1 = .0283$ rad.

With this value of K_1 and using graphical integration, the calculated RMS

value of the process $\phi_a(t)$ is found to be:

$$\phi_a\big|_{RMS} = .482 \quad \text{degrees}$$

The process $\phi_a(t)$ achieved in the simulation has a measured rms value of approximately:

$$\phi_a\big|_{\text{measured RMS}} \approx .425 \text{ degrees} .$$

This measurement was obtained from a one minute sample of the process. A histogram of the amplitude distribution of this sample is shown in Figure 15.

To obtain the spectral density of the system attribute due to this process considered alone, particular values of the random variable $\bar{A}$ must be selected. A table of values of A is shown below, where these are calculated from the expression for A given on Page 32:

ΔE_{ac-1}

ΔT	-12	0	+12
-26	1165	660	405
0	1088	622	406
+64	898	529	411

$\times 10^{-6}$

The maximum and minimum values of $\bar{A}$ are selected from this table, and corresponding to these values, the output spectral density is given by:

$$\Phi_\gamma(\omega)\Big|_{405 \times 10^{-6}} = \left| \frac{.0341s(\frac{s}{84.3} + 1)}{[(\frac{s}{49.7}) + \frac{s}{29.4} + 1]^2} \right|^2 \Phi_\phi(\omega)$$

$$\Phi_\gamma(\omega)\Big|_{1165 \times 10^{-6}} = \left| \frac{.0341s\ (\frac{s}{54.2} + 1)}{[(\frac{s}{29.1})^2 + \frac{s}{29.4} + 1]} \right|^2 \Phi_\phi(\omega)$$

These spectral densities are plotted in Figure 16. From this figure, it is evident that the random variable $\bar{A}$ has very little effect on the output spectral density. On the linear scaled plot, figure 17, the effect of $\bar{A}$ on $\Phi_\gamma(\omega)$ is not noticeable.

From the spectral density of process $\gamma_{ia}(t)$, a lower bound on the probability of no crossing of a given level $\pm$ c can be determined using the techniques outlined in reference [3].

$$\Pr(|\gamma_{ia}| < c \text{ in } T_{4/E_i T_j}) \geq 1 - E\,[N_{ij}(T_4)] \ .$$

Where here $E[N(T_4)]$ is the expected number of crossings of a level $\pm$ c by $\gamma_{ia}(t)$ during time period T_4, and is computed from:

$$E[N(T_4)] = \frac{2T_4}{\pi} \left(\frac{\lambda_2}{\lambda_o}\right)^{1/2} e^{-c^2/2\lambda_o}$$

$$\lambda_2 = \int_o^\infty \omega^2 \, \Phi_\gamma(\omega) \, d\omega$$

$$\lambda_o = \int_o^\infty \Phi_\gamma(\omega) \, d\omega \quad .$$

The integrand of the first integral is plotted in figure 17A , and by graphical integrations, there is obtained:

$$\lambda_o = 6.23 \times 10^{-4} \text{ degrees}^2$$

$$\lambda_2 = 131 \times 10^{-4} \text{ degrees}^2 \text{ rad}^2 \text{ sec}^{-2}$$

$$E[N(15 \text{ minutes})] = 2630 \exp \frac{-c^2}{12.46 \times 10^{-4}}$$

c in degrees.

A plot of the lower bound on the probability of no crossing of a level c by the process $\gamma_{ia}(t)$ for the fifteen minute mission time is shown in figure (18). The graph shows that almost certainly, a limit of $\pm$ .13 degrees will not be exceeded.

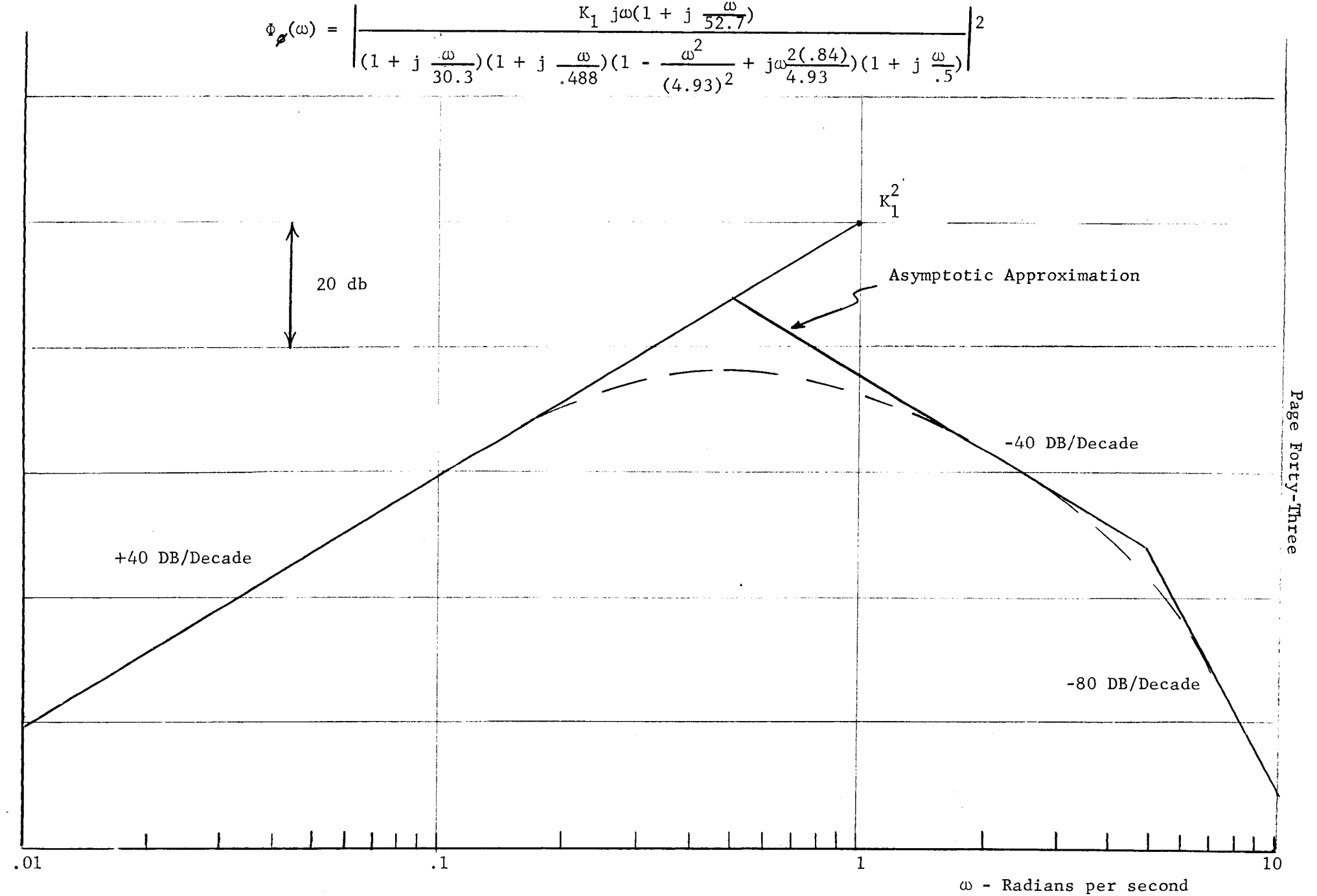

Figure 13 - Spectral density of input angle process $\phi_a(t)$ - log scale

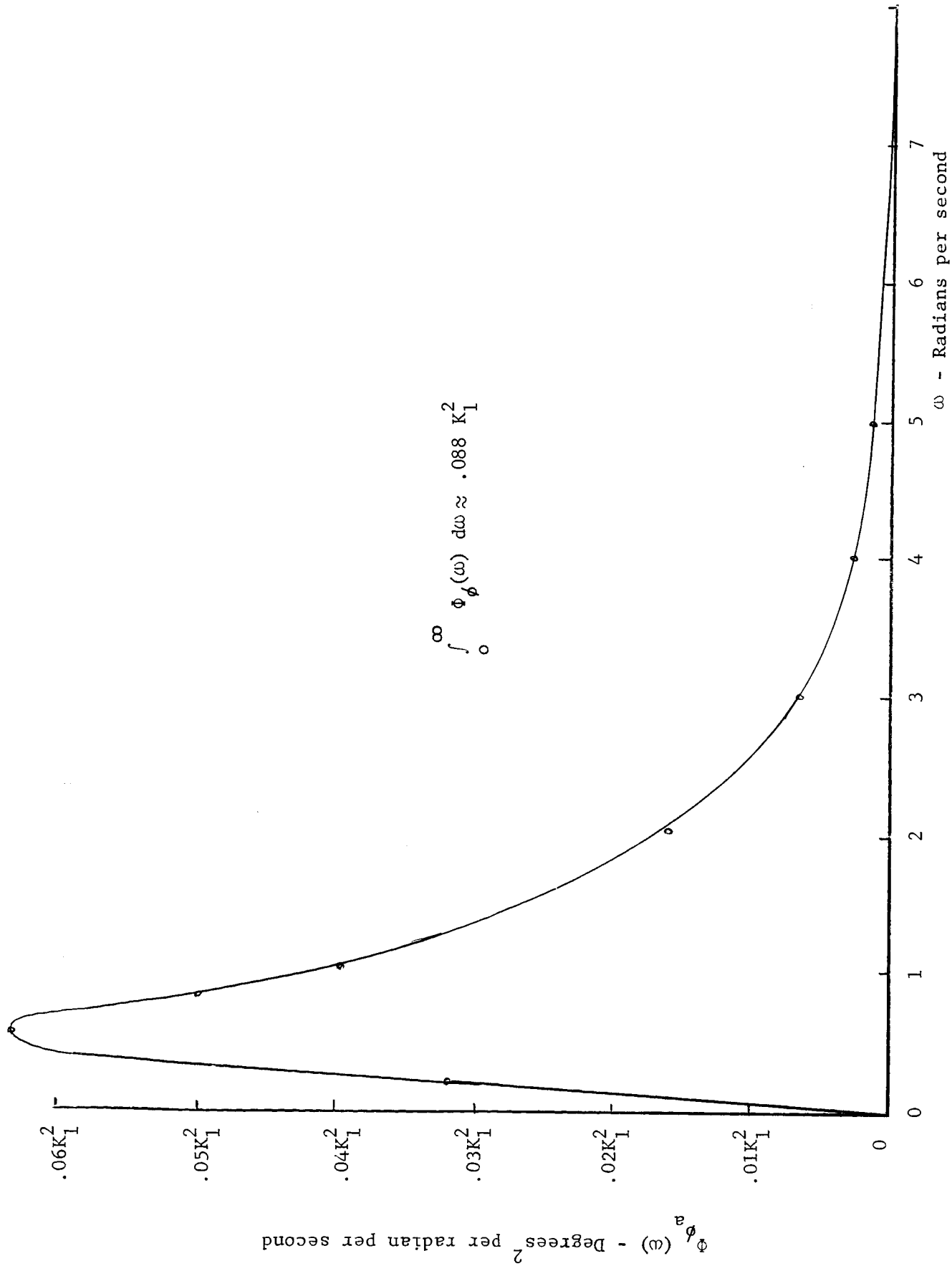

Figure 14 - Spectral density of pitch angle input process $\phi_a(t)$

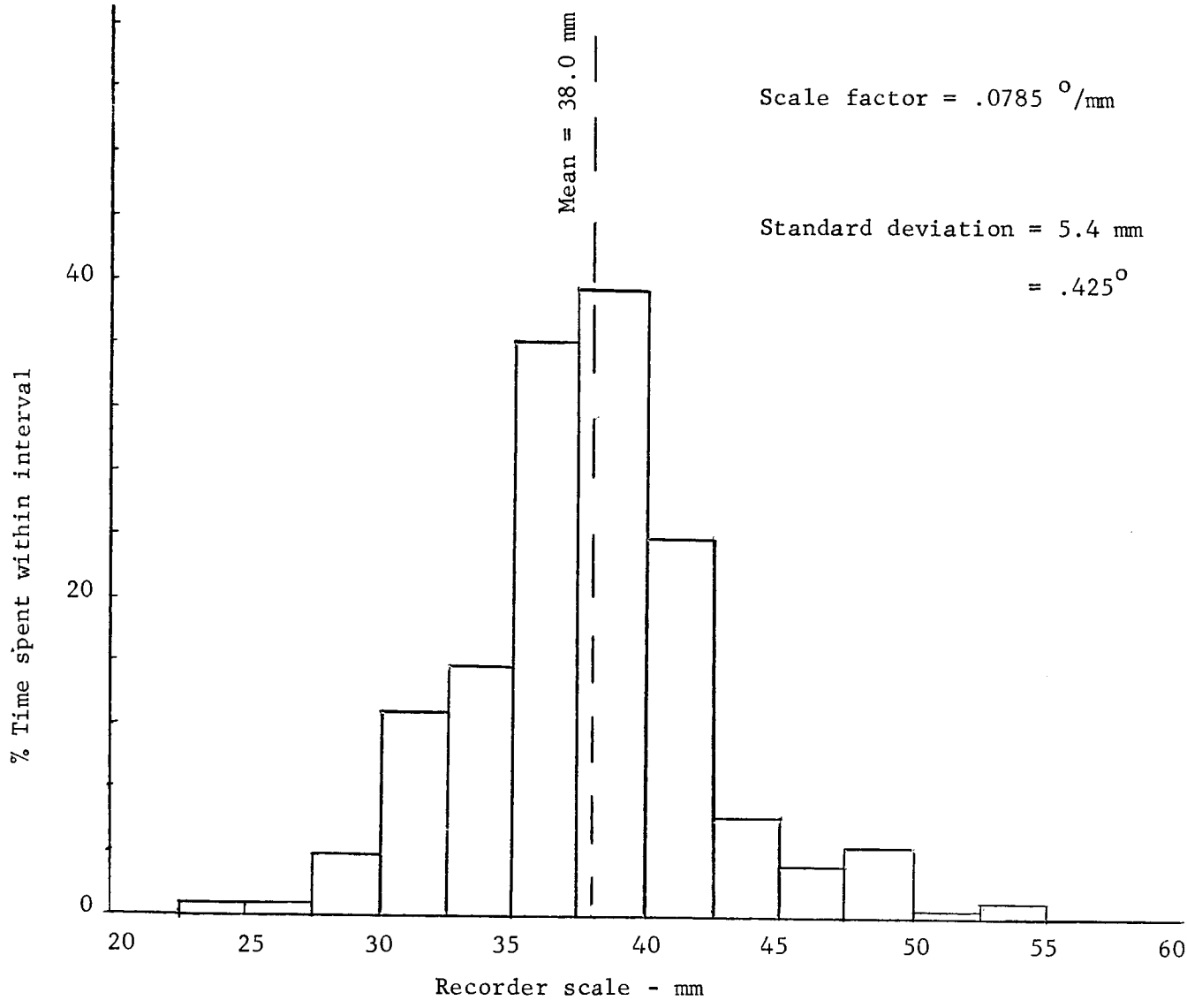

Figure 15 - Histogram of amplitude distribution of pitch angle input process - 1 minute sample

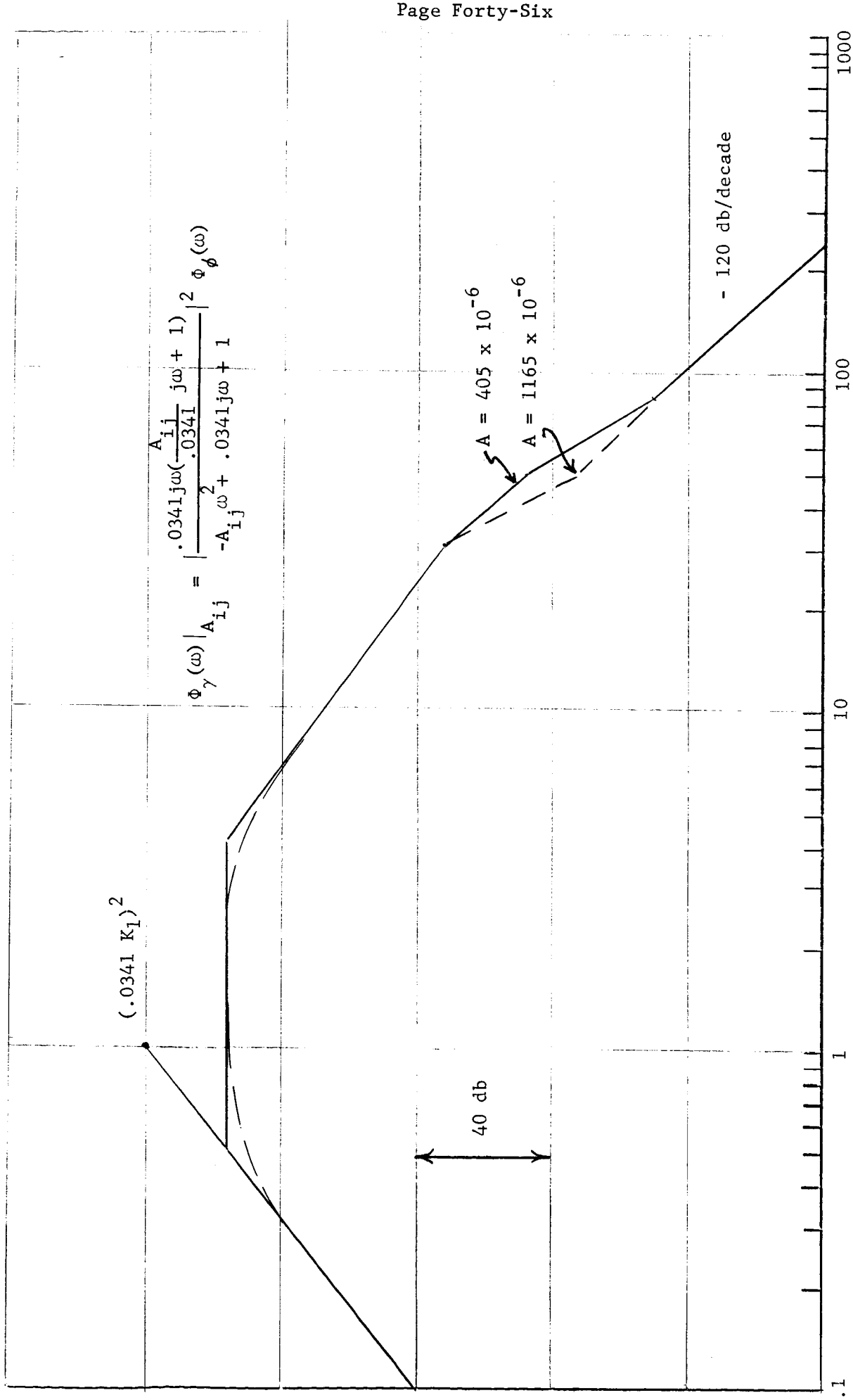

Figure 16 - Spectral density of output arm angular error $\gamma_{ia}(t)$ - log scale

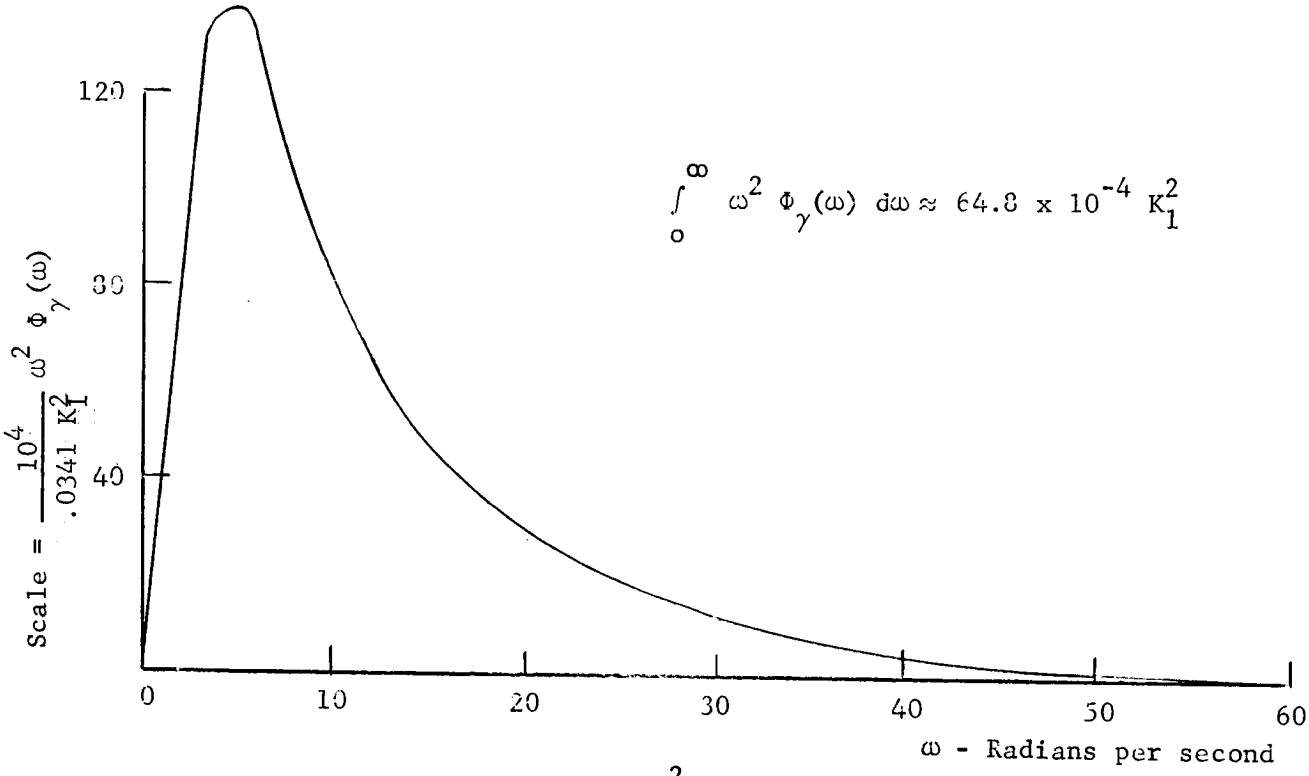

Figure 17A - Plot of $\omega^2\ \Phi_\gamma(\omega)$

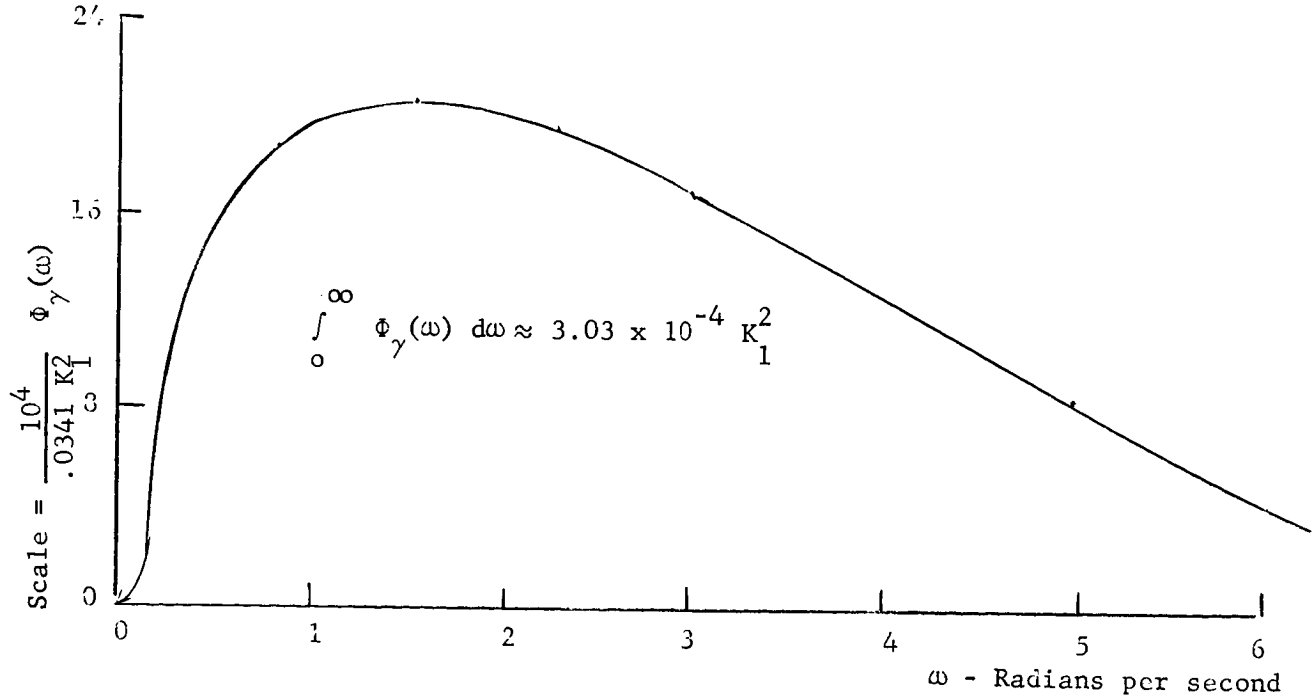

Figure 17 - Spectral Density of Output Arm Angular Error

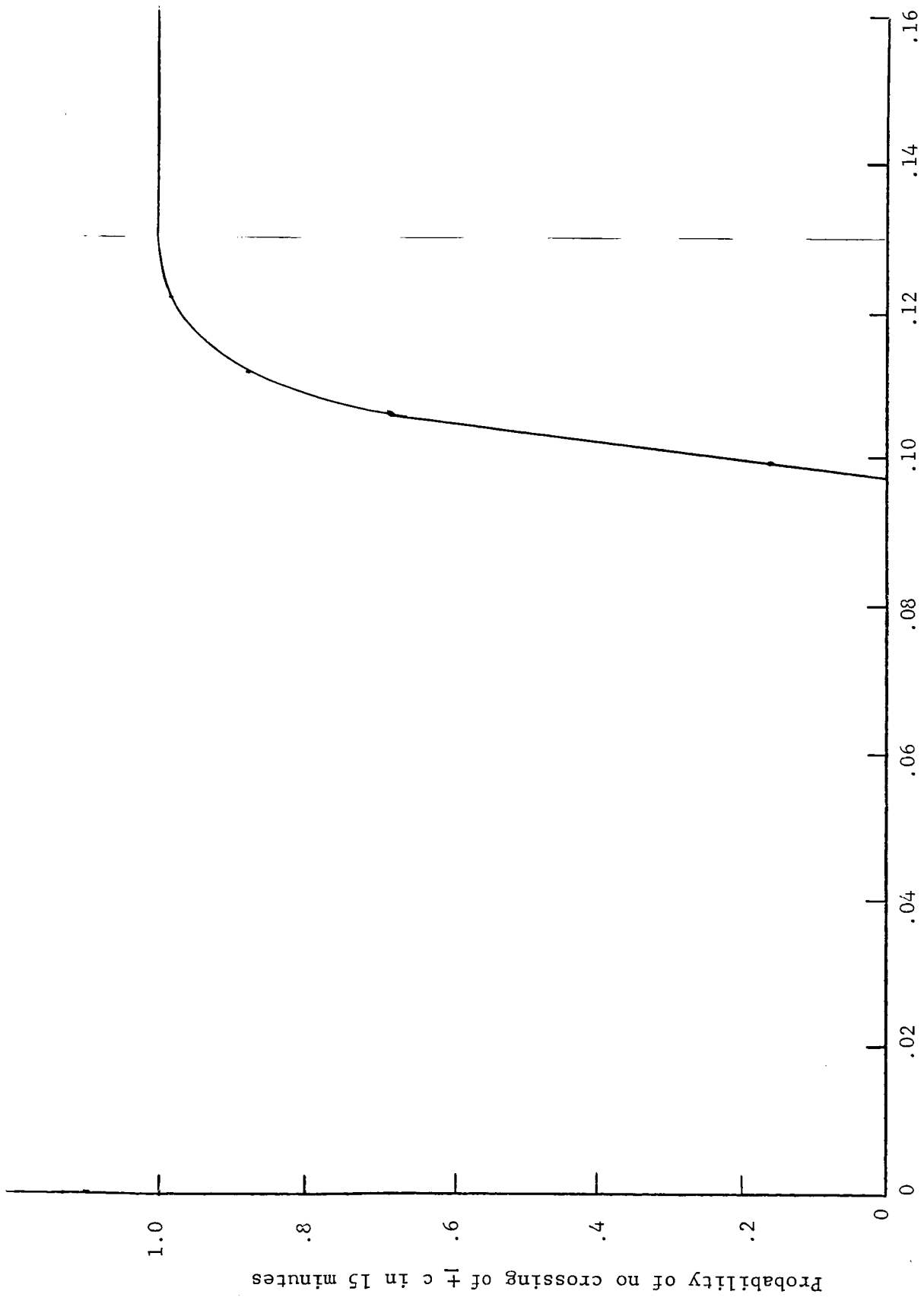

Figure 18 - Lower bound on the probability of no crossing of a level ± c by the process $\gamma_{ia}(t)$ during 15 minutes

5.0 ESTIMATION OF THE PROBABILITY OF A CATASTROPHIC FAILURE

To complete the system mathematical model, an estimate of the probability of a sudden system malfunction that is certain to cause the system output arm to exceed the specified level is required. In this study, no life tests on the elements or components were conducted, and it was decided to estimate this probability using conventional "failure rate" data on piece parts. In making use of this data, several important assumptions are required, as listed below:

1. The published "failure rate" data is applicable to the parts in the T.S.A. system.
2. The probability of a component attribute radically changing value is the same during any given time interval ΔT, under fixed environmental conditions.
3. The published "failure rate" data includes only failures such as opens, shorts, or sudden radical departures from nominal characteristics.

One difficulty in using the published data on piece parts is that the mode of failure of a given part is not determined, and within an element, the mode of failure determines the effect of the failure on the element attribute. Depending on the mode of failure and the functional relationships of the part within the element, a piece part failure may cause certain element failure, may induce element failure by overstressing other parts, may increase the probability of failure, or may have a slight or no effect on the element. To investigate the effects of individual part failures, experiments were conducted on the amplifier of the T.S.A., whereby, piece parts failures (shorts and opens) were simulated one by one, and the effects of these failures on the selected amplifier attribute, amplifier gain, were measured. The results of this experiment are tabulated in table 2, page 50. It is surprising that even in this simple circuit, certain modes of failure of piece parts would not cause certain failure of the system, as defined previously. If information were available on the probable modes of failure of the parts, the reliability calculation could be refined by weighting certain part failure probabilities with the probability of system failure given the part failure.

Using published data, such as that found in Military Handbook 217, and assuming that the part failure rates are truly representative of the particular parts in the T.S.A. system, a pessimistic estimation of the

Part	Mode of failure	Effect on amp. gain	Comments
R 657	short	K_a = .98 x nominal	may overstress tube
	open	K_a = 0	
R 652	short	K_a = 1.2 x nominal	
	open	K_a = 0	
R 651	short	K_a = 1.24 x nominal	unbalances output
	open	K_a = 0	
R 656	short	K_a = .78 x nominal	overstresses tube
	open	K_a = 0	
C 655	short	K_a = 0	
	open	K_a = .17 x nominal	
C 657	short	K_a = 0	
	open	K_a = .90 x nominal	
C 654	short	K_a = 0	
	open	K_a = 1.3 x nominal	unbalanced output
C 651 & C 652	short	K_a = 0	
	open	K_{a+} = 1.8 nominal K_{a-} = .7 nominal	unbalanced output
T 652	short	K_a = 0	
	open 1 winding of 3	K_a = nominal	inherent redundancy

Other parts either open or short cause $K_a = 0$.

NOTE: The function of these parts may be seen by referring to the amplifier circuit diagram, figure C1, page 89.

Table 2

Effect of Shorts and Opens of Piece Parts on Amplifier Gain Attribute (K_A)

probability of successful operation will be obtained by assuming piece part failure causes certain system failure. For a system with a small number of parts, the actual numerical error should not be great, however.

Making this assumption for the T.S.A. system, the failure rate of each element in the system is estimated using the techniques outlined in Military Handbook 217, and as described in detail in appendix C. The failure rates are calculated for three values of ambient temperature and three values of supply voltage to each element, to obtain tables as follows:

1. Amplifier, gyro, motor-tachometer, combined catastrophic failure rates in % per 1000 hours.

		Temp		
		0	26	90
E_{ac-1}	100	9.32	9.33	9.69
	112	10.88	10.89	11.46
	124	15.52	15.53	16.36

2. Inverter - catastrophic failure rates in % per 1000 hours.

		Temp		
		0	26	90
$E_{D.C.}$	20	13.88	14.29	15.12
	24	16.49	16.52	19.19
	28	16.79	16.83	19.49

A regression surface is then found for these tables, using the Taylor's series expansion, to obtain the expressions.

$$h_{amp,motor,gyro} \approx [10827 + 1.35\,\Delta T + .048\Delta T + 259.3\Delta E_{ac-1} + 10.70\,(\Delta E_{ac-1})^2 + .067\,(\Delta T)\,(\Delta E_{ac-1})]\;10^{-3}$$

$$(s = .012)$$

$$h_{inverter} \approx 18.11 + .0275\Delta T + .409\Delta E_{D.C.} - .08334(\Delta E_{D.C.})^2$$

$$(s = .593)\ .$$

Knowing these expressions and the relationship between E_{ac-1} and $E_{D.C.}$, permits the interpolation to five levels with d.c. supply voltage as the independent variable, and once the failure rates are on the same basis, to add them to obtain the table below:

		Temp				
		$0^{o}C$	$20^{o}C$	$40^{o}C$	$60^{o}C$	$80^{o}C$
$E_{D.C.}$	20	24.0	24.6	25.2	25.9	26.7
	22	26.8	26.9	28.2	28.8	29.6
	24	28.9	29.5	30.4	31.0	31.7
	26	30.0	30.6	31.5	32.1	32.9
	28	30.1	30.6	31.5	32.1	32.9

This table gives the estimated conditional catastrophic hazard rates in percent per 1000 hours for the complete system.

6.0. CALCULATION OF THE RELIABILITY OF THE T.S.A.

The study of the importance of the several drift processes in the T.S.A. system indicates that the gyro drift is the critical drift process in the system, as would be expected. The drift part of the system reliability will thus be calculated using only the gyro drift in the calculation, and considering the other drift processes as negligible by comparison in this particular system. This is not to imply that the other sources of error need not be considered in the design, but only that this particular design has been successful in minimizing the effect of the other drift processes in comparison with the gyro drift.

The estimate of the probability of the crossing of several levels c by the system attribute is tabulated in Table 1, and in Section 5.0 an estimate of the conditional catastrophic hazard rates was obtained. The only additional information needed for a numerical calculation is the joint probability density of the input random variables $\overline{E}$ and $\overline{T}$. Since these random variables are assumed independent, the probability density of each may be estimated separately. In practice, the estimate of the probability density of the temperature would be obtained from meteorological data, and an estimate of the probability density of the d.c. supply voltage would be furnished by the designer of the d.c. power supply, or would be obtained from tests similar to those conducted on the components of the T.S.A. system. Conversely, the specifications that must be placed on the d.c. supply to achieve a given level of reliability (within limits) for the T.S.A. can be determined. For purposes of this study, a numerical calculation is made using several different normal density functions for the input random variables.

Before proceeding to the calculation, the mission time intervals preceding the stabilization mode must be considered. In these intervals, the conditional catastrophic hazard rates are somewhat different. During interval T_1, the gyro is caged, there is no signal input to the amplifier, and the torque motor is not in use. During interval T_2, a switching operation takes place when a switch and relay close, and the caging motor runs through its sequence of operations. The hazard associated with this type of operation is usually found as "% failures per 1000 operations" and is not dependent upon time. An estimate of the various catastrophic hazard functions

from data in Appendix C is shown below for comparison, for supply voltage and temperature at nominal conditions:

$$h_1 = 24.359 \times 10^{-5}$$

$$h_2(t) = [24.359 + 1.02\ \delta(t-t_2)]\ 10^{-5}$$

$$h_3 = 30.400 \times 10^{-5}$$

$$h_4 = 30.400 \times 10^{-5}$$

where: $\delta(t-t_2) = 0 \quad \text{for } t \neq t_2$

$$\int_a^b \delta(t-t_2)\, dt = 1 \qquad a < t_2 < b$$

The probabilities associated with these catastrophic hazard rates for a one hour period are large ($\approx .9997$), hence little error is introduced by considering the catastrophic hazard rates to be the same during each time interval. Also, the density functions of the input random variables are assumed to be the same during each time interval. These steps are taken only to simplify the routine calculations. The numerical calculations are therefore made using:

$$R_{TSA}(1 \text{ hr}, 2 \text{ degrees}) = \sum_i^n \sum_j^m \left[e^{-(h_T/E_i T_j)(1 \text{ hour})}\right]$$

$$\cdot [\Pr(\gamma_i < 2^o; (15 \text{ min})/E_i T_j)]$$

$$\cdot [\Pr(E_{i-1/2} < E < E_{i+1/2})$$

$$\Pr(T_{j-1/2} < T < T_{j+1/2}]$$

Where the conditional catastrophic hazard rates are given on page 52 and the probabilities of no crossing of a $\pm\ 2^o$ level are listed on page 37, Table 1. The probabilities of no crossing of a 2^o level are first obtained in terms of the d.c. supply voltage instead of the a.c. supply voltage, as shown below:

$[R_D(2^o; 15 \text{ min})]$ d.c. supply voltage E_{DC}	Temperature T: 0^oC	20^oC	40^oC	60^oC	80^oC
20	.0001	.4300	.9800	.9990	.9984
22	.0001	.4300	.9800	.9990	.9984
24	.0001	.3900	.9730	.9983	.9976
26	.0001	.3500	.9660	.9975	.9968
28	.0001	.3200	.9600	.9970	.9960

For the input distributions, the following truncated normal distributions are used:

1. Temperature (Deg. C)	(-10)-10^o	10-30^o	30-50^o	50-70^o	70-90^o
$N(50^o, 32^o)$	.0798	.1765	.2835	.2835	.1765
$N(50^o, 20^o)$	.0219	.1393	.3497	.3497	.1393
$N(50^o, 0)$	0	0	.5000	.5000	0

2. Supply voltage (volts)	19-21v	21-23v	23-25v	25-27v	27-29v
N(24, 2.5)	.0968	.2404	.3256	.2404	.0968
N(24, 1.75)	.0347	.2389	.4528	.2389	.0347
N(24, 0)	0	0	1.000	0	0

where: $N(\mu, \sigma)$ is a normal distribution with mean μ and standard deviation σ.

For these input distributions, and using the conditional catastrophic failure rates as given in the preceding section, the calculation for R_{TSA}(1 hr, 2 degrees) yields:

Voltage Distribution \ Temperature Distribution	N(50,32)	N(50,20)	N(50,0)
N(24, 2.5)	.7986	.8715	.9850
N(24, 1.75)	.8078	.8820	.9852
N(24, 0)	.8043	.8826	.9854

R_{TSA}(1 hr, 2 degrees)

The above probabilities represent the estimated probability that the system output arm will remain within a limit of $\pm 2^o$ during the assumed mission,

given that the system is operating properly at t = 0, and that the inputs are within the range throughout which the element tests were conducted, or:

$$20 \leq E_{DC} \leq 30 \text{ volts}$$

$$0 \leq T \leq 90^{o}C$$

To remove the condition on the inputs being within these ranges, the system reliability is multiplied by the probability that the inputs are within the above ranges. This will yield an estimate of probability of successful operation of the system given only that it is operating at t = 0. This calculation gives, for the various assumed input distributions:

Supply Voltage Distribution	Temperature Distribution N(50,32)	N(50,20)	N(50,0)
N(24, 2.5)	.6751	.8120	.9403
N(24, 1.75)	.7134	.8585	.9826
N(24, 0)	.7122	.8614	.9854

R_{TSA} (1 hr, 2^{o}) Pr($20 < E < 30$, $0 < T < 90$)

The overall probability of remaining within the $\pm 2^{o}$ limits is strongly dependent upon the variance of the input random variables.

The contribution of the catastrophic failure probabilities to the overall calculation above is very small, and if the catastrophic failure probability were assumed zero, the figures in the table above would change only in the 3rd or 4th decimal place. For limits of $\pm 5^{o}$ or larger on the output error, the probability of a catastrophic failure becomes relatively more important.

7.0. OTHER USES OF THE PROBABILISTIC MODEL

7.1. Evaluation of a Tradeoff

To briefly demonstrate the type of design tradeoffs where the system model will prove useful as an aid to the designer's intuition, consider the problem of evaluating the effect of omitting the voltage regulator circuitry in the rotary inverter of the TSA. The regulator consists of several parts, and the catastrophic failure of any of these may cause complete power loss to the system. It would be advantageous to eliminate these parts, and thus decrease the chance of a catastrophic failure in the inverter if the system will not otherwise be affected adversely.

To evaluate this proposal, the probability of successful operation of the TSA will be calculated using the (hypothetical) inverter less the regulator, and this can be compared to the results of the previous calculation. The characteristics assumed for the inverter less regulator (inverter "B") are shown in figure 19. The nominal output voltage is the same, but the variation in output voltage with changing input voltage is greater than that of the original inverter.

The probability of an inverter catastrophic failure is reduced by the elimination of parts, and from the data in appendix C, the new inverter conditional catastrophic failure rates are calculated, and are shown below with the original for comparison:

		Inverter A (original) Temperature				Inverter B (less reg.) Temperature		
		0	26°	90°		0	26°	90°
D.C.	20	13.876	14.293	15.117	20	10.769	11.172	12.798
Supply	24	16.488	16.524	19.185	24	13.369	13.389	15.998
Voltage	28	16.790	16.826	19.591	28	13.670	13.689	16.298

Knowing the relationship between the d.c. supply voltage and the a.c. supply voltage for inverter B, and the conditional catastrophic and drift probabilities for the remainder of the system as a function of the a.c. voltage, permits the calculation of the new five level tables, as shown on the following page. The original tables of conditional drift and catastrophic probabilities are also listed for comparison. Note that the estimated system catastrophic failure rate has been decreased for the majority of input conditions but is increased at high d.c. voltage inputs. This reflects the

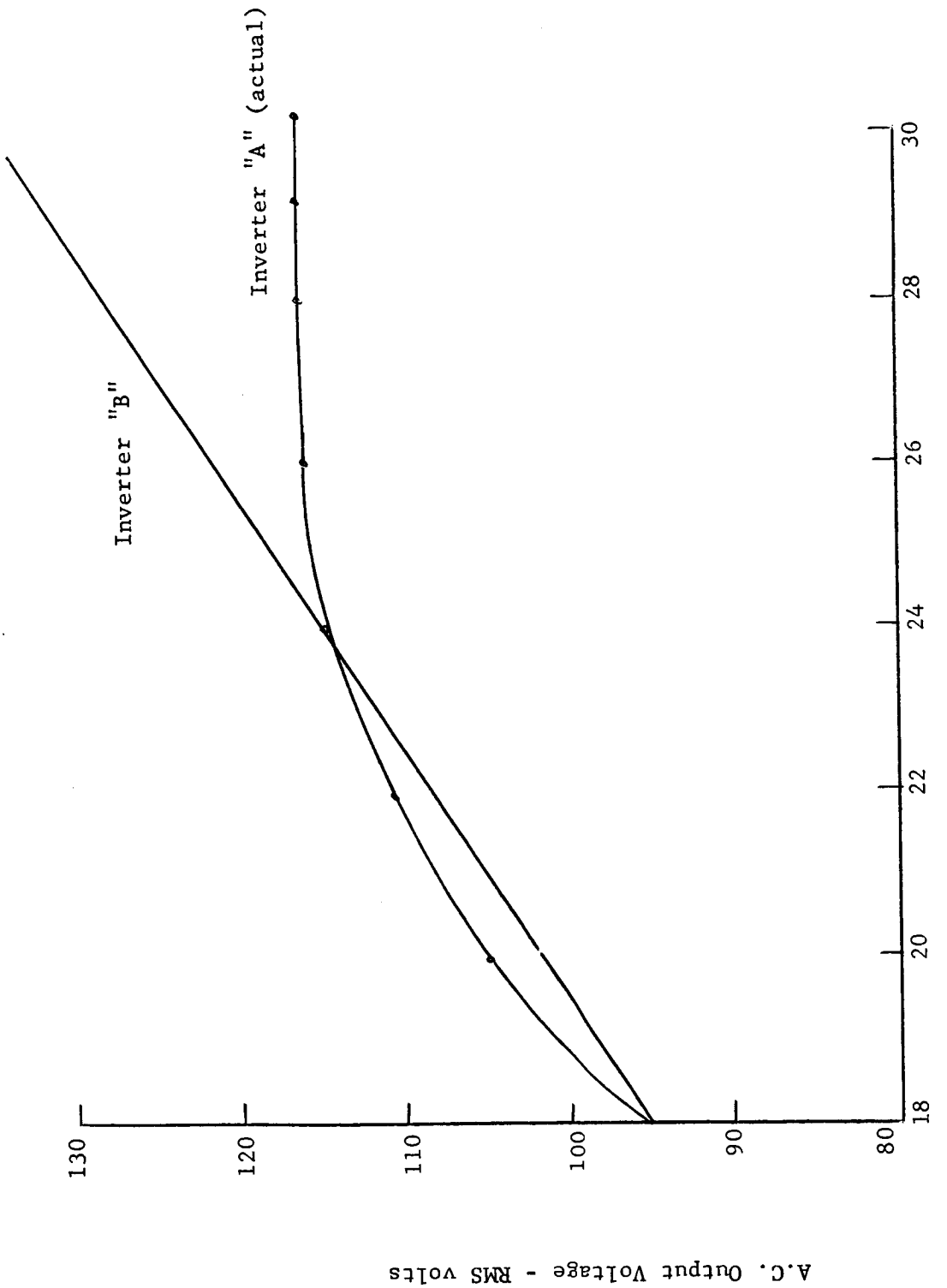

Figure 19 - Hypothetical & Actual Inverter Characteristics

1. Original Inverter

$E_{D.C.}$	Temperature 0	20°C	40°C	60°C	80°C
20	.0001	.4300	.9800	.9990	.9984
22	.0001	.4300	.9800	.9990	.9984
24	.0001	.3900	.9730	.9983	.9976
26	.0001	.3500	.9660	.9975	.9968
28	.0001	.3200	.9600	.9970	.9960

R_D(15 min, 2°)

$E_{D.C.}$	Temperature 0	20°C	40°C	60°C	80°C
20	24.0	24.6	25.2	25.9	26.7
22	26.8	26.9	28.2	28.8	29.6
24	28.9	29.5	30.4	31.0	31.7
26	30.0	30.6	31.5	32.1	32.9
28	30.1	30.6	31.5	32.1	32.9

h_c(% per 1000 hrs)

2. Inverter less regulator

$E_{D.C.}$	Temperature 0	20°C	40°C	60°C	80°C
20	.0001	.3300	.9640	.9980	.9965
22	.0001	.4300	.9800	.9990	.9984
24	.0001	.3900	.9730	.9983	.9976
26	.0001	.2300	.9225	.9920	.9880
28	.0001	.0500	.8475	.9820	.9720

R'_d(15 min, 2°)

$E_{D.C.}$	Temperature 0	20°C	40°C	60°C	80°C
20	20.1	20.5	21.2	21.8	22.5
22	22.2	22.4	23.3	24.1	25.0
24	24.9	24.9	26.2	27.1	28.1
26	27.7	27.7	29.0	30.0	31.0
28	31.4	31.5	32.9	33.9	35.0

h'_c(% per 1000 hrs)

Table 3 - Evaluation of Proposed Tradeoff

increased voltage stress on the amplifier, particularly the amplifier tubes, due to the elimination of the regulator. This added stress slightly increases the probability of a tube burnout at high d.c. voltage inputs. The probability of a drift failure is greater at higher d.c. voltages also. It thus appears that the advantage achieved by the elimination of parts is cancelled by the increased probability of failure due to other causes, and the calculation below confirms this. For the various input distributions, we have:

Supply Voltage Distribution	Temperature Distribution N(50,32)	N(50,20)	N(50,0)
N(24,2.5)	.6587	.7948	.9280
N(24,1.75)	.7022	.8469	.9744
N(24,0)	.7122	.8614	.9854

These are the estimated overall unconditional probabilities of system success, and when compared with the probabilities estimated previously using the original inverter, it is evident that the proposed tradeoff should not be undertaken.

6.2. Specifications at the interface

To extend the example of the comparison of different designs, we may ask the question: "What specifications should be placed on the d.c. to a.c. inverter to insure the best possible level of reliability for the overall system?" This is a synthesis problem where the system may be broken down into two elements as follows:

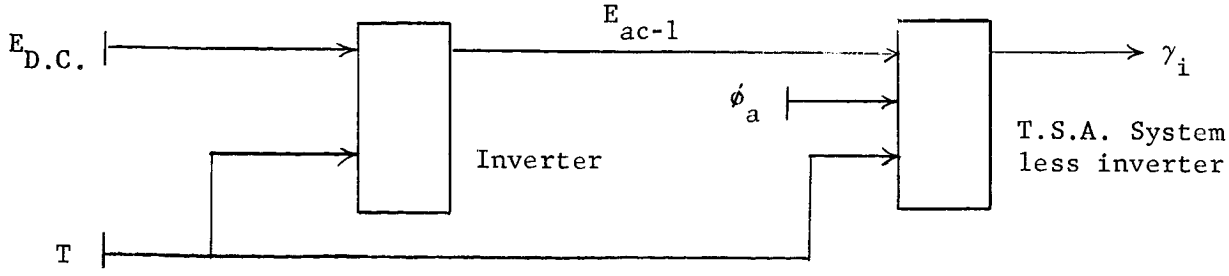

And specifications at the interface of the two elements are of interest. Specifically, the best design value of E_{ac-1} and the allowable deviation of E_{ac-1} from this value will be determined. We assume that the density function for the ambient temperature is known, and will be taken to be $N(50^{o},20^{o})$. The calculations are based on the same mission profile as before.

From the previous work, the conditional probabilities of system success with the above given temperature distribution may be found for various values of E_{ac-1}. These values are calculated for 9 levels and shown below:

	A.C. Voltage E_{ac-1}								
	100	103	106	109	112	115	118	121	124
R_{TSA} (less inverter)	.8707	.8840	.8908	.8940	.8908	.8825	.8674	.8460	.8104

The optimum design value for the inverter output voltage may be determined approximately by inspection of the above table as:

$$\text{design } E_{ac-1} \approx 109 \text{ volts}$$

We see from the above table that any variation in this value, due to differing d.c. input voltages or ambient temperature changes, will result in degradation of the reliability of the system. To achieve an absolutely fixed value of a.c. voltage will presumably require equipment of such complexity or weight so as not to be feasible. The only course of action for the designer will be to design the inverter for the best possible regulation subject to the constraints of weight, cost, size, and complexity. Since added complexity usually implies a higher probability of a "catastrophic" failure, a set of tradeoff curves between deviations in the output voltage and catastrophic hazard rate will be useful for making design decisions. Such a tradeoff curve is shown in figure 20.

To generate these curves, the a.c. output voltage is assumed to have a normal distribution. For the particular mission specified, and with the failure defined as the crossing of a $\pm 2^{o}$ level by the output arm angle, a considerable increase in catastrophic hazard rate could be tolerated in the inverter design if the variance of the inverter output could be reduced accordingly. In this particular case, cost, size or weight would be the most likely limitations in the degree of regulation of the inverter rather than the possibility of a catastrophic failure. From the tradeoff curves, a deviation in the output voltage of < 2 volts, and a catastrophic hazard rate of $< 40\%$ per 1000 hours will insure an estimated overall system reliability of $> .8920$, and this appears reasonable and in accord with the "state of the art."

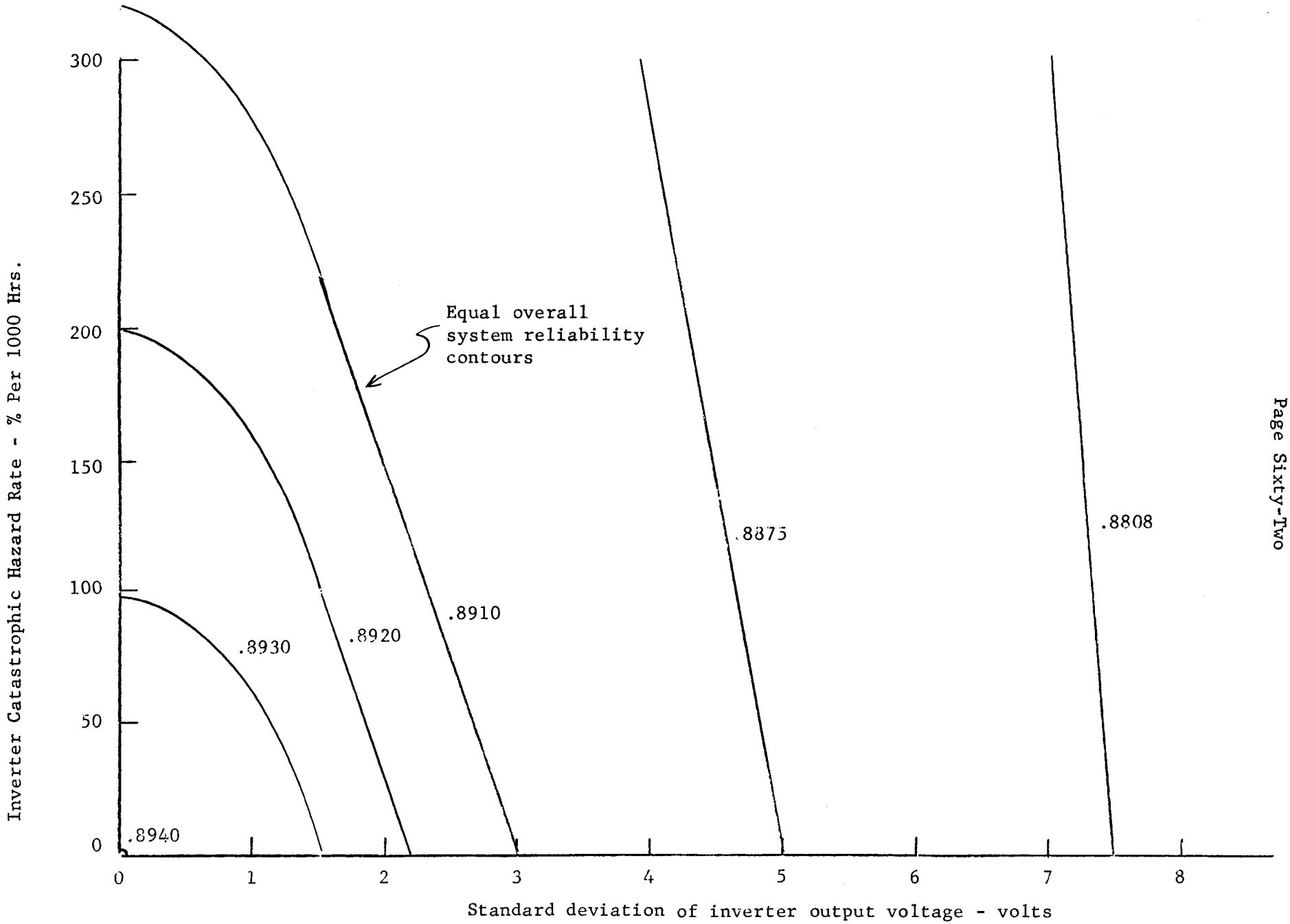

Figure - Tradeoff Curves - Inverter Deviation Vs. Catastrophic Failure Rates for Mean Output Voltage of 109 Volts.

8.0. SUMMARY

The general probabilistic modeling techniques developed in reference [1] have been applied to a representative electromechanical control system, and the actual numerical calculations carried out to obtain an estimate of the probability of system success for an assumed mission profile.

Several problems were encountered in this study that were left for investigation in the future. One of these problems is that of extending the representation of an attribute to include variations due to manufacturing tolerances, and variations due to failures of those piece parts that do not cause certain failure of the system. One such extension that appears feasible is to represent an attribute, amplifier gain for example, by an expression such as:

$$K_A = f(E_{ac-1}, T) + \bar{\epsilon}_A + \Delta K_{A(R1)} F_{R1} + \Delta K_{A(R2)} F_{R2} + \ldots \text{ etc.}$$

where: $f(E_{ac-1}, T)$ is the deterministic function that accounts for environmental variations.

$\bar{\epsilon}_A$ is a random variable describing the variation in gain due to the consideration of a population of amplifiers, rather than a single amplifier.

$\Delta K_{A(R1)}$ is the empirically determined change in gain that occurs when resistor R1 shorts.

F_{R1} is a continuous step function that has only the values 0 or 1, with the probability of either value being determined by the probability of R1 shorting.

Using functions such as those mentioned above, a computer simulation will probably be required to statistically determine the attribute behavior.

Another interesting problem is that of synthesizing a system to maximize the reliability, as was briefly noted in Section 7.2. If the variations in the element attributes with environment are known, it should be possible for a designer to choose nominal values of parameters such that the variation in the system attributes are minimized.

The question of the validity of the estimate is pertinent in view of the numerous assumptions and approximations made. The major mathematical approximations are summarized on the following page.

1. With fixed environment, the differential equations used to describe the system operation are linearized.
2. The effects of the environment on the system attributes are described approximately by the linear and quadratic terms of Taylor's expansion.
3. The integrals over the input random variable space are approximated by 5 level sums.

It is anticipated that as work progresses on modeling techniques, digital computers will be utilized more fully and the mathematical approximations that were necessary for this application will be refined.

The assumptions made to obtain numerical answers can be categorized into several classes:

1. Assumptions required because of lack of knowledge of the specific conditions under which the system operates. (Mission profile, input distributions, etc.).
2. Assumptions made as to the validity of the data used in the calculations (mil 217 data applies, etc.).
3. Assumptions concerning the physical behavior of the equipment. (past history has no effect, no failures when system power off, certain inputs unimportant, etc.).

The assumptions above, along with the mathematical approximations, will influence the accuracy of any particular application, and as yet it is not possible to place any sort of confidence limits on the validity of the estimated system reliability number. It should be recognized, however, that most of the approximations and assumptions above are inherent in any mathematical modeling of a physical situation, and the important point is that the application of the techniques used herein show with clarity the assumptions that must be made, and also the steps that must be taken to increase the accuracy of the estimate of system reliability. Furthermore, even though the degree of accuracy of the point estimate is not known, it is not the estimate itself, but the <u>variations</u> in the estimate that are of importance for assisting in the design evaluations and decisions.

REFERENCES

1. Lewis, J. B. and Wells, W. T., "Probabilistic Models for System Reliability," Technical Report No. 3, January, 1963, NASA contract NASw-334, Research Triangle Institute.
2. Britt, C. L., "Demonstrating Reliability Analysis and Prediction Techniques with Data Obtained from RTI Tests on a Representative System," Working Paper No. 7, April 12, 1963, NASA Contract NASw-334, Research Triangle Institute.
3. Leadbetter, M. R. and Lewis J. B., "Reliability of a Linear System with Random Inputs--An Example of the Use of Spectral Moments," Working Paper No. 5, December 4, 1962, NASA contract NASw-334, Research Triangle Institute.
4. Seamans, R. C., Barnes, F. A., Garber, T. B. and Howard, V. W., "Recent Developments in Aircraft Control," Journal of the Aeronautical Sciences, Vol. 22, pp. 145-164, 1955.
5. Department of Defense, "Reliability Stress and Failure Rate Data for Electronic Equipment," Mil-Hdbk-217, 8 August, 1962.
6. Truxal, J. G., Automatic Feedback Control System Synthesis, McGraw-Hill, 1955.
7. Anderson, R. L. and Bancroft, T. A., Statistical Theory in Research. McGraw-Hill, New York (1952).
8. Bennett, C. A. and Franklin, N. L., Statistical Analysis in Chemistry and the Chemical Industry. Wiley & Sons, New York (1954).
9. Kempthorne, O., The Design and Analysis of Experiments. Wiley & Sons, New York (1952).
10. Leone, F. C., "Statistical Programs for High Speed Computers." Technometrics, Vol. 3, 123-126 (1961).

9.0 APPENDICES

APPENDIX A

1. Check of Validity of Quasilinear Model - Nominal Environment

To check the validity of the nominal mathematical model of the system, the system equations are used to predict the response of the system to a particular input, a 5^{o} step change in aircraft pitch angle. This predicted response is then compared with the actual measured response of the system to this particular input.

The differential equations that approximately describe the behavior of the T.S.A., for nominal environmental conditions and supply voltages, are as follows:

$$\left\{ \begin{array}{l} \epsilon = \phi_a - \gamma - \dfrac{K_T}{K_e R}\ \dot{\gamma} \\ \\ \tau_m \ddot{\gamma} + \dot{\gamma} = K_A K_m K_e R \epsilon \end{array} \right\} \text{ for } |\epsilon| \leq \frac{V_s}{K_A K_e}$$

$$\left\{ \begin{array}{l} \epsilon = \phi_a - \gamma - \dfrac{K_T}{K_e R}\ \dot{\gamma} \\ \\ \tau_m \ddot{\gamma} + \dot{\gamma} = \pm R K_m V_s \end{array} \right\} \text{ for } |\epsilon| > \frac{V_s}{K_A K_e}$$

Substituting the numerical values obtained by experiment into these equations yields:

$$\left\{ \begin{array}{l} \epsilon = \phi_a - \gamma - .035\ \dot{\gamma} \\ \\ .375\ \ddot{\gamma} + \dot{\gamma} = 598\ \epsilon \end{array} \right\} \ |\epsilon| \leq .296^{o}$$

$$\left\{ \begin{array}{l} \epsilon = \phi_a - \gamma - .035\ \dot{\gamma} \\ \\ .375\ \ddot{\gamma} + \dot{\gamma} = \pm\ 177 \end{array} \right\} \ |\epsilon| > .296^{o}$$

To find the response of the system to a 5^{o} step input, a graphical technique may be used. The equations are first combined to eliminate ϵ:

$$.375\ \ddot{\gamma} + 1.95\ \dot{\gamma} + 598\ \gamma = 0 \qquad |\epsilon| \leq .296^{o}$$

$$.375\ \ddot{\gamma} + \dot{\gamma} - 177 = 0 \qquad \epsilon > .296^{o}$$

$$.375\ \ddot{\gamma} + \dot{\gamma} + 177 = 0 \qquad \epsilon < -.296^{o}$$

Now make the substitution $y = \dot{\gamma}$, and divide each equation by y to obtain:

$$.375\ \alpha + 21.95 + 598\ \gamma/y \qquad |\epsilon| \leq .296^{o}$$

$$.375\ \alpha + 1 - 177/y \qquad \epsilon > .296^{o}$$

$$.375\ \alpha + 1 + 177/y \qquad \epsilon < -.296^{o}$$

Where α is the slope of the solution curve at a particular point in the γ - $\dot{\gamma}$ plane. Solving for the slopes in the various regions gives:

$$\alpha = -58.6 - 1595\ \gamma/y \qquad |\epsilon| \leq .296^{o}$$

$$\alpha = -2.67 + 472/y \qquad \epsilon > .296^{o}$$

$$\alpha = -2.67 - 472/y \qquad \epsilon < -.296^{o}$$

The isoclines are plotted in figure A1 and the trajectory for a 5^{o} step input is plotted using the known slopes as a guide. From the plot of $\gamma(t)$ vs $\dot{\gamma}(t)$, the time response can be obtained by plotting $\frac{1}{\dot{\gamma}}$ vs γ and performing a graphical integration:

$$t_b - t_a = \int_a^b \frac{1}{\dot{\gamma}}\, d\gamma \qquad \text{(seconds)}$$

This procedure is followed in the plot of figure A2 to obtain the calculated time response to the 5^{o} step input. The measured and calculated time responses are compared in figure A3.

2. System Stability

The linear model of the system indicates that little trouble with instability will be encountered. The locus of the roots of the system characteristic equation,

$$\bar{A}s^2 + \bar{B}s + 1 = 0$$

are plotted below. As temperature and supply voltage increase, the roots

progress away from the imaginary axis as shown.

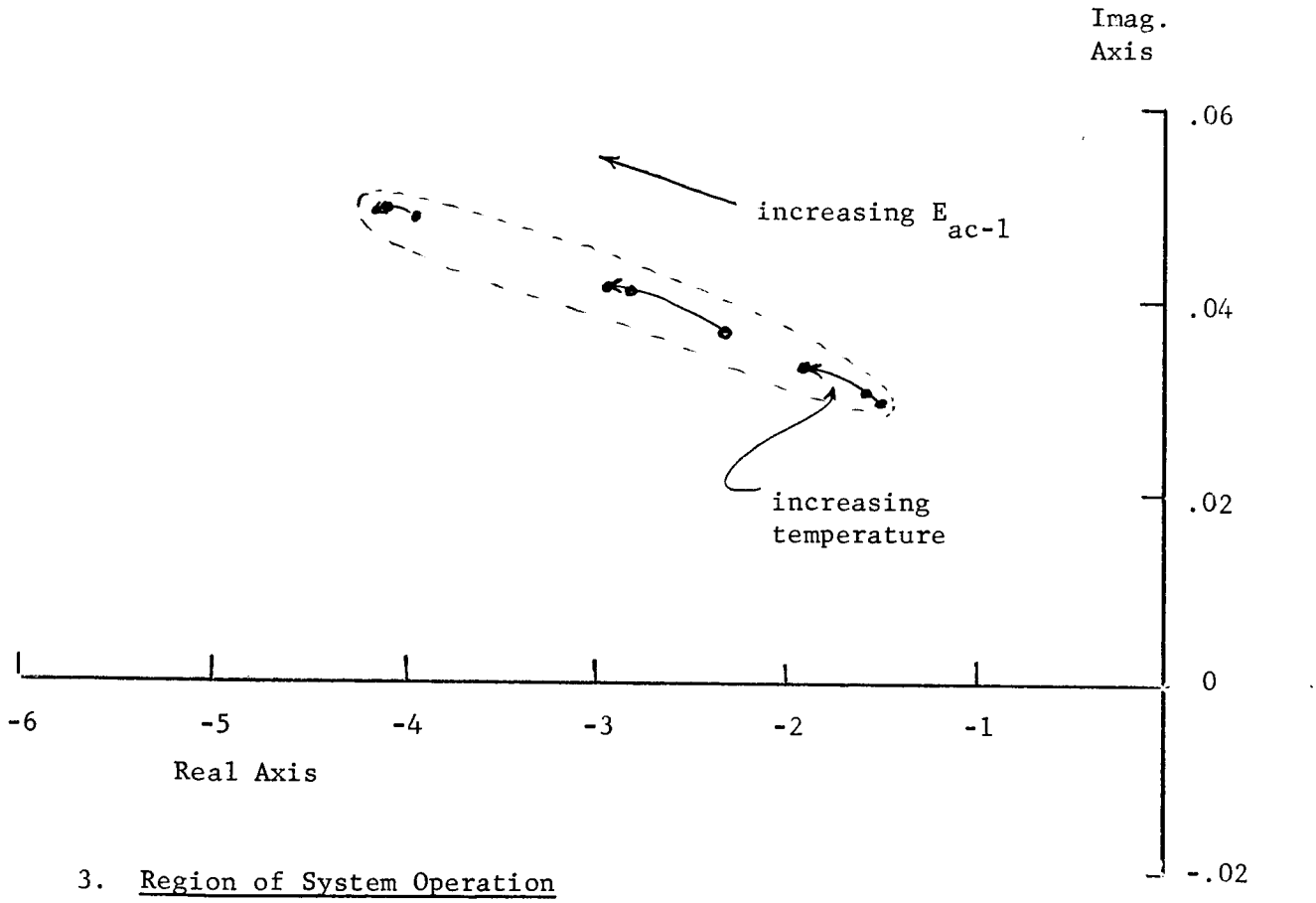

3. Region of System Operation

To check the possibility of amplifier saturation with the signal levels used, it is useful to obtain an expression for the system error ϵ as a function of the input signal $\phi_a(t)$. Under nominal conditions:

$$\hat{\epsilon} \approx \frac{\frac{s}{545}\left(\frac{s}{2.7} + 1\right)}{As^2 + Bs + 1} \hat{\phi}_a$$

For a sinusoidal input $\phi_a(t) = A \sin \omega t$, the amplitude of the error signal $|\epsilon|$ vs frequency may be plotted. The amplifier does not saturate under nominal environmental conditions so long as $|\epsilon| \leq .296$. From the plot, figure A5, we see that for $\omega = 5$ radians per second, the amplitude A corresponding to $|\epsilon| = .296$ is $\approx$ 16 degrees. Since the spectral density of the actual input

signal contains little energy above 5 radians per second, and has an RMS value $\approx$ .425 degrees, we would expect amplifier saturation to be a relatively rare occurrence.

By using the same techniques as used for the analysis of the output error due to system time lags, the probability of amplifier saturation could be calculated, but this degree of analysis is not thought necessary in view of the above considerations.

We thus conclude that the amplifier operates in the linear region to a high degree of approximation.

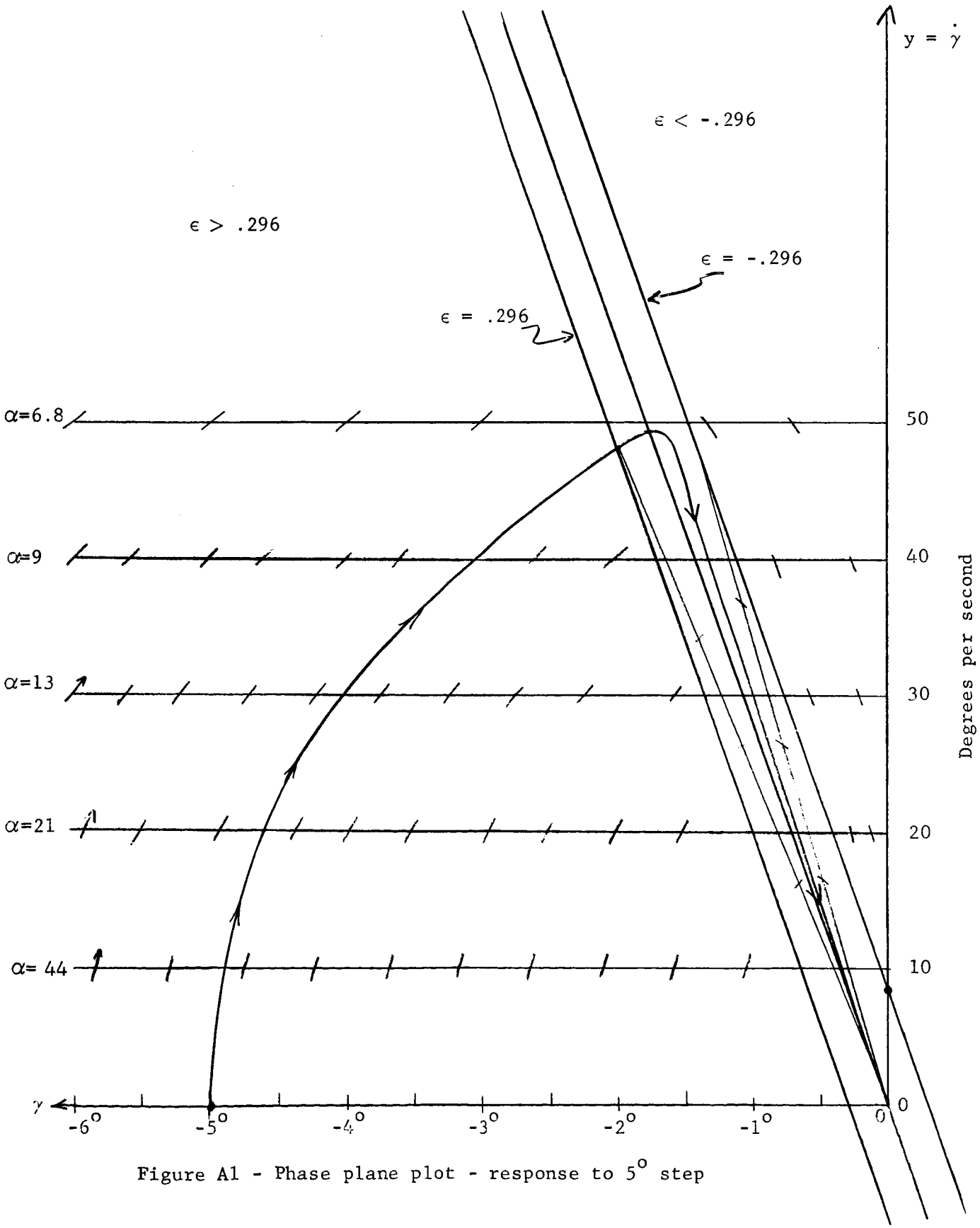

Figure A1 - Phase plane plot - response to 5^{o} step

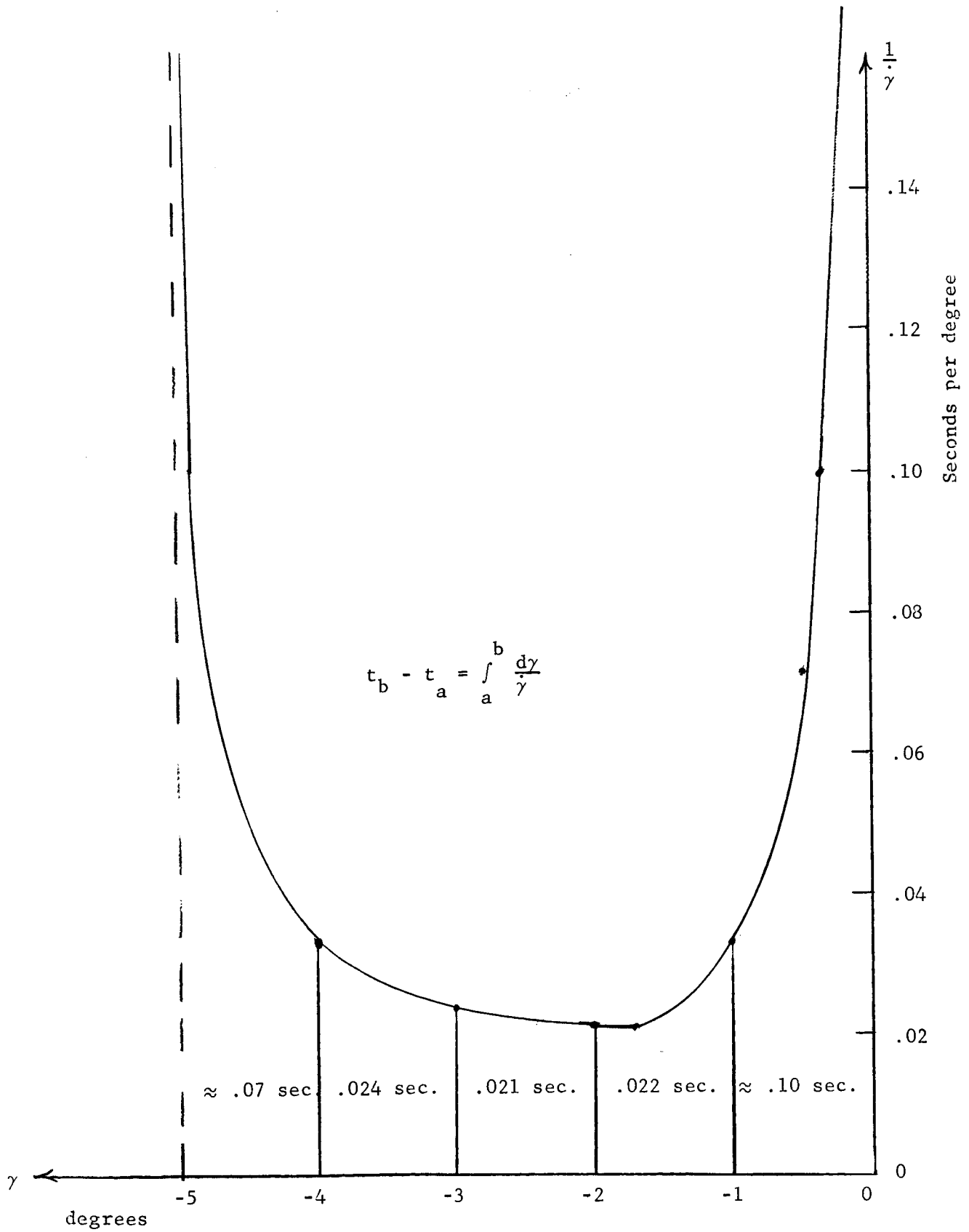

Figure A2 - Plot of $\frac{1}{\dot{\gamma}}$ vs γ for numerical integration

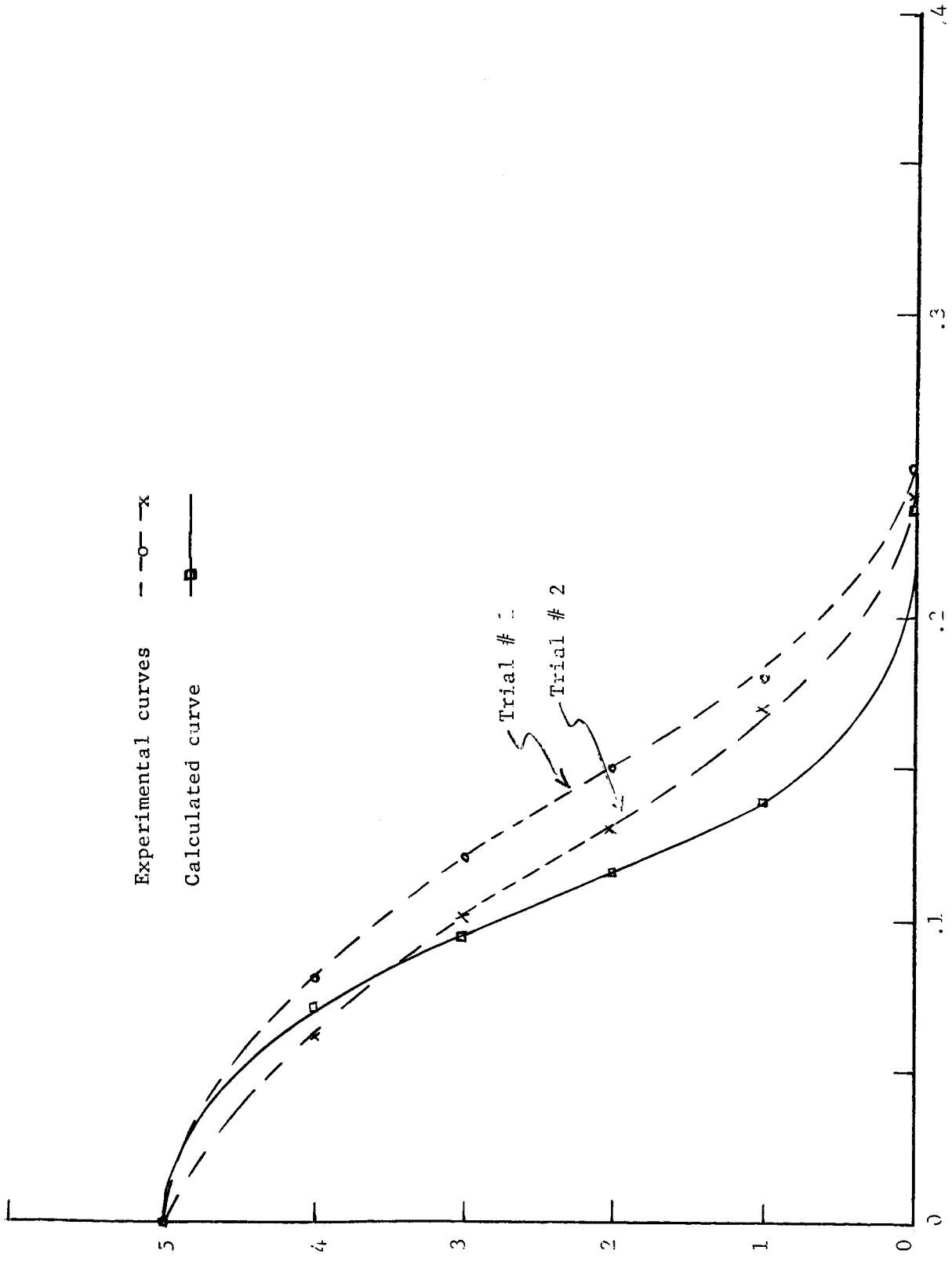

Figure A3 - Measured and Calculated response of system to 5^{o} step input

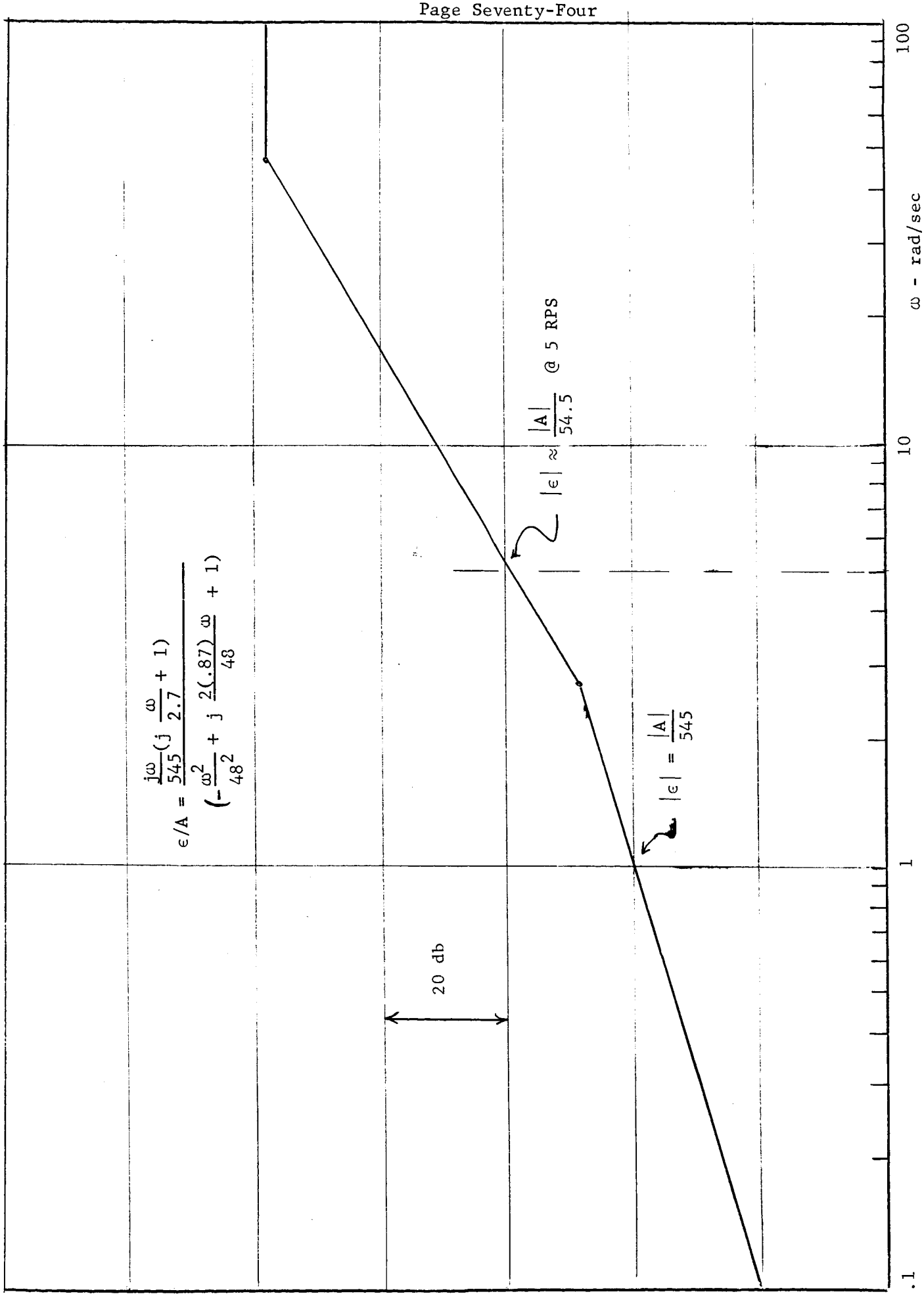

Figure A4 - Amplitude of error signal for sinusoidal input

APPENDIX B

Representation of pitching motion of a typical aircraft

The pitching motions of an aircraft in flight are determined by the motions of the airplane control surfaces, the dynamics of the airplane with its associated control systems, and by disturbing moments and forces that arise from atmospheric turbulance. The disturbances due to turbulance are usually called "gust disturbances" and are a random phenomena that require statistical methods for the description of their effects.

The input-output relationships for aircraft pitching motion may be represented functionally as:

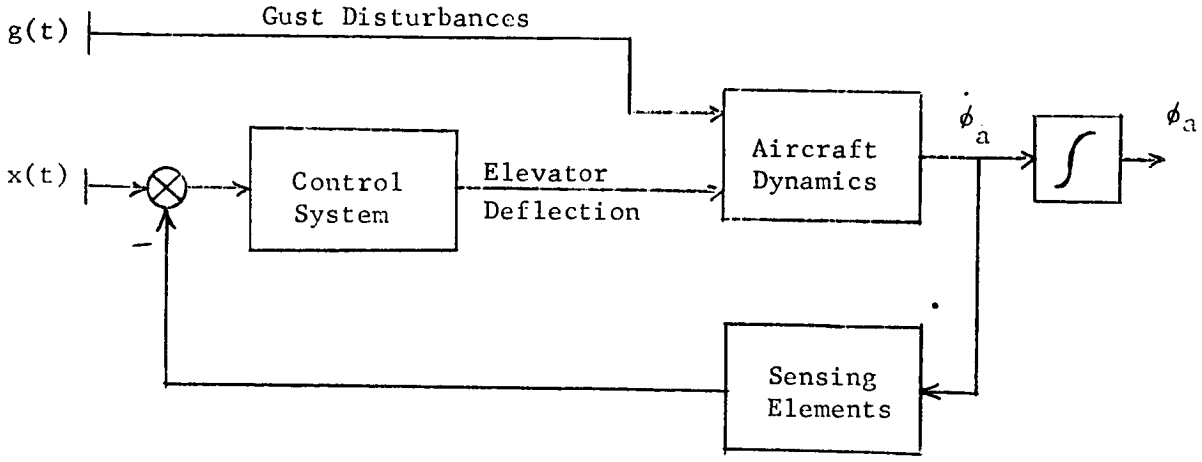

To simulate typical pitching motion for a given aircraft, the mathematical relationships giving pitch angle as a function of x(t) and g(t) are required. A statistical description of g(t) is available in the form of the power spectral density of the vertical and horizontal velocity components. The knowledge of the power spectral density of g(t) and the linearized airplane dynamical equations permits the approximate determination of the spectral density of the airplane pitch angle due to wind gust disturbances. Experimental work by Clementson (reference 4) indicates that gust velocity may be considered as a stationary Gaussian random process and that the power spectral density of vertical gust velocities may be described satisfactorily by the relationship:

$$[(\text{P.S.D.})\ w_G/V] = \frac{4(ms)/\pi^*}{1 + (2\omega)^2}$$

where: w_G/V = ratio of gust velocity to aircraft air speed.
ω = frequency in radians per second.

This relationship is derived from averaged meteorological data.

Reference (4) furnishes a set of numerical parameters for a typical aircraft that permits the determination of the aircraft transfer functions relating the vertical gust velocity to the aircraft pitch angle, as follows:

$$\frac{\hat{\phi}_G}{\hat{w}_G/V} = \frac{.86}{[1 + .452s + .327s^2]} .$$

And for the transfer function relating pitch angle to elevator deflection angle with gusts absent, reference (4) gives:

$$\frac{\hat{\phi}_e}{\hat{\delta}} = \frac{.7(1 + 1.6s)}{s(1 + .452s + .327s^2)} .$$

The above transfer functions have been simplified by neglecting the long period phugoid motion of the airplane. It is felt that this motion will not be important since the pilot or autopilot will correct for these long term oscillations.

The above transfer functions do not include the effects of pitch rate and pitch angle feedback loops that are used to stabilize the aircraft. The aircraft with the above dynamical characteristics, according to reference (4), will usually contain sensing elements for feedback to the airplane elevator with transfer functions:

$$\frac{\hat{\delta}_r}{\hat{\phi}_A} = \frac{1.2}{1 + .019s}$$

$$\frac{\hat{\delta}_p}{\hat{\phi}_A} = \frac{3.15}{1 + .019s}$$

*(ms) = mean square value of w_G/V. For purposes of this study, a value of 46×10^{-4} is used.

Thus to represent the aircraft with these particular characteristics, the system functional diagram will be:

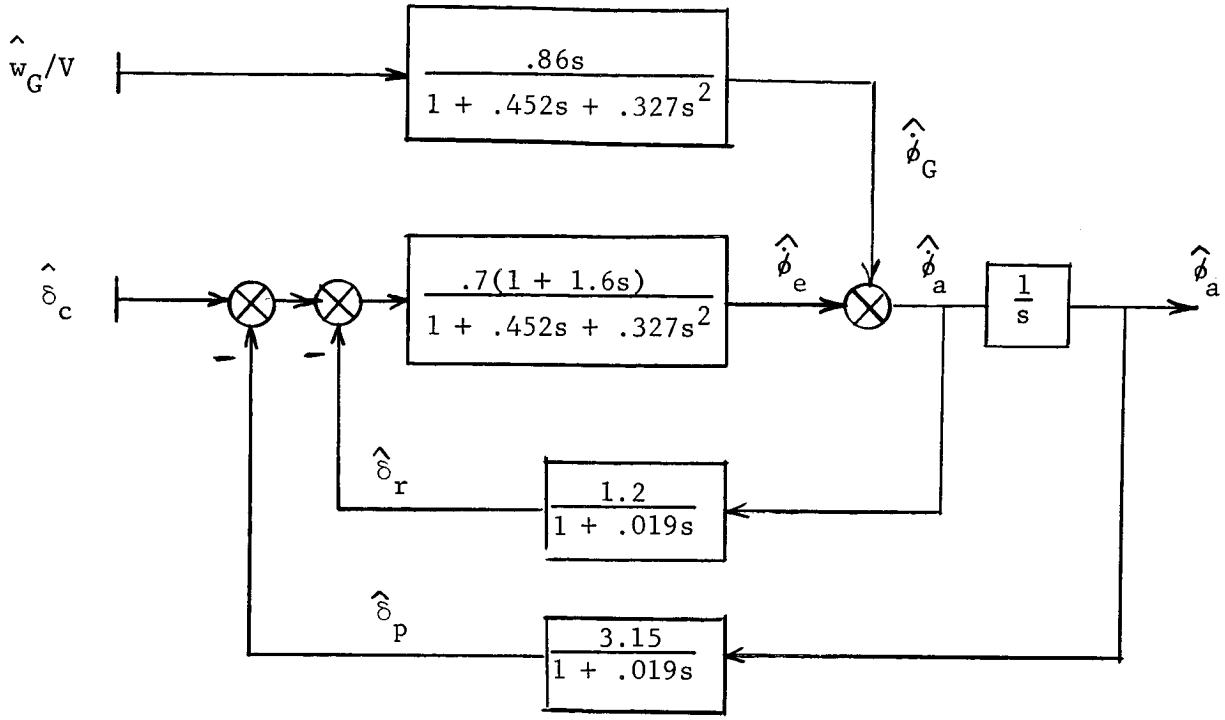

From this functional diagram it is possible to obtain the transfer function relating aircraft pitch angle to wind gust velocity, with the command input $\delta_c(t) = 0$.

$$\frac{\hat{\phi}_a}{\hat{w}_G/V} = \frac{.391s(1 + .019s)}{.00282s^4 + .152s^3 + .823s^2 + 2.43s + 1}$$

or:

$$\frac{\hat{\phi}_a}{\hat{w}_G/V} \approx \frac{.391s(1 + .019s)}{(.033s + 1)(2.05s + 1)(.0415s^2 + .342s + 1)}$$

To generate a voltage analogous to $\phi_a(t)$ on an analog computer, a "white" noise generator is used. The transfer function from white noise, $n(t)$, of spectral density η, to pitch angle is obtained by noting that:

$$[\text{P.S.D. } w_G/V] = \left|\frac{1}{1 + 2s}\right|^2 \eta$$

Hence:

$$\frac{\hat{w}_G/V}{\hat{n}} = \frac{1}{1 + 2s}$$

Where the amplitude of the noise source must be adjusted to obtain a spectral density of $\eta = 58.6 \times 10^{-4}$ volts^2 per radian per second. (For 1 volt=1 rad.).

Thus the transfer function from white noise to pitch angle is:

$$\frac{\hat{\phi}_a}{\hat{n}} = \frac{.391s(1 + .019s)}{(.033s + 1)(2.05s + 1)(.0415s^2 + .342s + 1)(1 + 2s)}$$

Mechanization

The computer circuit used to achieve the simulation of the pitch angle input is shown in figure (B1). A Donner analog computer, model 3400, and a General Radio noise generator, model 1390B, were used for the simulation. This noise generator provides a noise with a flat spectrum from 5 to 20,000 cycles per second. The noise signal was sampled at a rate of 30 times per second to flatten the spectrum in the 0-5 cps region.

The computer output was used to modulate a 400 cycle reference signal, and the resulting double side band suppressed carrier signal was used to drive the tilt table servomechanism. The table position was sensed by generating an electrical signal with a multiple turn potentiometer geared to the table.

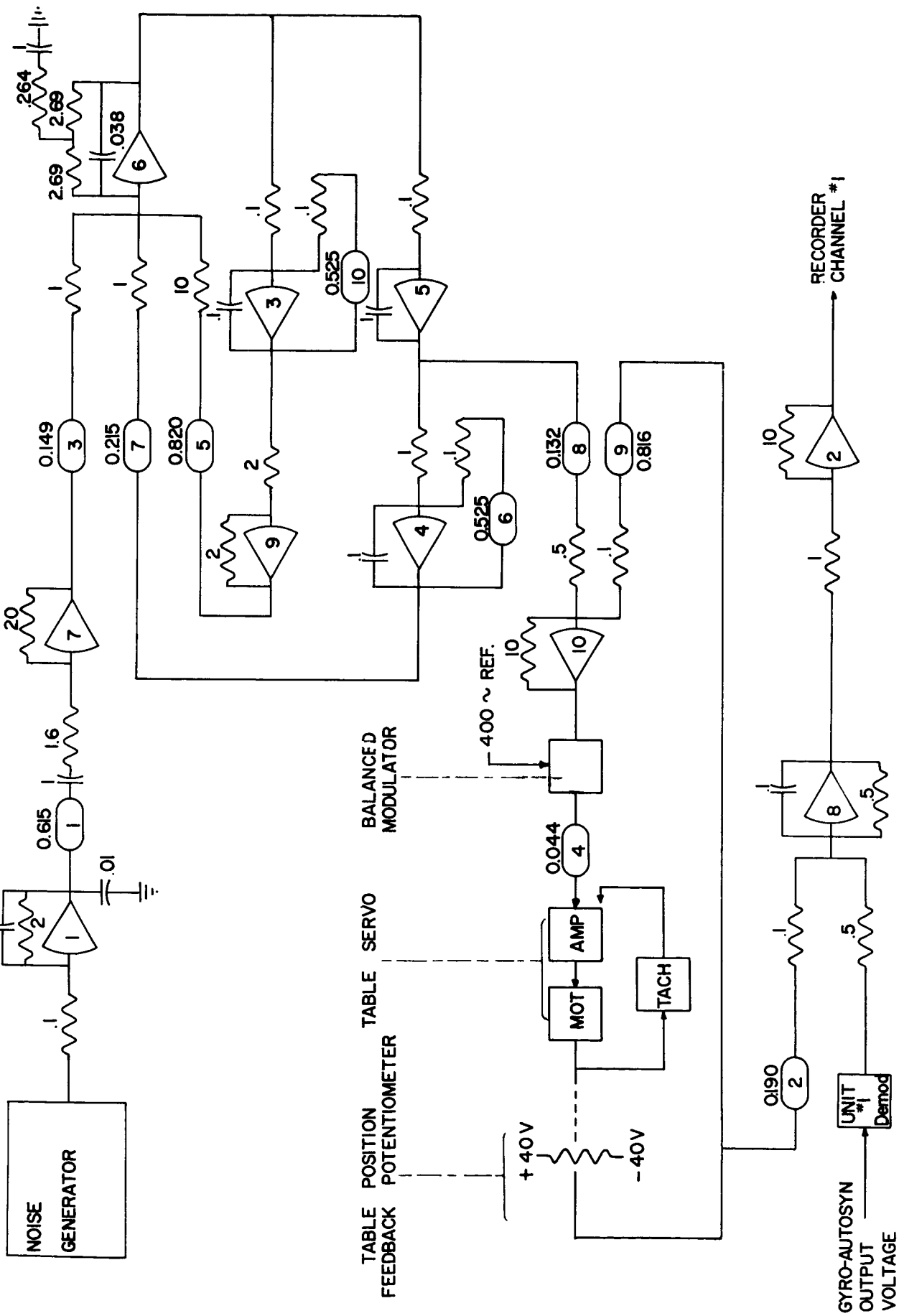

Figure B1. ANALOG COMPUTER DIAGRAM

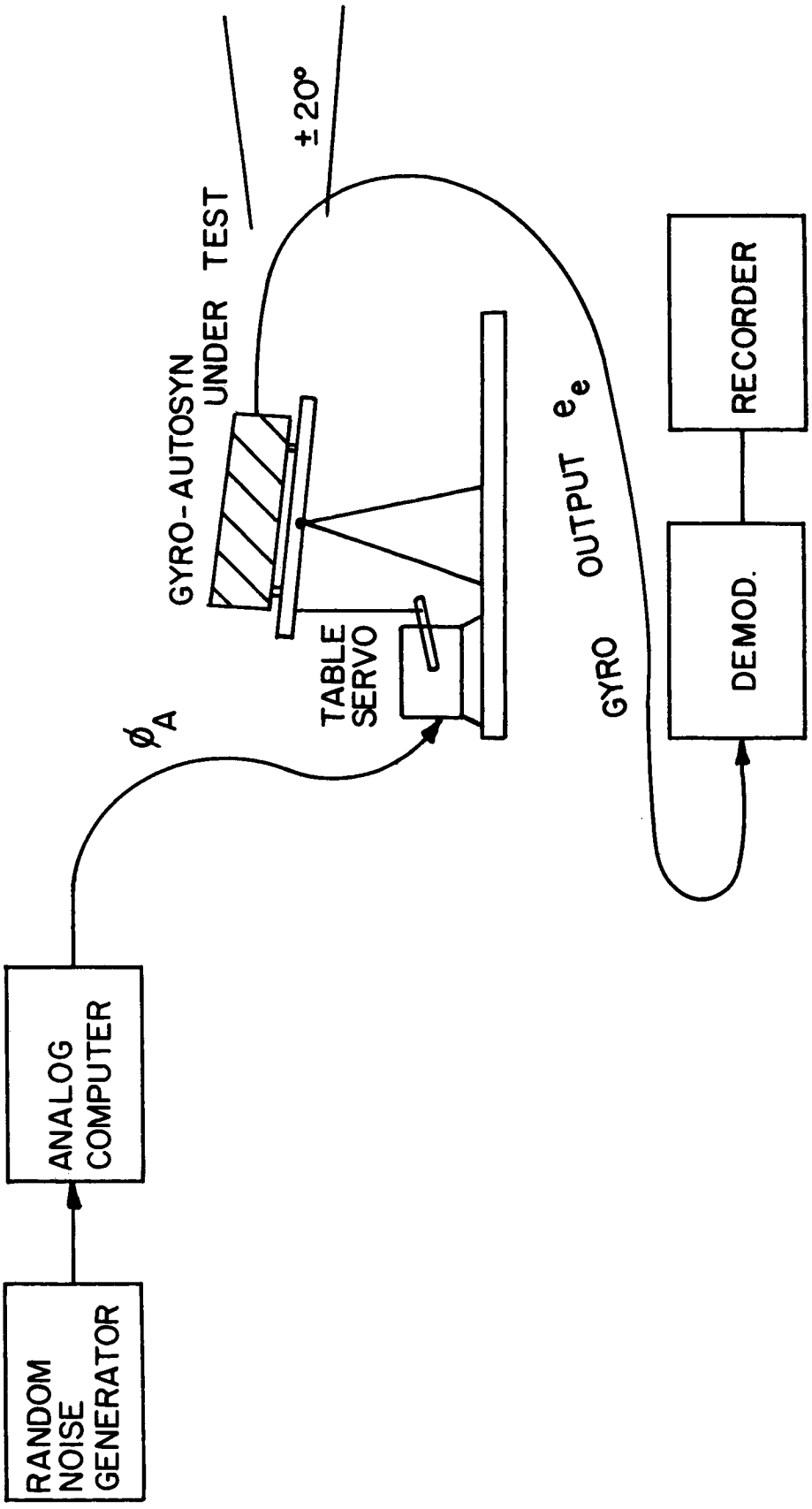

FIGURE B2
MECHANIZATION OF PITCH ANGLE INPUT

APPENDIX C

1. Part Failure Rates - Amplifier

From Mil-Hdbk-217, "Reliability Stress and failure rate data for electronic equipment," the following catastrophic failure rate data is obtained for each part in the amplifier. For each part a "failure rate" is obtained for each of three levels of supply voltage to the amplifier (100, 112, 124 volts) and three levels of temperature (0^{o}, 26^{o}, $85^{o}C$), and where important, three levels of signal input voltage (0, 20, 50 MV. RMS). The failure rates are given as "percent per 1000 hours." The inputs and environments of the amplifier are converted into stresses on the individual parts by use of the circuit diagram and by actual measurements made in the laboratory. The data is listed in the form of tables as follows:

		Amplifier Ambient Temperature		
		$0^{o}C$	$26^{o}C$	$85^{o}C$
Amplifier Supply Voltage	100	h/100, 0	h/100, 26	h/100, 85
	112	h/112, 0	h/112, 26	h/112, 85
	124	h/124, 0	h/124, 26	h/124, 85

for e_e = 20 MV RMS unless otherwise noted

For the individual parts we have:

1. Resistor R651 (Balance pot.); 500 Ω, 1 w, composition. (Mil R-94B data)

$$[h_{R651}] = \begin{bmatrix} .011 & .011 & .013 \\ .011 & .011 & .013 \\ .011 & .011 & .013 \end{bmatrix}$$

2. Resistor R652 (cathode bias); 200 Ω, 1/2 w., composition. (Mil R-11C data)

$$[h_{R652}] = \begin{bmatrix} .001 & .001 & .003 \\ .001 & .001 & .003 \\ .001 & .001 & .003 \end{bmatrix}$$

3. Resistor R653 (Gain pot.); 500,000 Ω, 1 w. composition (Mil R-94B data)

$$[h_{R653}] = \begin{bmatrix} .011 & .011 & .013 \\ .011 & .011 & .013 \\ .011 & .011 & .013 \end{bmatrix}$$

4. Resistor R654 (Plate load); 250,000 Ω, 1/2 w. composition (Mil R-11C data)

$$[h_{R654}] = \begin{bmatrix} .001 & .001 & .003 \\ .001 & .001 & .003 \\ .001 & .001 & .003 \end{bmatrix}$$

5. Resistor R655 (Power supply load); 100,000 Ω, 1/2 w. composition (Mil R-11C data)

$$[h_{R655}] = \begin{bmatrix} .001 & .001 & .010 \\ .001 & .001 & .015 \\ .001 & .001 & .022 \end{bmatrix} \quad \begin{matrix} P/P_{rated} \\ .39 \\ .48 \\ .58 \end{matrix}$$

6. Resistor R656 (Cathode bias); 10,000 Ω, 1/2 w. composition (Mil R-11C data)

$$[h_{R656}] = \begin{bmatrix} .001 & .001 & .003 \\ .001 & .001 & .003 \\ .001 & .001 & .003 \end{bmatrix}$$

7. Resistor R657 (Grid); 250,000 Ω, 1/2 w. composition (Mil R-11C data)

$$[h_{R657}] = \begin{bmatrix} .001 & .001 & .003 \\ .001 & .001 & .003 \\ .001 & .001 & .003 \end{bmatrix}$$

8. Resistor R658 (Tach gain); 300 Ω, 10 w., wire wound (Mil R-26C data)

$$[h_{R658}] = \begin{bmatrix} .014 & .016 & .025 \\ .017 & .019 & .032 \\ .019 & .023 & .037 \end{bmatrix} \quad \begin{matrix} P/P_{rated} \\ .2 \\ .25 \\ .30 \end{matrix}$$

9. Capacitors C651 & C652 (Output phase); .1 MFD, 600 w.v. paper. (Mil C-25 data)

$$[h_{C651}] = [h_{C652}] = \begin{bmatrix} .001 & .001 & .002 \\ .001 & .001 & .002 \\ .001 & .001 & .002 \end{bmatrix} \quad \begin{matrix} V/V_{rated} \\ .081 \\ .094 \\ .104 \end{matrix}$$

10. Capacitor C653 (Coupling); .01 mfd., 600 mv., paper. (Mil C-25 data)

$$[h_{C653}] = \begin{bmatrix} .001 & .001 & .001 \\ .001 & .001 & .001 \\ .001 & .001 & .001 \end{bmatrix}$$

11. Capacitor C654 (Filter), 1 mfd, 200 vdc, paper (Mil C-25 data)

$$[h_{C654}] = \begin{bmatrix} .026 & .034 & .070 \\ .031 & .038 & .080 \\ .038 & .045 & .100 \end{bmatrix}$$

12. Capacitor C655, (input), .001 mfd, 200 v, mica. (Mil C-5B data)

$$[h_{C655}] = \begin{bmatrix} .001 & .001 & .001 \\ .001 & .001 & .001 \\ .001 & .001 & .001 \end{bmatrix}$$

13. Capacitor C656, (output) 1 mfd, 150 v, 400 c.p.s., paper. (Mil C-25 data)

$$[h_{C656}] = \begin{bmatrix} .001 & .001 & .001 \\ .001 & .001 & .001 \\ .001 & .001 & .001 \end{bmatrix}$$

for $e_e = 0$

$$[h_{C656}] = \begin{bmatrix} .004 & .005 & .010 \\ .007 & .009 & .019 \\ .010 & .012 & .026 \end{bmatrix}$$

for e_e = 20 mv. RMS

$$[h_{C656}] = \begin{bmatrix} .018 & .022 & .044 \\ .030 & .036 & .080 \\ .033 & .042 & .088 \end{bmatrix}$$

for e_e = 50 mv. RMS

14. Capacitor C657 (Cathode by-pass), .1 mfd, 600 wv, paper. (Mil C-25 data)

$$[h_{C657}] = \begin{bmatrix} .001 & .001 & .001 \\ .001 & .001 & .001 \\ .001 & .001 & .001 \end{bmatrix}$$

15. Tube V652 - X652 (Voltage amp - rect.), 12SN7. Rated filament voltage 12.6 volts, rated plate dissipation 7.5 watts. Bulb temperature: 115°C @ 85° ambient; 100°C @ 26° ambient; 90°C @ 0° ambient. Actual plate dissipation less than .5 watt. Ratio of operating to rated heater voltage

is .94 @ 100 v.; 1.07 @ 112 v; 1.18 @ 124 v.

$$[h_{V652}] = \begin{bmatrix} .55 & .55 & .55 \\ 1.31 & 1.31 & 1.31 \\ 3.58 & 3.58 & 3.58 \end{bmatrix}$$

16. Tube V651 - X651, (Power amp.), 12SN7, operating conditions same as item 15 except the operating plate dissipation is estimated at 3 watts total.

$$[h_{V651}] = \begin{bmatrix} .56 & .56 & .56 \\ 1.36 & 1.36 & 1.36 \\ 3.72 & 3.72 & 3.72 \end{bmatrix}$$

17. Transformers T651A and T651B (Saturable reactors), hermetically sealed construction. Insulation class B. (Mil T 27A data)

$$[h_{T651A}] = [h_{T651B}] = \begin{bmatrix} .020 & .020 & .028 \\ .020 & .020 & .028 \\ .020 & .020 & .028 \end{bmatrix}$$

18. Transformer T652 (Power - 3 phase) hermetically sealed construction. Insulation class B. (Mil T 27A data) (Assumed 20°C temperature rise at full load conditions).

$$[h_{T652}] = \begin{bmatrix} .025 & .025 & .130 \\ .025 & .025 & .160 \\ .025 & .025 & .225 \end{bmatrix}$$

19. Transformer T653 (Input interstage) hermetically sealed construction. Class B insulation. (Mil T 27A data).

$$[h_{T653}] = \begin{bmatrix} .015 & .015 & .021 \\ .015 & .015 & .021 \\ .015 & .015 & .021 \end{bmatrix}$$

20. Connectors J653 (4 pin), and connector J652 (10 pin)

$$h_{J653} \approx .005$$

$$h_{J652} \approx .009$$

21. Relay K651, (Cage-Uncage) telephone type, 24 vdc, SPDT.

$$[h_{K651}]_A \approx \begin{bmatrix} .01 & .01 & .035 \\ .01 & .01 & .035 \\ .01 & .01 & .035 \end{bmatrix}$$

% per 1000 operating hours

$$[h_{K651}]_B \approx \begin{bmatrix} .01 & .01 & .01 \\ .01 & .01 & .01 \\ .01 & .01 & .01 \end{bmatrix}$$ % per 1000 operations

From the above data, the conditional hazard functions for the amplifier gain attribute can be calculated. Each part that could cause failure of the gain is used in the calculation. This calculation therefore includes all parts except relay K651 and resistor R658. The conditional failure rates of the other parts are added to give:

$$[h_{\text{amp gain}}] = \begin{bmatrix} 1.263 & 1.271 & 1.467 \\ 2.828 & 2.835 & 3.062 \\ 7.465 & 7.472 & 7.784 \end{bmatrix}$$

for $e_e = 0$

$$[h_{\text{amp gain}}] = \begin{bmatrix} 1.266 & 1.275 & 1.478 \\ 2.834 & 2.843 & 3.080 \\ 7.474 & 7.483 & 7.809 \end{bmatrix}$$

for $e_e = 20$ mv

$$[h_{\text{amp gain}}] = \begin{bmatrix} 1.280 & 1.292 & 1.510 \\ 2.857 & 2.870 & 3.151 \\ 7.497 & 7.513 & 7.871 \end{bmatrix}$$

for $e_e = 50$ mv

2. Part Failure Rates - Inverter

The regulated d.c. to a.c. inverter has nameplate specifications as follows:

d.c. input = 24 v.d.c.; 12 amps

a.c. output = 115 v; 3 phase, 400 c.p.s., .5 amps

RPM = 12,000

Temp. rise 45°C

In the same way that the amplifier part failure rates were estimated, the conditional catastrophic failure rates for the inverter are calculated from the individual part failure rates. The failure rates will be calculated for three levels of d.c. supply voltage (20v, 24v, 28v) and three levels of ambient temperature (0, 26°C, 85°C). Data from Mil Handbook 217 is used, and is listed in tabular form as follows:

		Ambient Temperature		
		0	26°C	85°C
d.c. supply voltage	20	h/20, 0	h/20, 26	h/20, 85
	24	h/24, 0	h/24, 26	h/24, 85
	28	h/28, 0	h/28, 26	h/28, 85

1. Resistor R_1, 1250 Ω, 10w, wirewound. (Mil R 26C data)(Note: regulator box temperature assumed to be ambient + 10°C)

$$h_{R1} = \begin{bmatrix} .022 & .028 & .044 \\ .028 & .034 & .056 \\ .028 & .034 & .056 \end{bmatrix}$$

2. Resistor R_2, 500 Ω, variable, 5w, wirewound (Mil R 26C data).

$$h_{R2} = \begin{bmatrix} .032 & .038 & .058 \\ .038 & .044 & .066 \\ .038 & .044 & .066 \end{bmatrix}$$

3. Resistor R_3, 50 Ω, 10 w, wirewound (Mil R 26C data).

$$h_{R3} = \begin{bmatrix} .010 & .012 & .018 \\ .010 & .012 & .018 \\ .010 & .012 & .018 \end{bmatrix}$$

4. Capacitors C_1 and C_2, 1 mfd, 100 vdc, paper. (Mil C 62A data).

$$h_{C1} = h_{C2} = \begin{bmatrix} .001 & .001 & .002 \\ .001 & .002 & .003 \\ .002 & .003 & .006 \end{bmatrix}$$

5. Capacitors C_3, C_4, C_5, C_6 .1 mfd, 600 v paper.

$$h_{C3} = h_{C4} = h_{C5} = h_{C6} = \begin{bmatrix} .001 & .001 & .002 \\ .001 & .001 & .002 \\ .001 & .001 & .002 \end{bmatrix}$$

6. Capacitor C_7, .001 μfd, mica. 600 v (Mil C - 5B data).

$$h_{C7} = \begin{bmatrix} .001 & .001 & .001 \\ .001 & .001 & .001 \\ .001 & .001 & .001 \end{bmatrix}$$

7. Inductor L_2, L_3, iron core, class B insulation.

$$h_{L1} = h_{L2} = \begin{bmatrix} .050 & .050 & .320 \\ .050 & .050 & .320 \\ .050 & .050 & .320 \end{bmatrix}$$

8. Selenium rectifier S_1 17 plates, 4 sections.

$$h_{S1} = \begin{bmatrix} 2.94 & 2.94 & 2.94 \\ 2.94 & 2.94 & 2.94 \\ 2.94 & 2.94 & 2.94 \end{bmatrix}$$

9. Carbon pile voltage regulator P_1 115 v rated.

$$h = \begin{bmatrix} .100 & .100 & .100 \\ .100 & .100 & .100 \\ .100 & .100 & .100 \end{bmatrix}$$

10. Field windings and armature, class B insulation.

a. Failure rate-electrical failures

$$h_{ea} = \begin{bmatrix} .065 & .068 & 1.150 \\ .065 & .085 & 2.150 \\ .065 & .085 & 2.150 \end{bmatrix}$$

b. Failure rate - mechanical failures (Data for 12,000 RPM Brush type motor).

$$h_{ma} = \begin{bmatrix} 10.60 & 11.00 & 11.00 \\ 13.20 & 13.20 & 13.20 \\ 13.50 & 13.50 & 13.50 \end{bmatrix}$$

The inverter failure rate is found by adding the individual part failure rates under each condition:

$$[h_c] = \begin{bmatrix} 13.876 & 14.293 & 15.117 \\ 16.488 & 16.524 & 19.185 \\ 16.790 & 16.826 & 19.491 \end{bmatrix}$$

3. Failure rates - Motor and Gyro

a. Gyro - 3 phase, 24 volts, 400 cps., speed 24,000 RPM

The gyro failure rate as a function of input voltage and temperature cannot be determined from the available data in Mil Hdbk 217. However, an average failure rate of 5% per 1000 hours is given, and will be used under all conditions of temperature and supply voltage, hence:

$h_G \approx$ 5% per 1000 hrs under all conditions of temp. and supply voltage.

b. Motor-tachometer - 2 phase, 115 v, max. speed 6000 RPM, Class B insulation, estimated temperature rise 20°C.

Considering both mechanical and electrical catastrophic failures, the estimated gyro-tach failure rate is estimated using the techniques of

Mil 217 as:

$h_m \approx$ voltage		Temp. 0°	$26^{\circ}C$	$85^{\circ}C$
	100	3.05	3.05	3.20
	112	3.05	3.05	3.38
	124	3.05	3.05	3.55

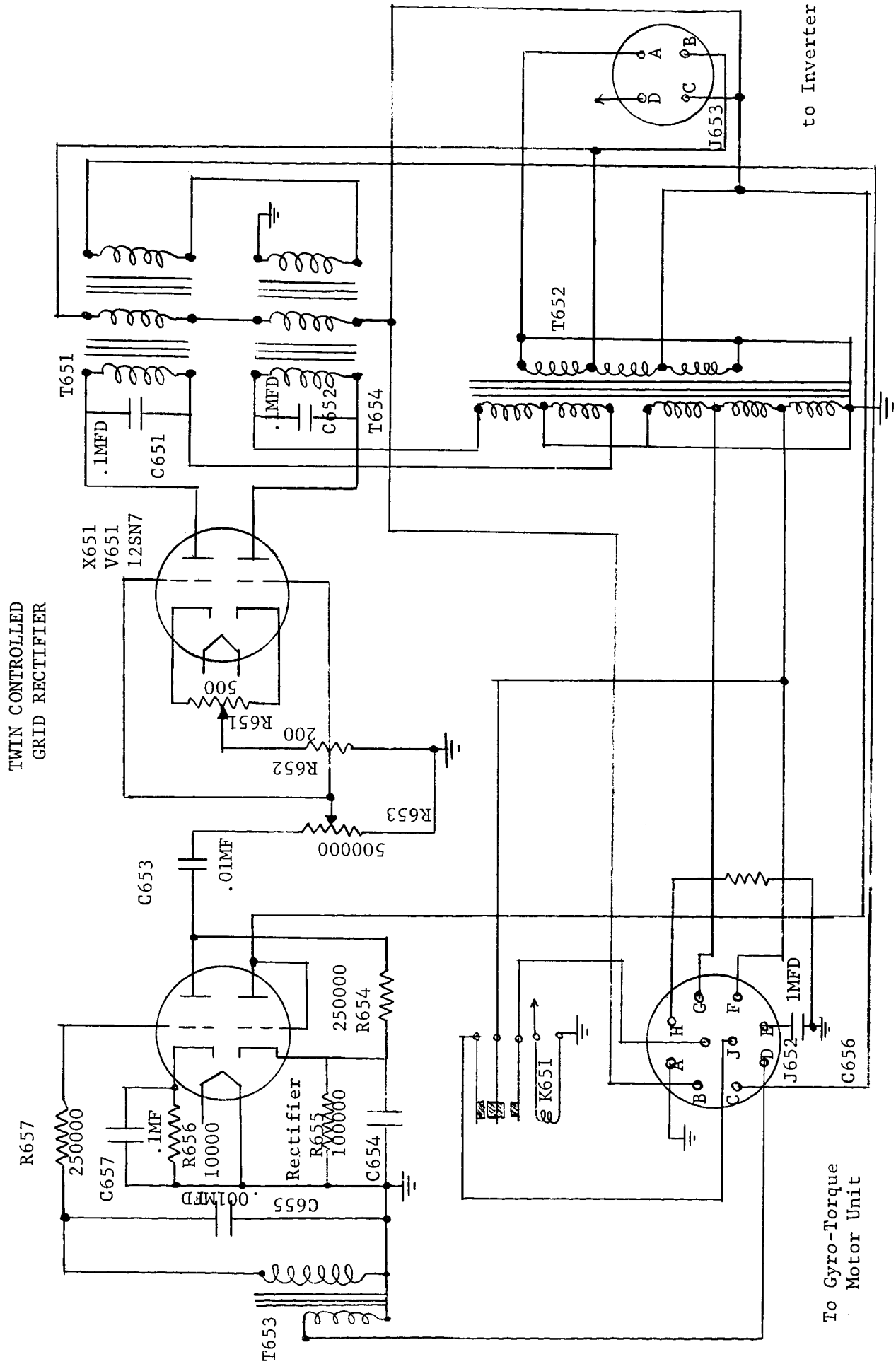

Figure Schematic Diagram of TSA Amplifier Circuit

APPENDIX D -

1. Amplifier gain - nominal conditions

The amplifier nominal gain measurements were made by feeding the amplifier input with a voltage of the proper frequency and phase, and recording the RMS value of the input and output voltage. The input voltage was recorded on a Hewlett-Packard HP 400H, and the output voltage read from a Simpson 267 voltmeter. The amplifier output was loaded with a spare 2 phase servomotor with locked rotor. Data taken is as follows:

Input Voltage (Millivolts)	Output Voltage (Volts)
-60	-113.0
-50	-113.0
-40	-110.0
-30	-100.0
-20	-71.0
-10	-41.0
+10	+37.2
+20	+70.0
+30	+100.0
+40	+110.0
+50	+117.0
+60	+117.0

Temperature 27^{o}C, Average A.C. voltage input (3 phase) = 112 v, Amplifier Unit #1

The plot of figure 5 shows the amplifier gain characteristic. On this figure a two segment straight line approximation has been plotted for comparison with the actual gain characteristics of the amplifier.

2. Amplifier characteristics with changing input conditions

The following data was taken using the same test set up as above, except that provision is made for changing the ambient temperature and the 3 phase supply voltage to the amplifier. An equipment warm up period of 10 minutes is allowed before data is recorded.

a. Conditions: Low temperature, Low voltage

	initial	final
Temperature:	5°C	3°C
Supply voltage (V_{12},V_{13},V_{23})	101,97,103	101,95,102
Output voltage:		

	Time (min)					
Vin (MV)	5	10	15	20	25	30
0	1.7	2.2	2.7	2.6	2.4	2.1
+10	28.3	28.2	28.8	28.8	28.5	28.2
-10	31.5	32.5	33.0	33.0	33.0	32.8
+30	81	81	81	82	82	80
-30	80	80	80	81	81	80
+60	92	91	92	92	92	92
-60	92	91	91	91	91	91

b. Conditions: Low temperature, Nominal voltage

	initial	final
Temperature:	3°C	3.8°C
Supply voltage (V_{12},V_{13},V_{23})	112,104,114	111,104,114
Output voltage:		

	Time (min)					
Vin (MV)	5	10	15	20	25	30
0	1.2	1.4	1.8	1.5	1.5	1.5
+10	35.5	36.0	35.5	36.0	36.0	36.0
-10	38.0	39.0	38.8	39.4	39.5	39.5
+30	98	98	98	98	98	99
-30	96	96	96	96	96	97
+60	112	112	112	112	112	112
-60	108	108	108	108	108	108

c. Conditions: Low temperature, High voltage

	initial	final
Temperature:	1°C	1°C
Supply voltage (V_{12},V_{13},V_{23})	125,117,126	121,115,120
Output voltage:		

	Time (min)					
Vin (MV)	5	10	15	20	25	30
0	.95	.95	.95	1.00	.95	1.00
+10	45.0	45.0	44.0	46.0	43.0	42.5
-10	46.0	46.0	46.0	46.5	45.0	44.5
+30	108	107	107	107	105	105
-30	108	107	107	107	105	105
+60	123	121	121	121	120	119
-60	120	119	117	117	117	115

d. Conditions: Nominal temperature, Low voltage

	initial	final
Temperature:	26°C	26°C
Supply voltage (V_{12},V_{13},V_{23})	101,97,103	102,96,104
Output voltage:		

	Time (min)					
Vin (MV)	5	10	15	20	25	30
0	1.9	2.1	2.0	2.6	2.5	2.4
+10	29.5	29.0	29.0	29.2	29.2	29.8
-10	32.5	33.0	33.5	33.8	33.5	33.5
+30	82	82	83	83	83	83
-30	82	82	82	82	83	82
+60	93	93	94	94	94	93
-60	92	93	93	93	93	92

e. Conditions: Nominal temperature, Nominal voltage

	initial	final
Temperature:	26°C	26°C
Supply voltage (V_{12},V_{13},V_{23})	113,105,115	113,105,115
Output voltage:		

	Time (min)					
Vin (MV)	5	10	15	20	25	30
0	1.6	3.0	3.1	3.1	3.2	3.2
+10	37.5	37.2	37.2	37.2	37.2	37.2
-10	42	41	41	41	41	41
+30	100	100	100	100	100	100
-30	100	100	100	100	100	100
+60	117	117	117	117	117	117
-60	113	113	113	113	113	113

f. Conditions: Nominal temperature, High voltage

	initial	final
Temperature:	26°C	26°C
Supply voltage (V_{12},V_{13},V_{23})	125,114,128	125,113,127
Output voltage:		

	Time (min)					
Vin (MV)	5	10	15	20	25	30
0	.9	2.0	1.6	2.1	2.1	2.1
+10	45.5	46.0	45.5	45.0	44.5	44.8
-10	48.2	49	49	49	48.8	48.8
+30	109	109	109	110	109	109
-30	109	109	110	110	109	109
+60	122	124	124	123	123	123
-60	120	121	121	121	120	120

g. Conditions: High temperature, Low voltage

	initial	final
Temperature:	85°C	85°C
Supply voltage (V_{12},V_{13},V_{23})	102,97,104	101,96,103
Output voltage:		

	Time (min)					
Vin (MV)	5	10	15	20	25	30
0	2.4	2.8	2.9	2.9	3.0	3.0
+10	33.0	30.0	28.0	26.5	27.5	27.5
-10	33.0	36.0	34.0	32.0	33.5	33.5
+30	77	83	82	82	82	81
-30	77	83	83	82	82	81
+60	92	93	93	93	93	92
-60	92	93	93	93	92	91

h. Conditions: High temperature, Nominal voltage

	initial	final
Temperature:	85°C	85°C
Supply voltage (V_{12},V_{13},V_{23})	113,105,115	113,105,115
Output voltage:		

	Time (min)					
Vin (MV)	5	10	15	20	25	30
0	2.8	3.0	2.6	3.4	3.0	2.8
+10	35.8	35.0	35.0	36.0	36.5	35.0
-10	40.5	40.8	40.5	41.0	42.0	41.0
+30	100	100	100	100	98	100
-30	100	100	100	99	98	100
+60	115	115	114	115	114	114
-60	112	112	112	112	111	112

i. Conditions: High temperature, High voltage

	initial	final
Temperature:	85°C	85°C
Supply voltage (V_{12},V_{13},V_{23})	127,114,129	125,113,128
Output voltage:		

	Time (min)					
Vin (MV)	5	10	15	20	25	30
0	.95	1.60	2.10	2.10	2.30	2.20
+10	46.5	45.0	44.5	43.5	44.0	43.5
-10	49.2	48.0	49.5	48.5	50.0	48.5
+30	109	109	109	110	110	110
-30	109	109	109	110	109	110
+60	125	124	124	124	125	124
-60	122	122	122	122	122	122

3. Motor gain - nominal environmental conditions

The motor was driven with a variable control voltage of proper phase, and the resulting speed of the motor was measured by recording the time per revolution of the output arm on a strip chart recorder. The motor operates under load. The data taken is as follows:

Motor Control Voltage (volts)	Period of Output Arm (sec) TRIAL 1	2	3	4	Avr. Speed (deg./sec)
15	36.0	33.5	33.8	30.5	3,295
20	17.6	17.2	16.8	16.8	6,440
25	11.0	11.2	11.2	11.2	9,810
30	8.4	8.4	8.4	8.4	13,100
35	6.8	6.8	6.8	6.8	16,200
40	5.6	5.6	5.6	5.6	19,650
60	3.6				30,500

Test Conditions: Temperature = 27°C, Average a.c. supply voltage (3 phase) = 112 volts. Gyro unit #3.

To convert the period of the output arm into motor speed, the motor-output arm gear ratio of 306:1 is used:

$$\text{Motor speed (deg/sec)} = \frac{306}{\text{arm period}} \times 360 \text{ deg/rev.}$$

The data taken in the four trials above is averaged at each value of control voltage and is plotted in figure 8, page 27.

4. Motor gain - changing environmental conditions

Several measurements are made of the motor speed, holding the control phase voltage fixed at $\pm$ 41 volts, and changing the reference phase voltage and ambient temperature. Data taken under various conditions is recorded below, where the motor speed is measured in mm. To convert to degrees per second, the conversion is:

$$\text{deg. per second} = \frac{5}{(\text{mm})} \times 360 \times 306$$

Values in table are motor speed measured in mm.

Voltage E_{ac-1}	Temperature: Low		Room		High	
	-41*	+41*	-41	+41	-41	+41
Low	43.0	39.0	32.0	32.0	24.5	23.0
	43.5	38.1	32.0	31.2	24.5	23.1
	42.5	38.0	33.0	31.5		23.5
	42.0	37.0	33.0			23.7
	T=0	E_{ac-1}=100.3	T=26°	E_{ac-1}=100.3	T=85°	E_{ac-1}=100.7
Voltage E_{ac-1}	Low		Room		High	
	-41	+41	-41	+41	-41	+41
Med	35.0	34.0	28.0	27.5	25.0	25.0
	36.0	33.5	28.8	27.3	25.0	25.1
	36.2	32.8	28.5	27.6	25.0	25.2
	37.2	33.9	28.2	27.7	25.0	25.0
	T=3°	E_{ac-1}=109.3	T=26°	E_{ac-1}=112.7	T=85.0	E_{ac-1}=110.7
Voltage E_{ac-1}	Low		Room		High	
	-41	+41	-41	+41	-41	+41
High	37.0	35.0	33.0	30.0	26.5	26.0
	37.0	34.0	32.0	30.0	26.5	25.5
	36.0	33.0	31.0	29.5	26.5	25.5
	36.0	33.0	31.0	29.2	26.0	26.0
	T=-5°	E_{ac-1}=123.3	T=26°	E_{ac-1}=124.0	T=85°	E_{ac-1}=122.7

*Values of control phase voltage

5. Motor time response - nominal environmental conditions

The servo motor time response was measured by recording the tachometer output voltage on a strip chart recorder while providing a step control voltage input into the motor. The time for the tachometer output trace to reach 63.3% of the final value is read from the chart recording. Results indicate that this time depends strongly upon the magnitude of the step input voltage. The extent of this input dependence is shown in the following data:

Step input voltage (volts)	Time for speed to reach 63.3% of final value (secs)		
	TRIAL 1	2	Avr.
+40	.35	.40	.375
-40	.41	.34	.375
+74	.21	.22	.215
-74	.20	.20	.200
+115	.16	.14	.150
-115	.11	.11	.110

Test conditions: Temperature 27°C, average supply voltage (3 phase) = 112v
Motor unit # 3.

6. Motor time response - changing environmental conditions

The table below gives values of the motor time constant in seconds, using a step input voltage of ± 41 volts, for various environmental conditions.

Voltage E_{ac-1}	Temperature: Low		Room		High	
	-41*	+41*	-41	+41	-41	+41
Low	.34	.36	.38	.47	.39	.34
	.37	.39	.38	.45	.39	.34
	.37	.39		.41		
	.45	.32				
	.42					
	.35					
	T=0 E_{ac-1}=100.3		T=26° E_{ac-1}=100.3		T=85° E_{ac-1}=100.7	

Voltage E_{ac-1}	Low		Room		High	
	-41	+41	-41	+41	-41	+41
Nom.	.38	.37	.42	.34	.37	.31
	.36	.32	.34	.40	.35	.33
		.34	.37	.33		
		.35	.37	.35		
				.34		
				.34		
	T=3° E_{ac-1}=109.3		T=26° E_{ac-1}=112.7		T=85° E_{ac-1}=110.7	

Time Constant (secs)

*Values of control phase voltage.

Voltage E_{ac-1}	Temperature: Low -41*	Low +41*	Room -41	Room +41	High -41	High +41
High	.26	.24	.26	.32	.28	.27
	.23	.25	.25	.29	.28	.26
	.25	.26		.27		
	.22	.23				
	$T=-5^{o}$ $E_{ac-1}=123.3$		$T=26^{o}$ $E_{ac-1}=124.0$		$T=85^{o}$ $E_{ac-1}=122.7$	

Time Constant (secs)

*Values of control phase voltage.

7. Tachometer gain - nominal conditions

While driving the motor with variable control voltages of the proper phase, the output of the tachometer windings on the motor was measured with a Triplet Model 850 voltmeter. The resulting data is:

Motor Speed (deg/sec)	Tach voltage (volts) TRIAL 1	2	3	4	Avr.
3,295	.020	.030	.035	.035	.030
6,440	.055	.060	.065	.070	.062
9,810	.100	.110	.115	.115	.110
13,100	.150	.160	.170	.165	.161
16,200	.210	.230	.225	.225	.222
19,650	.270	.280	.280	.275	.276

Test conditions: Temperature $27^{o}C$; average supply voltage (3 phase) = 112v, Motor #3

The nominal tachometer data is plotted in figure 9 page 29.

8. Tachometer gain - changing environmental conditions

Holding the motor speed fixed, the tachometer output voltage is measured as the ambient temperature and supply voltage are set at several levels.

Supply[1] Voltage	Temperature Low -41	Low +41	Nom. -41	Nom. +41	High -41	High +41
Low	.142	.100 .166	.184	.203	.191	.199
Nom.	.174	.122	.192 .225	.240 .240	.210	.235
High	.175	.206	.210	.243	.221	.232

Tachometer Output Voltage

[1]Note: Each reading in this table corresponds to the reading in the table of section 4.

To convert this data into Tachometer gain, the voltage readings are divided by the corresponding motor speed readings calculated from the table of section 4, this appendix.

9. Experimental Measurement of Nominal Autosyn Gain

In this experiment, the temperature and power supply voltage are fixed at nominal values, and measurements made of autosyn output voltage under load while angular displacements are introduced by shims of different thickness placed under the output arm of the TSA. These shims then give known angular deflections of the autosyn rotor. The resulting autosyn output voltage is measured using a Hewlett-Packard 400-H voltmeter.

The resulting data is:

Autosyn Rotor Angle

Total Shim Thickness (mills)	Degrees	Output Voltage (volts) Trial #1	Trial #2	Trial #3	Trial #4
0	0	.017	.016	.017	.017
5		.023	.017	.024	.021
10	.143	.025	.024	.025	.025
15		.026	.022	.026	.024
20	.286	.037	.029	.037	.033
25		.041	.042	.041	.038
30	.428	.045	.042	.054	.042
35		.059	.054	.057	.057
40	.573	.063	.058	.066	.060
44		.077	.070	.076	.075
50	.716	.082	.077	.078	.075
54		.095	.091	.093	.091
60	.859	.099	.095	.100	.099
64		.110	.110	.106	.106
70	1.00	.114	.114	.110	---

Test conditions: Temperature 27°C, Average a.c. voltage input (3 phase)=112v
Gyro-autosyn unit # 2.

10. Autosyn gain - changing environmental conditions

The autosyn rotor angle is held fixed and the autosyn supply voltage and ambient temperature set at several levels. The resulting data is:

Voltage	Temperature Low	Nom.	High
123	.065	.063	.053
112	.060	.058	.050
101	.056	.050	.041

Autosyn Output Voltage, input angle .52°

11. Experimental Measurement of Inverter Characteristics

In this experiment the inverter is supplied with varying d.c. supply voltages, and the resulting a.c. output voltage is measured under load using an a.c. voltmeter and a frequency counter.

Each data point below is the average value of 6 observations taken at each d.c. voltage level. No change with time is measurable.

1. Temperature = 26°C

d.c. voltage (volts)	a.c. voltage (volts)	frequency (cps)
29.25	117.0	418.5
28.37	117.0	417.2
26.03	116.0	414.7
23.95	114.2	413.5
21.92	110.5	402.2
19.90	104.5	376.8
17.97	94.5	350.2

2. Temperature = 5°C

d.c. voltage (volts)	a.c. voltage (volts)	frequency (cps)
29.52	117.8	419.0
28.53	117.7	417.7
26.07	117.0	417.7
24.03	115.6	414.3
21.92	112.3	397.5
19.90	106.7	370.3
17.92	97.3	342.7

The inverter characteristics are plotted in figure 10, page 31.

12. Gyro drift

From the chart recordings of gyro drift, the maximum amplitude during the last 15 minute portion of a 30 minute test period is determined. For the various ambient temperatures and supply voltages, these maximum amplitudes are listed in the table below: (in degrees)

MAXIMUM DEVIATIONS OF GYRO FROM VERTICAL FOR $t_3 \leq t \leq t_4$ AT AVERAGE FREQUENCIES: HIGH = 417, NOMINAL = 400, LOW = 365 CYCLES

Average Voltage E_{ac-1}	Average Temperature 0°C		26°C			90°C	
	High[b]	Low	Nom.			High	Low
100v	3.71	12.38	2.31			.82	.66
	4.95	7.26	1.57			1.32	.50
	5.36	5.61	.66			.50	.99
	10.72	8.91	1.82			.82	.33
	Nom.	Low	Nom.	Nom.	Nom.	Nom.	
112v	10.72	18.98[a]	2.23	.33	5.44	.66	
	10.72	19.80[a]	1.32	.41	3.96	.33	
	13.20	17.32[a]	1.65	1.90	4.62	.82	
	9.90	13.20[a]	1.48	2.06	2.80	.66	
			1.90	4.04	.74		
			1.65	6.93	.74		
			1.57	2.14	.91		
			2.48	2.97	1.65		
	High		Nom.			High	Low
124v	14.85		1.07			.50	.82
	12.38		2.48			.82	.66
	17.32		1.65			.50	1.48
	16.50		5.36			.82	2.48

[a] 107 volts

[b] Frequency

In addition, the following data were collected and used at 26°C and nominal frequency for 80 v: 4.78, 3.80 and for 135 v: 7.42, 6.19. Prior to statistical analyses, the gyro data were adjusted for autosyn gain, transformed to logarithms, and weighted.

13. Measured response of TSA to 5° step input

The complete TSA system was energized using nominal values for supply voltage and the output arm displaced 5 degrees. The arm was released and

allowed to return to the original position. The output arm displacement was recorded on a strip chart recorder and the following values were read from the chart:

Arm Displacement (degrees)	Cumulative time measured from t=0 (secs) TRIAL 1	TRIAL 2
5	0	0
4	.08	.06
3	.12	.10
2	.15	.13
1	.18	.17
0	.25	.24

Test Conditions: Temperature 27°C. Average supply voltage (3 phase) = 112v
Amplifier # 1; Gyro # 3; Inverter # 1.

This measured response curve is plotted in figure A3, for comparison to the calculated curve.

14. Data Summary

When the measurements on the previous pages are properly averaged and corrected for slight changes in the input-environmental conditions, and converted into the parameter of interest, the data can be summarized in convenient tabular form as:

a) Tachometer gain - K_T

		Temperature 5°C	26°C	85°C	
Supply Voltage E_{ac-1}	100	1126	1125	844	$\times 10^{-8}$
	112	1286	1150	1007	
	124	1386	1258	1071	

b) Motor gain - K_m

		Temperature 5°C	26°C	85°C
Supply Voltage E_{ac-1}	100	332	419	562
	112	387	475	539
	124	366	438	515

c) Autosyn gain - K_e

		Temperature 5°C	26°C	85°C
Supply Voltage E_{ac-1}	100	.1105	.0986	.0808
	112	.1183	.1144	.0986
	124	.1282	.1243	.1045

d) Motor time constant - τ_m

		Temperature 5°C	26°C	85°C
Supply Voltage E_{ac-1}	100	.374	.411	.365
	112	.357	.362	.340
	124	.242	.274	.272

e) Amplifier gain - K_A

		Temperature 5°C	26°C	85°C
Supply Voltage E_{ac-1}	100	2730	2790	2770
	112	3290	3390	3370
	124	3630	3750	3750

f) Saturation level (amplifier) - V_s

		Temperature 5°C	26°C	85°C
Supply Voltage E_{ac-1}	100	91.4	93.2	92.6
	112	110.0	115.0	113.1
	124	118.7	122.1	123.0

g) Coefficient $A = \frac{\tau_m}{K_e R K_A K_m}$

		Temperature 5°C	26°C	85°C	
Supply Voltage E_{ac-1}	100	1130	1090	887	$\times 10^{-6}$
	112	729	589	583	
	124	429	410	412	

h) Coefficient $B = \frac{1 + K_A K_m K_T}{K_e R K_A K_m}$

		Temperature 5°C	26°C	85°C	
Supply Voltage E_{ac-1}	100	342	376	344	$\times 10^{-4}$
	112	353	324	330	
	124	349	325	329	

10.0. NOMENCLATURE

ϕ_a - Aircraft pitch angle, inertial reference

ϕ_r - Gyro gimbal-autosyn rotor angle, inertial reference

ϕ_s - Autosyn stator angle, case reference

γ - Angle between system output arm and airframe

γ_i - System output arm angle, inertial reference

θ - Motor shaft angle

K_A - Amplifier gain (volts per volt)

K_e - Autosyn signal generator gain (volts per degree)

K_T - Tachometer gain (volts per degree per second)

K_m - Motor gain (deg. per sec. per volt)

τ_m - Motor time constant (seconds)

V_s - Amplifier saturation voltage (RMS volts)

V_c - Motor control phase voltage (RMS volts)

V_e - Autosyn output voltage (RMS volts)

$E_{D.C.}$ or E - D.C. supply voltage from airframe (volts)

E_{ac-1} - A.C. inverter output voltage (RMS volts)

E_{ac-2} - A.C. output voltage from amplifier (RMS volts)

N_a - Amplifier output voltage with zero input voltage

N_G - Component of gyro-autosyn output representing gyro drift

T - Ambient temperature

WG/V - Ratio of vertical wind gust velocity to aircraft speed

R - Gear ratio

h - Catastrophic hazard rate

ω - Frequency in radians per second

s - Laplace variable or complex frequency

S.D. - Standard deviation